ARL-TR-8840 • Oct 2019

DEVCOM ARMY RESEARCH LABORATORY

Viscoelastic-Damage Theory Based on a QR Decomposition of Deformation Gradient

by John D Clayton and Alan D Freed

NOTICES

Disclaimers

The findings in this report are not to be construed as an official Department of the Army position unless so designated by other authorized documents.

Citation of manufacturer's or trade names does not constitute an official endorsement or approval of the use thereof.

Destroy this report when it is no longer needed. Do not return it to the originator.

ARL-TR-8840 ● Oct 2019

Viscoelastic-Damage Theory Based on a QR Decomposition of Deformation Gradient

by John D Clayton and Alan D Freed
Weapons and Materials Research Directorate, CCDC Army Research Laboratory

REPORT DOCUMENTATION PAGE

Form Approved
OMB No. 0704-0188

PLEASE DO NOT RETURN YOUR FORM TO THE ABOVE ADDRESS.

1. REPORT DATE *(DD-MM-YYYY)*	2. REPORT TYPE	3. DATES COVERED (From - To)
October 2019	Technical Report	November 2018–October 2019

4. TITLE AND SUBTITLE
Viscoelastic-Damage Theory Based on a QR Decomposition of Deformation Gradient

5a. CONTRACT NUMBER

5b. GRANT NUMBER

5c. PROGRAM ELEMENT NUMBER

6. AUTHOR(S)
John D Clayton and Alan D Freed

5d. PROJECT NUMBER

5e. TASK NUMBER

5f. WORK UNIT NUMBER

7. PERFORMING ORGANIZATION NAME(S) AND ADDRESS(ES)
US Army Combat Capabilities Development Command Army Research Laboratory
ATTN: FCDD-RLW-PC
Aberdeen Proving Ground, MD 21005-5066

8. PERFORMING ORGANIZATION REPORT NUMBER
ARL-TR-8840

9. SPONSORING/MONITORING AGENCY NAME(S) AND ADDRESS(ES)

10. SPONSOR/MONITOR'S ACRONYM(S)

11. SPONSOR/MONITOR'S REPORT NUMBER(S)

12. DISTRIBUTION/AVAILABILITY STATEMENT
Approved for public release; distribution is unlimited.

13. SUPPLEMENTARY NOTES
primary author's email: <john.d.clayton1.civ@mail.mil>.

14. ABSTRACT
A novel thermodynamic framework for the continuum mechanical response of nonlinear solids is described. Large deformations, nonlinear hyperelasticity, viscoelasticity, and property changes due to evolution of damage in the material are encompassed. The deformation gradient is decomposed in Gram-Schmidt fashion into the product of an orthogonal matrix Q and an upper triangular matrix R, where the latter can be populated by six independent strain attributes. Strain attributes, in turn, are used as fundamental independent variables in the thermodynamic potentials. A complementary set of internal variables enters the thermodynamic potentials to enable history and rate dependence through viscoelasticity and irreversible stiffness degradation via damage. Governing equations and thermodynamic restrictions imposed by the entropy production inequality are derived. Mechanical, thermodynamic, and kinetic relations are presented for materials of certain cubic or isotropic symmetries. Representative models and example problems demonstrate utility and flexibility of this theory for depicting nonlinear hyperelasticity, large-strain viscoelasticity, and/or damage from cracks or voids, with physically measurable parameters.

15. SUBJECT TERMS
continuum mechanics, nonlinear elasticity, viscoelasticity, damage mechanics, soft solids

16. SECURITY CLASSIFICATION OF:			17. LIMITATION OF ABSTRACT	18. NUMBER OF PAGES	19a. NAME OF RESPONSIBLE PERSON
a. REPORT	b. ABSTRACT	c. THIS PAGE			John D Clayton
Unclassified	Unclassified	Unclassified	UU	82	19b. TELEPHONE NUMBER (Include area code) 410-278-6146

Standard Form 298 (Rev. 8/98)
Prescribed by ANSI Std. Z39.18

Contents

List of Figures

Acknowledgments

John D Clayton acknowledges support of the US Army Combat Capabilities Development Command (CCDC) Army Research Laboratory. Alan D Freed acknowledges support of a Joint Faculty Appointment with the CCDC Army Research Laboratory.

1. Introduction

An increased understanding of the mechanics of soft biological tissues is needed to develop improved practices or products in medical, transportation, and defense industries. For example, models of the static soft tissue response can be used to inform novel surgical procedures and to aid design of medical implants with surrogate materials of similar properties. Dynamic tissue models are important for describing the response of the human body to impacts encountered in sporting activities, vehicular collisions, and ballistic events. Such models, in turn, support design of protective systems in automobiles and personal protective equipment for police, security, and military personnel.

Deformations are very often large, even within normal ranges of everyday biological activity (e.g., muscle functions, circulation, and breathing), necessitating nonlinear constitutive models.[1–3] The equilibrium nonlinear elastic response dominates for low loading rates, while viscoelasticity becomes important to account for rate dependence, hysteresis, and stress relaxation. For traumatic events, damage may be incurred in the tissue, and models linking degradation of mechanical properties to loss of biological function are sought.[4,5] The present work seeks to develop a general theoretical framework enabling modeling of the physical phenomena of nonlinear elasticity, viscoelasticity, and damage. The framework should be applicable to a host of soft biological tissues (e.g., muscle, skin, and internal organs) as well as other viscoelastic solids, such as polymers, capable of sustaining very large deformations. Dynamic behaviors (i.e., inertial effects) and irreversible structure changes that accompany damage are also encompassed. At the microscopic level, many if not most tissues are heterogeneous and contain fluid; the present approach treats the material as a homogeneous solid body whereby local microstructure effects are embedded in macroscopic state variables and commensurate effective properties, as opposed to more intricate theories enabling fluid-structure interactions, for example.[6,7]

The thermodynamic framework developed herein accounts for nonlinear viscoelasticity in a general setting similar, but not identical, to the theoretical-computational schemes of Simo, Holzapfel, and coworkers.[8–11] In these prior approaches, tensor internal variables are used to account for time dependence, essentially leading to an additive decomposition of the second Piola-Kirchhoff stress tensor into equilib-

rium (i.e., limiting hyperelastic) and non-equilibrium (i.e., viscous) parts. Evolution equations for these internal variables generalize standard viscoelastic spring-dashpot models in a setting consistent with positive dissipation mandated by the second law of thermodynamics.[9,10] Some formulations enable different material-specific kernels in the convolution representation of the internal variable or its thermodynamic conjugate force.[8] Particular choices of internal variables are consistent with a multiplicative decomposition of the deformation gradient into elastic and viscous parts,[8,12] similar to constructions used in elastic-plastic crystal mechanics.[13–15] Multiplicative decompositions have also been proposed as fundamental kinematic assertions in viscoelasticity[11]; their usage is not mandatory, however, for thermodynamic consistency of a general theory. Another noteworthy and innovative approach for shape memory polymers invokes a multiplicative decomposition of the deformation gradient into an instantaneous thermoelastic part and an upper triangular matrix for temporarily frozen deformation of the permanent network.[16]

When nonlinear elastic and viscoelastic theories are extended to include damage, one or more scalar internal state variables are often used to represent degradation incurred in a soft solid when deformed to a regime exceeding some strain-history dependent tolerance, for example a critical strain or stored energy. Progressive degradation of the stiffness may be incurred in polymers[8] as well as biological tissues[5] when subjected to cyclic deformations of increasing amplitude. If the load level is fixed, then the stress hysteresis converges to a saturated response curve, though remnant strains may persist. Sophisticated kinetic laws consistent with these physics and the laws of thermodynamics have been developed for collagenous soft tissues comprising arterial walls.[5] Similar concepts, with extension to stochastic aspects, have been invoked for other fibrous soft tissues.[4]

Herein, damage is distinguished physically from viscoelasticity as follows. The former is associated with irreversible changes in microstructure that remain upon unloading of the solid to its original undeformed shape. Typically damage evolution involves bond breaking corresponding to crack extension, void nucleation, and other tearing modes in the solid that generate free internal surfaces. In polymers, damage may be attributed to permanent chain and multi-chain breakages and micro-void formation.[8] Such mechanisms tend to impart a reduction in overall stiffness of the material, which is evident on unloading to, and subsequent reloading from, the origin in stress-strain space. In contrast, viscoelasticity is associated with dissipative,

rate-dependent structural rearrangements that are restored or removed when the material is unloaded to its original shape. Hysteresis is evident in cyclic loading, depending on rate. Stress relaxation behavior is characteristic of viscoelastic solids. Transient changes in microstructure may occur under a purely viscoelastic response, but these are impermanent, in contrast to damage that is evident upon inspection of a material element with residual cracks or pores.

The current formulation differs from the above-mentioned constitutive models in several respects. With regard to kinematics, emphasized here is a Gram-Schmidt factorization or QR decomposition: $\boldsymbol{F} = \boldsymbol{Q}\boldsymbol{R}$. This is a decomposition of the deformation gradient $\boldsymbol{F}$ into a product of an orthogonal matrix, often written as $\boldsymbol{Q}$, and an upper triangular matrix, often written as $\boldsymbol{R}$. This QR decomposition is contrasted to the more traditional emphasis on a split of deformation into volumetric and deviatoric parts[8,17] via $\boldsymbol{F} = J^{1/3}\bar{\boldsymbol{F}}$, where $J = \det \boldsymbol{F}$. The QR decomposition results in a field of local physical frames, each back-rotated from a global Cartesian spatial frame of reference, where material response data are most readily measured and interpreted.[18,19]

The upper triangular matrix $\boldsymbol{R}$, called the "Laplace stretch"[19,20] can be calculated explicitly from terms in the deformation gradient. Seven physically descriptive scalar strain attributes, in the terminology of Criscione,[21] are associated with dilatation, squeeze, and shear, and six of which are independent, can be obtained readily from components of $\boldsymbol{R}$. Conjugate scalar measures of stress can be derived from rates of the strain attributes and the definition of stress power.[19] The QR decomposition apparently was first proposed in the setting of continuum mechanics of solids by McClellan[22] and has received renewed attention in recent years following work of Srinivasa.[23]

Advantages of use of the QR decomposition in the context of finite hyperelasticity are discussed at length in previous works.[18–20,23–25] Explicit hyperelastic potentials can be constructed from the strain attributes rather than classical strain invariants, where the former approach appears more physically intuitive than the latter.[23] This approach is permissible and objective since six independent strain attributes exist in one-to-one fashion with six independent components of the deformation tensor $\boldsymbol{C} = \boldsymbol{F}^{\mathrm{T}}\boldsymbol{F} = \boldsymbol{R}^{\mathrm{T}}\boldsymbol{R}$. Components of $\boldsymbol{Q}$ and $\boldsymbol{R}$ can be obtained from $\boldsymbol{F}$ by simple algebraic formula, without recourse to an expensive eigenvalue calculation necessary

for determination of terms entering a polar decomposition of $\boldsymbol{F}$ into rotation and stretch. Upper triangular matrices are closed under both addition and multiplication, and their determinants and inverses are trivially calculated, so constraints such as incompressibility are easily enforced.[16] Another benefit is that derivatives of the strain energy can be calculated simply and directly from measured or prescribed values of stress and deformation. Depending on the choice of strain attributes used, stresses can be written in terms of (nearly) orthogonal components consisting of derivatives of strain energy density with respect to each attribute. Such orthogonality is beneficial in the context of formulation of energy potentials for hyperelasticity under large deformations when the form of such potentials is undecided a priori.[21,23] Classical invariant-based theories, on the other hand, suffer from the coupling among invariants that forbids isolation of contributions to energy of each from data obtained in traditional stress-strain experiments. The QR decomposition also appears well-suited for addressing symmetry requirements in materials of monoclinic, orthotropic, and transversely isotropic symmetry groups.[23]

Implicit elastic models, to which Fung-type exponential theories can be manipulated,[26–30] have also been proposed whereby both strain and stress attributes simultaneously enter the thermodynamic potentials. Implicit theoretical representations may offer a more intuitive calibration procedure than usual explicit hyperelasticity for biological tissues that demonstrate a strain-limiting response.[27,28] Explicit and implicit models invoking QR kinematics have been developed for planar analysis of biological tissues (i.e., membranes[24]), but have not been fully applied to 3-D continua until the present work.

The present report also newly invokes scalar stress-like attributes in its description of viscoelasticity, rather than tensor-valued viscous stresses as in prior models.[8–10,12] Along similar lines, kinetic equations for damage evolution herein utilize thermodynamic driving forces ultimately depending on strain attributes rather than strain invariants as implemented in biomechanics applications.[4,5] It is anticipated that the same advantages mentioned already in the context of QR hyperelastic materials will be inherited in analogous formulations of viscoelasticity and damage. The present approach ultimately seeks a constitutive framework with more physically descriptive, fewer, and easier calibrated parameters for a given soft solid than existing models. Demonstrative examples will be presented that seek to achieve this goal.

Most of the present work is of general nature, intended to account phenomenologically for viscoelastic and damage phenomena through generic internal state variables whose kinetics can be calibrated to macroscopic stress-strain data, for example. This is the approach taken in works dealing with polymers and biological tissues.[5,8] Linkages between fine-scale material structure and effective properties are highly microstructure-specific, and analytical formulae can be obtained only under ideal circumstances (e.g., otherwise homogeneous linear elastic solids with rather dilute concentrations of voids or cracks[31–33]). For elastic solids with Griffith cracks, a general expression for compliance changes in terms of integration of local stress intensity factors is given by Rice.[34] Derivation of new multi-scale relations between microscopic structure changes and macroscopic behavior is beyond the present scope, and it may not be feasible for highly complex nonlinear materials such as heterogeneous biological tissues.

Effective moduli obtained for elastic solids with penny-shaped cracks[32] and spherical voids[31] are invoked in a few specific examples towards the end of the present work. The intent is demonstration of how a phenomenological damage variable can be explicitly related to flaws, possibly evolving, in real materials, and how realistic effective moduli can be incorporated from micromechanical studies in a thermodynamically consistent way, such that damage is dissipative. These moduli are extrapolations of solutions from micromechanics for isotropic linear elastic bodies, since exact solutions for effective moduli of solids with cracks or voids do not exist for the present nonlinear constitutive theory. The results do become rigorous for small deformations because the present theory is consistent with linear elasticity in the limit of small deformations.

This report is organized as follows. Kinematics and balance laws of continuum mechanics, with emphasis on aspects derived from the QR decomposition, are given in Section 2. Constitutive assumptions and resulting derived thermodynamic relations are given in Section 3, where very general internal state variable frameworks are admitted. The equilibrium responses of solids with several material symmetries (e.g., approximately cubic and isotropic) are addressed via hyperelasticity in Section 4. Viscoelasticity and damage are addressed in respective Section 5 and Section 6. Conclusions are given in Section 7. Notation follows conventions of modern continuum mechanics, where vectors and tensors of higher order are written in boldface type, and scalars and scalar components are written in italics. When in-

dex notation is used for clarity, summation is implied over repeated indices. Other mathematical devices are defined as necessary when they appear.

2. Kinematics and Balance Laws

Kinematics and balance laws of geometrically nonlinear continuum mechanics are presented with an emphasis on the QR decomposition and its ramifications.

2.1 Kinematics of Finite Deformation

Let $\boldsymbol{X}$ and $\boldsymbol{x}$ denote Lagrangian and Eulerian position vectors of a material particle in respective reference and spatial configurations, each referred to a global Cartesian system with fixed origin to be described in more detail later. Let t denote time. Motions between configurations are the mappings

$$\boldsymbol{x} = \boldsymbol{\varphi}(\boldsymbol{X}, t), \qquad \boldsymbol{X} = \boldsymbol{\Phi}(\boldsymbol{x}, t). \tag{1}$$

Herein, these are presumed sufficiently smooth to enable existence of all subsequent space-time derivatives. The present work does not deal with shocks or other surfaces of singularity. Denote the material time derivative, material gradient, and spatial gradient of a generic quantity f by the respective operations

$$\dot{f}(\boldsymbol{X}, t) = \frac{\partial f(\boldsymbol{X}, t)}{\partial t}, \quad \nabla_0 f(\boldsymbol{X}, t) = \frac{\partial f(\boldsymbol{X}, t)}{\partial \boldsymbol{X}}, \quad \nabla f(\boldsymbol{X}(\boldsymbol{x}, t), t) = \frac{\partial f(\boldsymbol{X}(\boldsymbol{x}, t), t)}{\partial \boldsymbol{x}}. \tag{2}$$

Particle velocity and acceleration are

$$\boldsymbol{v}(\boldsymbol{X}, t) = \dot{\boldsymbol{x}}(\boldsymbol{X}, t), \qquad \boldsymbol{a}(\boldsymbol{X}, t) = \dot{\boldsymbol{v}}(\boldsymbol{X}, t). \tag{3}$$

Arguments of functions, for example $(\boldsymbol{X}, t)$ in the Lagrangian description, are dropped henceforth unless needed for clarity.

The deformation gradient and its inverse are

$$\boldsymbol{F} = \nabla_0 \boldsymbol{\varphi} = \partial \boldsymbol{x} / \partial \boldsymbol{X}, \qquad \boldsymbol{F}^{-1} = \nabla \boldsymbol{\Phi} = \partial \boldsymbol{X} / \partial \boldsymbol{x}. \tag{4}$$

Consequences of Eq. 4 include the local integrability conditions[15,35]

$$\begin{aligned} \frac{\partial F^i_J}{\partial X^K} = \frac{\partial^2 x^i}{\partial X^J \partial X^K} = \frac{\partial F^i_K}{\partial X^J} = 0 \quad &\Leftrightarrow \quad \nabla_0 \times \boldsymbol{F} = \boldsymbol{0}, \\ \frac{\partial (F^{-1})^I_j}{\partial x^k} = \frac{\partial^2 X^I}{\partial x^j \partial x^k} = \frac{\partial (F^{-1})^I_k}{\partial x^j} = 0 \quad &\Leftrightarrow \quad \nabla \times \boldsymbol{F}^{-1} = \boldsymbol{0}. \end{aligned} \tag{5}$$

The referential and spatial velocity gradients are

$$\nabla_0 \boldsymbol{v} = \dot{\boldsymbol{F}}, \qquad \nabla \boldsymbol{v} = \dot{\boldsymbol{F}} \boldsymbol{F}^{-1}. \tag{6}$$

Let $\mathrm{d}v$ and $\mathrm{d}V$ denote spatial and referential volume elements. Then

$$\mathrm{d}v = (\det \boldsymbol{F}) \mathrm{d}V = J \mathrm{d}V, \qquad \dot{J} = J \nabla \cdot \boldsymbol{v} = J \mathrm{tr}(\dot{\boldsymbol{F}} \boldsymbol{F}^{-1}), \tag{7}$$

with $J > 0$ the Jacobian determinant and $\mathrm{tr}(\cdot)$ the trace operator. All relations above are standard.

2.2 QR Kinematics

A fixed global Cartesian frame with spatial basis vectors $\{\boldsymbol{e}_i\}$, $i = 1, 2, 3$, is introduced, to which all vector and tensor components are referred unless noted otherwise. Thus, with capital Roman indices $J = 1, 2, 3$ denoting Lagrangian components,

$$\boldsymbol{e}_i = \boldsymbol{e}^i = \delta^i_J \boldsymbol{e}^J = \delta^i_J \boldsymbol{e}_J. \tag{8}$$

The deformation gradient is

$$\boldsymbol{F} = F^i_J \boldsymbol{e}_i \otimes \boldsymbol{e}^J = F_{ij} \boldsymbol{e}_i \otimes \boldsymbol{e}_j. \tag{9}$$

The deformation gradient can be decomposed uniquely into the product of a rotation $\boldsymbol{Q}$ and upper triangular matrix $\boldsymbol{R}$, where the latter is called the Laplace stretch:

$$\boldsymbol{F} = \boldsymbol{Q}\boldsymbol{R} = Q^i_\alpha R^\alpha_J \boldsymbol{e}_i \otimes \boldsymbol{e}^J; \qquad \boldsymbol{Q}^{-1} = \boldsymbol{Q}^{\mathrm{T}}, \quad \det \boldsymbol{Q} = +1. \tag{10}$$

Greek indices $\alpha = 1, 2, 3$ correspond to an intermediate configuration whose tangent vectors are pulled back from the spatial configuration by $\boldsymbol{Q}^{-1}$ or pushed forward from the reference configuration by $\boldsymbol{R}$. The same global Cartesian basis is

chosen for this configuration, called the "physical configuration" in prior work[19]:

$$\boldsymbol{e}_\alpha = \boldsymbol{e}^\alpha = \delta^i_\alpha \boldsymbol{e}_i = \delta^J_\alpha \boldsymbol{e}_J. \tag{11}$$

Refer to Fig. 1.

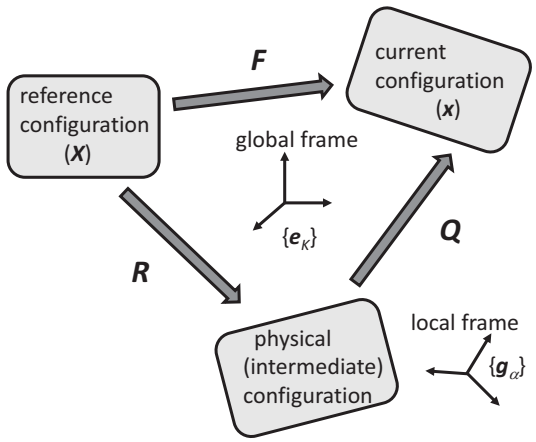

Fig. 1 Configurations, deformations, and coordinate frames

The Laplace stretch is written as follows in matrix form, where all components are referred to the global Cartesian coordinate system of Eq. 8 and Eq. 11:

$$\boldsymbol{R} = \begin{bmatrix} R_{11} & R_{12} & R_{13} \\ 0 & R_{22} & R_{23} \\ 0 & 0 & R_{33} \end{bmatrix} = \begin{bmatrix} a & a\gamma & a\beta \\ 0 & b & b\alpha \\ 0 & 0 & c \end{bmatrix} = \begin{bmatrix} a & 0 & 0 \\ 0 & b & 0 \\ 0 & 0 & c \end{bmatrix} \begin{bmatrix} 1 & \gamma & \beta \\ 0 & 1 & \alpha \\ 0 & 0 & 1 \end{bmatrix} = \boldsymbol{\Lambda\Gamma}. \tag{12}$$

Physically descriptive deformation measures are the three positive elongation ratios a, b, c that enter the extension tensor $\boldsymbol{\Lambda}$ and the three shear magnitudes α, β, γ that enter the simple shear tensor $\boldsymbol{\Gamma}$. Volume change is measured by

$$J = \det \boldsymbol{R} = \det \boldsymbol{\Lambda} = abc. \tag{13}$$

Parameters $a, b, c, \alpha, \beta, \gamma$ are physical attributes because they can be measured directly by an experimentalist in the physical coordinate system to be introduced in Eq. 18 without need for post analysis.[18,19,25]

Let

$$\boldsymbol{C} = \boldsymbol{F}^{\mathrm{T}}\boldsymbol{F} = \boldsymbol{R}^{\mathrm{T}}\boldsymbol{R} = C_{IJ}\boldsymbol{e}^I \otimes \boldsymbol{e}^J = F^i_I \delta_{ij} F^j_J \boldsymbol{e}^I \otimes \boldsymbol{e}^J = R^\alpha_I \delta_{\alpha\beta} R^\beta_J \boldsymbol{e}^I \otimes \boldsymbol{e}^J \tag{14}$$

denote the right Cauchy-Green deformation tensor. Nonzero components of $\boldsymbol{R} = R_{IJ}\boldsymbol{e}^I \otimes \boldsymbol{e}^J$ are obtained explicitly from C_{IJ} by the following sequence of basic recursive calculations[23]:

$$\begin{aligned} &R_{11} = \sqrt{C_{11}}, \quad R_{12} = C_{12}/R_{11}, \quad R_{13} = C_{13}/R_{11}, \quad R_{22} = \sqrt{C_{22} - (R_{12})^2}, \\ &R_{23} = (C_{23} - R_{12}R_{13})/R_{22}, \qquad R_{33} = \sqrt{C_{33} - (R_{13})^2 - (R_{23})^2}. \end{aligned} \tag{15}$$

Elongations and shears are

$$a = R_{11}, \quad b = R_{22}, \quad c = R_{33}; \qquad \alpha = R_{23}/R_{22}, \quad \beta = R_{13}/R_{11}, \quad \gamma = R_{12}/R_{11}. \tag{16}$$

The inverse of $\boldsymbol{R}$ is also upper triangular and can be written explicitly in matrix form in the global Cartesian coordinate system as

$$\boldsymbol{R}^{-1} = \boldsymbol{\Gamma}^{-1}\boldsymbol{\Lambda}^{-1} = \begin{bmatrix} 1/a & -\gamma/b & (\alpha\gamma - \beta)/c \\ 0 & 1/b & -\alpha/c \\ 0 & 0 & 1/c \end{bmatrix}. \tag{17}$$

With Eq. 17 at hand, $\boldsymbol{Q} = \boldsymbol{F}\boldsymbol{R}^{-1}$ can then be calculated by matrix multiplication. A stated benefit from the perspective of computations is that, given F^i_J, no diagonalization (e.g., eigenvalue analysis) is required to calculate any terms in a QR decomposition, in contrast to a polar decomposition.

2.3 Physical and Convected Bases

There is a choice of assignment of index numbers $1, 2, 3$ to the $\{\boldsymbol{e}_i\}$ that is ideal when the QR decomposition is used. Let the $\{\boldsymbol{e}_i\}$ be rotated by an amount $\boldsymbol{Q}$. Then for this ideal choice, the direction aligned with the rotated 1-axis and the direction normal to the rotated 1-2-plane remain invariant under the transformation $\boldsymbol{R}$. It is assumed henceforth that the $\{\boldsymbol{e}_i\}$ have been so ideally labeled. An algorithm for pivoting to achieve the corresponding upper triangular dominance of $\boldsymbol{R}$ is presented

in another reference.[19]

The so-called physical basis of Freed and Zamani,[19] denoted here by $\{\boldsymbol{g}_\alpha\}$, $\alpha = 1, 2, 3$, corresponds to the aforementioned rotated coordinate system:

$$\boldsymbol{g}_\alpha = \boldsymbol{g}^\alpha = Q^i_\alpha \boldsymbol{e}_i = Q^i_\alpha \delta^J_i \boldsymbol{e}_J, \qquad \boldsymbol{e}_i = (Q^{-1})^\alpha_i \boldsymbol{g}_\alpha = (Q^{\mathrm{T}})^\alpha_i \boldsymbol{g}_\alpha. \tag{18}$$

It is in this physical frame that the three elongations a, b, c and three shears α, β, γ, which are the physical attributes of the Laplace stretch $\boldsymbol{R}$, are measured. The $\{\boldsymbol{g}_\alpha\}$ comprise a local Cartesian frame (i.e., orthonormal right-handed triad) at each material point $\boldsymbol{X}$. If $\boldsymbol{Q}_t(\boldsymbol{X}) = \boldsymbol{Q}(\boldsymbol{X}, t)$ is not homogeneous in space, then obviously the $\boldsymbol{g}_\alpha$ do not comprise a global rectilinear frame.

Apply Eq. 10 to a simply connected region of a body deforming by $\boldsymbol{F}$ and parameterized by reference coordinates $\{X^K\}$ and spatial coordinates $\{x^k\}$. At a fixed time instant t, these coordinate charts are related by a diffeomorphism as implied by Eq. 1. Then the same region in the physical (intermediate) configuration can be covered by a chart of coordinates $\{y^\alpha\}$ that exist in one-to-one correspondence with $\{x^k\}$ and $\{X^K\}$ if and only if integrability conditions analogous to Eq. 5 hold simultaneously for $\boldsymbol{Q}^{-1}$ and $\boldsymbol{R}$. The former requires that Q^i_α be spatially constant, since a pure rotation must be homogeneous (i.e., of rigid-body type) to be integrable to a vector field: its contortion must vanish (proven elsewhere,[35] p. 112). The Laplace stretch need not be homogeneous to be integrable (i.e., for conditions $R^\alpha_I = \partial y^\alpha / \partial X^I$ to hold globally over the region). Rather, only the curl-free conditions $\partial R^\alpha_I / \partial X^J = \partial R^\alpha_J / \partial X^I$ need be fulfilled when $\{y^\alpha\}$ exist and correspondingly, when $\boldsymbol{Q}$ is homogeneous. Thus, when chart $\{y^\alpha\}$ exists with the aforementioned properties, then the orthonormal physical basis $\{\boldsymbol{g}_\alpha\}$ is global over the corresponding domain. Otherwise it is a local basis, and the $\{y^\alpha\}$ are anholonomic coordinates.[36]

In the physical coordinate system, introduce a unit cube with edges parallel to the $\{\boldsymbol{g}_\alpha\}$. The Laplace stretch of the deformation gradient, $\boldsymbol{R} = \boldsymbol{Q}^{\mathrm{T}}\boldsymbol{F}$, deforms such a cube to a parallelepiped whose edges are the oblique basis vectors $\{\boldsymbol{\gamma}_\alpha\}$, neither orthogonal nor of unit length, in general. The specific operation by which these

"convected basis vectors" are calculated is[18]

$$\boldsymbol{\gamma}_\alpha = \Lambda^\delta_\alpha \Gamma_{\beta\delta} \boldsymbol{g}^\beta \leftrightarrow \{\boldsymbol{\gamma}_\alpha\} = \boldsymbol{\Lambda}\boldsymbol{\Gamma}^{\mathrm{T}}\{\boldsymbol{g}_\alpha\} \leftrightarrow \begin{Bmatrix} \boldsymbol{\gamma}_1 \\ \boldsymbol{\gamma}_2 \\ \boldsymbol{\gamma}_3 \end{Bmatrix} = \begin{bmatrix} a & 0 & 0 \\ b\gamma & b & 0 \\ c\beta & c\alpha & c \end{bmatrix} \begin{Bmatrix} \boldsymbol{g}_1 \\ \boldsymbol{g}_2 \\ \boldsymbol{g}_3 \end{Bmatrix}. \quad (19)$$

The convected basis vectors $\{\boldsymbol{\gamma}_\alpha\}$ are generally neither homogeneous over a simply connected body nor tangent to any global material lines. An in-depth analysis of compatibility conditions that would ensure existence of a curvilinear coordinate chart in which such lines are embedded is outside the present scope.

A convected metric tensor with covariant components $\gamma_{\alpha\beta} = \boldsymbol{\gamma}_\alpha \cdot \boldsymbol{\gamma}_\beta$ can be constructed to enable a geometric description of strain. It was stated without proof in a previous work[18] that Christoffel symbols associated with gradients of $\gamma_{\alpha\beta}$ vanish identically in a local convected coordinate system. This assertion is obviously true if $\boldsymbol{F}$ is homogeneous with respect to $\boldsymbol{X}$, since then $\boldsymbol{Q}$ and $\boldsymbol{R}$ must also both be homogeneous as the Gram-Schmidt decomposition is unique. When $\boldsymbol{R}$, and thus any of a, b, c and/or any of α, β, γ are heterogeneous, material gradients of $\gamma_{\alpha\beta}$ are generally nonzero, so connection coefficients constructed from $\{\boldsymbol{\gamma}_\alpha\}$ may not vanish, depending on how these coefficients are defined.

2.4 Velocity Gradient

The mixed-variant velocity gradient in the second of Eq. 6 can be written

$$\nabla \boldsymbol{v} = \dot{\boldsymbol{F}}\boldsymbol{F}^{-1} = \dot{\boldsymbol{Q}}\boldsymbol{Q}^{-1} + \boldsymbol{Q}\dot{\boldsymbol{R}}\boldsymbol{R}^{-1}\boldsymbol{Q}^{-1} = \boldsymbol{\Omega} + \boldsymbol{Q}\boldsymbol{\eta}\boldsymbol{Q}^{-1}, \quad (20)$$

where $\boldsymbol{\Omega}$ is a skew (spin) tensor and the rate contribution from the Laplace stretch is contained in

$$\boldsymbol{\eta} = \dot{\boldsymbol{R}}\boldsymbol{R}^{-1} = \begin{bmatrix} \dot{a}/a & a\dot{\gamma}/b & a(\dot{\beta} - \alpha\dot{\gamma})/c \\ 0 & \dot{b}/b & b\dot{\alpha}/c \\ 0 & 0 & \dot{c}/c \end{bmatrix}. \quad (21)$$

All components in the matrix representation in Eq. 21 are referred to the global basis $\{\boldsymbol{e}_i\}$ of Eq. 8 and Eq. 11. These components follow readily from Eq. 12 and Eq. 17, noting that the product of two upper triangular matrices is also always upper triangular. These components are also notably equal to the components of the

second term in the last of Eq. 20 when referred to the local physical basis $\{\boldsymbol{g}_\alpha\}$:

$$\begin{aligned}\boldsymbol{Q}\dot{\boldsymbol{R}}\boldsymbol{R}^{-1}\boldsymbol{Q}^{-1} &= Q^i_\alpha \dot{R}^\alpha_J (R^{-1})^J_\beta (Q^{-1})^\beta_j \boldsymbol{e}_i \otimes \boldsymbol{e}^j = \dot{R}^\alpha_J (R^{-1})^J_\beta Q^i_\alpha \boldsymbol{e}_i \otimes (Q^{-1})^\beta_j \boldsymbol{e}^j \\ &= \eta^\alpha_\beta \boldsymbol{g}_\alpha \otimes \boldsymbol{g}^\beta.\end{aligned} \tag{22}$$

Rate terms in Eq. 21 are mostly orthogonal in the terminology of Criscione,[21] the exception being η_{13} that contains both $\dot{\beta}$ and $\dot{\gamma}$.

2.5 Strain Attributes

Let a_0, b_0, c_0 and $\alpha_0, \beta_0, \gamma_0$ denote respective values of a, b, c and α, β, γ in an initial reference state corresponding to time instant $t = t_0$. Two different sets of dimensionless scalar strain attributes and their rates are then defined as follows, the first consisting of six attributes e_i, $i = 1, \ldots, 6$:

$$\{e_i\} = \begin{Bmatrix} e_1 \\ e_2 \\ e_3 \\ e_4 \\ e_5 \\ e_6 \end{Bmatrix} = \begin{Bmatrix} \ln(a/a_0) \\ \ln(b/b_0) \\ \ln(c/c_0) \\ \gamma - \gamma_0 \\ \alpha - \alpha_0 \\ \beta - \beta_0 \end{Bmatrix}, \qquad \{\dot{e}_i\} = \begin{Bmatrix} \dot{e}_1 \\ \dot{e}_2 \\ \dot{e}_3 \\ \dot{e}_4 \\ \dot{e}_5 \\ \dot{e}_6 \end{Bmatrix} = \begin{Bmatrix} \dot{a}/a \\ \dot{b}/b \\ \dot{c}/c \\ \dot{\gamma} \\ \dot{\alpha} \\ \dot{\beta} \end{Bmatrix}. \tag{23}$$

The six strain attributes in Eq. 23 are independent with regard to reconstruction of $\boldsymbol{R}$, where e_1, e_2, e_3 quantify logarithmic extensions and e_4, e_5, e_6 quantify simple shears.

The second set consists of seven attributes ϵ_i, $i = 0, \ldots, 6$:

$$\{\epsilon_i\} = \begin{Bmatrix} \epsilon_0 \\ \epsilon_1 \\ \epsilon_2 \\ \epsilon_3 \\ \epsilon_4 \\ \epsilon_5 \\ \epsilon_6 \end{Bmatrix} = \begin{Bmatrix} \ln(abc/a_0b_0c_0) \\ \frac{1}{3}\ln(ab_0/a_0b) \\ \frac{1}{3}\ln(bc_0/b_0c) \\ \frac{1}{3}\ln(ca_0/c_0a) \\ \gamma - \gamma_0 \\ \alpha - \alpha_0 \\ \beta - \beta_0 \end{Bmatrix}, \qquad \{\dot{\epsilon}_i\} = \begin{Bmatrix} \dot{\epsilon}_0 \\ \dot{\epsilon}_1 \\ \dot{\epsilon}_2 \\ \dot{\epsilon}_3 \\ \dot{\epsilon}_4 \\ \dot{\epsilon}_5 \\ \dot{\epsilon}_6 \end{Bmatrix} = \begin{Bmatrix} \dot{a}/a + \dot{b}/b + \dot{c}/c \\ \frac{1}{3}(\dot{a}/a - \dot{b}/b) \\ \frac{1}{3}(\dot{b}/b - \dot{c}/c) \\ \frac{1}{3}(\dot{c}/c - \dot{a}/a) \\ \dot{\gamma} \\ \dot{\alpha} \\ \dot{\beta} \end{Bmatrix}. \tag{24}$$

Only six of the seven strain attributes in Eq. 24 are independent kinematic variables

since

$$\epsilon_1 + \epsilon_2 + \epsilon_3 = 0 \quad \Rightarrow \quad \dot{\epsilon}_1 + \dot{\epsilon}_2 + \dot{\epsilon}_3 = 0. \tag{25}$$

A logarithmic measure of the dilatation occupies position ϵ_0. When $a_0 = b_0 = c_0 = 1$ is chosen as the datum reference state, then $\epsilon_0 = \ln J$ follows from Eq. 13. This choice is used henceforth for convenience, as are the convenient prescriptions $\alpha_0 = \beta_0 = \gamma_0 = 0$, meaning the reference volume element at $t = t_0$ is considered undeformed. Logarithmic squeeze modes occupy $\epsilon_1, \epsilon_2, \epsilon_3$; these are collectively isochoric in the sense that the sum of their rates equals zero, though isolated individual modes do not preserve volume. Simple shears occupy $\epsilon_4, \epsilon_5, \epsilon_6$; these do individually preserve volume since none of α, β, γ affects J. Reasoning behind the definitions in Eq. 23 and Eq. 24 will become clear later in the context of stress power.

2.6 Stresses and Stress Power

Denote by $\boldsymbol{\sigma}$, $\boldsymbol{k}$, $\boldsymbol{s}$, and $\boldsymbol{P}$ the Cauchy stress tensor, Kirchhoff stress tensor, rotated Kirchhoff stress tensor, and first Piola-Kirchhoff stress tensor, respectively. Evaluating all components in the global Cartesian frame $\{\boldsymbol{e}_i\} = \{\boldsymbol{e}_J \delta_i^J\}$, these stress tensors are related by

$$\begin{aligned} \boldsymbol{\sigma} &= J^{-1}\boldsymbol{P}\boldsymbol{F}^{\mathrm{T}} = J^{-1}\boldsymbol{k} = J^{-1}\boldsymbol{Q}\boldsymbol{s}\boldsymbol{Q}^{-1} \quad \leftrightarrow \\ \sigma_j^i &= J^{-1}P_K^i F_j^K = J^{-1}k_j^i = J^{-1}Q_\alpha^i s_\beta^\alpha (Q^{-1})_j^\beta. \end{aligned} \tag{26}$$

The first two stress measures, $\boldsymbol{\sigma}$ and $\boldsymbol{k}$, are always symmetric in covariant and contravariant forms as follows from the usual local angular momentum balance. Symmetry of $s_{\alpha\beta} = JQ_{i\alpha}\sigma^{ij}Q_{j\beta}$ then follows immediately in Cartesian coordinate systems since $Q_{\alpha i}^{-1} = Q_{i\alpha}$.

Components of the rotated stress $\boldsymbol{s}$ are equal to those of the Kirchhoff stress when the latter is referred to the local physical basis $\{\boldsymbol{g}_\alpha\}$:

$$\boldsymbol{k} = k_j^i \boldsymbol{e}_i \otimes \boldsymbol{e}^j = k_j^i (Q^{-1})_i^\alpha \boldsymbol{g}_\alpha \otimes Q_\beta^j \boldsymbol{g}^\beta = s_\beta^\alpha \boldsymbol{g}_\alpha \otimes \boldsymbol{g}^\beta. \tag{27}$$

For this reason, $\boldsymbol{s}$ is also referred to as a physical stress tensor. The Cauchy pressure is

$$p = -\frac{1}{3}\mathrm{tr}\boldsymbol{\sigma} = -\frac{1}{3J}\mathrm{tr}\boldsymbol{k} = -\frac{1}{3J}\mathrm{tr}\boldsymbol{s}. \tag{28}$$

The stress power per unit reference or initial volume is

$$\boldsymbol{P} : \dot{\boldsymbol{F}} = J\boldsymbol{\sigma} : \nabla\boldsymbol{v} = \boldsymbol{k} : \nabla\boldsymbol{v} = \boldsymbol{s} : \boldsymbol{\eta}, \tag{29}$$

with $\boldsymbol{\eta}$ defined in Eq. 21. The final expression relies on the symmetry of $\boldsymbol{k}$ and the anti-symmetry of Ω and is derived in component form as

$$k^i_j \nabla_i v^j = k^i_j \dot{F}^j_K (F^{-1})^K_i = k^i_j Q^j_\alpha \dot{R}^\alpha_K (R^{-1})^K_\beta (Q^{-1})^\beta_i = s^\alpha_\beta \eta^\beta_\alpha. \tag{30}$$

Stress power can also be expressed in terms of rates of strain attributes in Eq. 23 or Eq. 24 and their scalar stress conjugates. For the former six-attribute form in Eq. 23, define the stress conjugates $\{\hat{t}_i\}$, $i = 1, \ldots, 6$ in terms of components of $\boldsymbol{s} = s_{\alpha\beta}\boldsymbol{e}^\alpha \otimes \boldsymbol{e}^\beta$ referred to the global frame $\{\boldsymbol{e}^\alpha = \boldsymbol{e}_\alpha = \boldsymbol{e}_i \delta^i_\alpha\}$ as[19]

$$\{\hat{t}_i\} = \begin{Bmatrix} \hat{t}_1 \\ \hat{t}_2 \\ \hat{t}_3 \\ \hat{t}_4 \\ \hat{t}_5 \\ \hat{t}_6 \end{Bmatrix} = \begin{Bmatrix} s_{11} \\ s_{22} \\ s_{33} \\ (a/b)s_{21} - \alpha(a/c)s_{31} \\ (b/c)s_{32} \\ (a/c)s_{31} \end{Bmatrix}. \tag{31}$$

Normal stresses are $\hat{t}_1, \hat{t}_2, \hat{t}_3$; shearing stresses are $\hat{t}_4, \hat{t}_5, \hat{t}_6$. Note that $s_{21} = s_{12}$, $s_{31} = s_{13}$, and $s_{32} = s_{23}$.

For the seven-attribute form in Eq. 24, define $\{\hat{\tau}_i\}$, $i = 0, \ldots, 6$ in terms of $s_{\alpha\beta}$ as[19]

$$\{\hat{\tau}_i\} = \begin{Bmatrix} \hat{\tau}_0 \\ \hat{\tau}_1 \\ \hat{\tau}_2 \\ \hat{\tau}_3 \\ \hat{\tau}_4 \\ \hat{\tau}_5 \\ \hat{\tau}_6 \end{Bmatrix} = \begin{Bmatrix} \frac{1}{3}(s_{11} + s_{22} + s_{33}) \\ s_{11} - s_{22} \\ s_{22} - s_{33} \\ s_{33} - s_{11} \\ (a/b)s_{21} - \alpha(a/c)s_{31} \\ (b/c)s_{32} \\ (a/c)s_{31} \end{Bmatrix}. \tag{32}$$

Negative pressure per unit reference volume occupies the first entry $\hat{\tau}_0 = -Jp$. Normal stress differences are $\hat{\tau}_1, \hat{\tau}_2, \hat{\tau}_3$. Shear stresses are $\hat{\tau}_4, \hat{\tau}_5, \hat{\tau}_6$. The following

constraint applies, suggesting the deviatoric nature of the normal stress differences:

$$\hat{\tau}_1 + \hat{\tau}_2 + \hat{\tau}_3 = 0. \tag{33}$$

With these definitions at hand, which differ by a factor of J from those in prior work,[19] it can be shown that stress power per unit reference volume obeys

$$\boldsymbol{P} : \dot{\boldsymbol{F}} = \sum_{i=1}^{6} \hat{t}_i \dot{e}_i = \sum_{i=0}^{6} \hat{\tau}_i \dot{\epsilon}_i. \tag{34}$$

The first term in the rightmost sum is the rate of pressure-volume working: $\hat{\tau}_0 \dot{\epsilon}_0 = -p\dot{J}$.

2.7 Conservation Laws and Entropy Production

Denote by ρ and ρ_0 the local spatial and initial mass density of the material. Let $\boldsymbol{b}$ denote body force per unit initial volume. Local conservation laws for mass, linear momentum, and angular momentum are of the usual forms:

$$\dot{\rho} + \rho \nabla \cdot \boldsymbol{v} = 0, \qquad \nabla_0 \cdot \boldsymbol{P} + \boldsymbol{b} = \rho_0 \boldsymbol{a}, \qquad \boldsymbol{P}\boldsymbol{F}^{\mathrm{T}} = \boldsymbol{F}\boldsymbol{P}^{\mathrm{T}}. \tag{35}$$

Thermodynamic potentials are expressed on a per unit initial volume basis. These include the internal energy density U, Helmholtz free energy density Ψ, and entropy density η, related by

$$U = \Psi + T\eta. \tag{36}$$

Absolute temperature is denoted by $T > 0$. Denote the heat flux in the reference configuration by the vector $\boldsymbol{q}$ and a scalar heat source per unit reference volume by r. The local balance of energy is

$$\dot{U} = \boldsymbol{P} : \dot{\boldsymbol{F}} - \nabla_0 \cdot \boldsymbol{q} + r. \tag{37}$$

A local entropy production inequality and an alternative expression that follows from Eq. 36 and Eq. 37 are, respectively,

$$\dot{\eta} \geq \frac{1}{T}\left(r + \frac{\boldsymbol{q} \cdot \nabla_0 T}{T} - \nabla_0 \cdot \boldsymbol{q}\right), \qquad \boldsymbol{P} : \dot{\boldsymbol{F}} - \frac{\boldsymbol{q} \cdot \nabla_0 T}{T} \geq \dot{\Psi} + \dot{T}\eta. \tag{38}$$

Stress power $\boldsymbol{P} : \dot{\boldsymbol{F}}$ in Eq. 37 and the second of Eq. 38 can be written in any of the equivalent forms in Eq. 29 and Eq. 34.

3. Constitutive Assumptions and Thermodynamics

A general thermodynamic formulation invoking explicit hyperelasticity in conjunction with dissipative internal state variables is presented. Strain attributes are used as elastic state variables, while internal state variables will ultimately be invoked to account for viscoelasticity and damage.

3.1 Thermodynamic Potentials

Thermodynamic potentials are assumed to depend on temperature (T) or entropy (η), internal state variables, and strain attributes. The present derivations make use of the strain attributes $\{\epsilon_i\}$ introduced in Eq. 24, noting that a similar theory could be constructed using those in Eq. 23 instead. The present choice is advantageous for modeling problems involving isolated volume changes and pressures since the hydrostatic response is obtained directly. However, orthogonality of terms involving derivatives of the free or internal energy with respect to each of the strain attributes is compromised as a result of the constraint in Eq. 25.

Denote by $\{\chi_i^\alpha\}$ a set of dimensionless, strain-like scalar variables associated with viscoelasticity, where $i = 0, \dots, 6$ and $\alpha = 1, \dots, m$, with m a discrete number of relaxation times. Most generally, each of the $\{\chi_i^\alpha\}$ is regarded as an independent internal state variable. A constraint

$$\chi_1^\alpha + \chi_2^\alpha + \chi_3^\alpha = 0, \tag{39}$$

analogous to Eq. 25, will be imposed in specific examples later to ensure thermodynamic consistency of particular free energy functions. Viscoelasticity may be anisotropic or isotropic.

Denote by $D \in [0, 1]$ an internal state variable linked to damage processes in the solid. Damage, by construction, is limited to isotropy here in the sense that its effects are manifested by a single scalar function. Anisotropic damage, whereby material integrity degrades differently in different material directions, can be addressed via vector- or tensor-valued internal state variables.[37]

Denote the sets of strain attributes and viscoelastic state variables, respectively, by the column vectors

$$\boldsymbol{\epsilon} = [\epsilon_0, \epsilon_1, \epsilon_2, \epsilon_3, \epsilon_4, \epsilon_5, \epsilon_6]^{\mathrm{T}}, \qquad \boldsymbol{\chi}^\alpha = [\chi_0^\alpha, \chi_1^\alpha, \chi_2^\alpha, \chi_3^\alpha, \chi_4^\alpha, \chi_5^\alpha, \chi_6^\alpha]^{\mathrm{T}}. \tag{40}$$

Free and internal energy densities are assigned, respectively, the functional forms

$$\Psi = \Psi(\boldsymbol{\epsilon}, T, \boldsymbol{\chi}^\alpha, D), \qquad U = U(\boldsymbol{\epsilon}, \eta, \boldsymbol{\chi}^\alpha, D). \tag{41}$$

Note that dependence of energy functions on redundant variable ϵ_3 [and ξ_3^α when Eq. 39 is imposed] requires that these variables explicitly enter the energy functions when physically appropriate for the symmetry class of the material. An alternative method, whereby elimination of explicit dependence on redundant variables via use of Eq. 25 is given in prior work[25]; this alternative, which produces equivalent end results, is avoided here to avoid cumbersome algebraic manipulations in forthcoming constitutive equations for stresses. The current presentation addresses materials with homogeneous physical properties in the sense that explicit dependence of the material response on $\boldsymbol{X}$ is omitted in Eq. 41. For example, functionally graded solids are excluded.

3.2 Constitutive Laws

Expansion of the first of Eq. 41 using the chain rule, followed by substitution of the result and Eq. 34 into the second of Eq. 38 gives the following dissipation inequality:

$$\sum_{i=0}^{6} \hat{\tau}_i \dot{\epsilon}_i - \frac{\partial \Psi}{\partial \boldsymbol{\epsilon}} \cdot \dot{\boldsymbol{\epsilon}} - \left(\eta + \frac{\partial \Psi}{\partial \eta} \right) \dot{T} - \sum_{\alpha=1}^{m} \frac{\partial \Psi}{\partial \boldsymbol{\chi}^\alpha} \cdot \dot{\boldsymbol{\chi}}^\alpha - \frac{\partial \Psi}{\partial D} \dot{D} - \frac{\boldsymbol{q} \cdot \nabla_0 T}{T} \geq 0. \tag{42}$$

Stress power can be written, using Eq. 25 and Eq. 33, in terms of components of $\dot{\boldsymbol{\epsilon}}$:

$$\sum_{i=0}^{6} \hat{\tau}_i \dot{\epsilon}_i = \sum_{i=0}^{2} \hat{\tau}_i \dot{\epsilon}_i + (\hat{\tau}_1 + \hat{\tau}_2)(\dot{\epsilon}_1 + \dot{\epsilon}_2) + \sum_{i=4}^{6} \hat{\tau}_i \dot{\epsilon}_i. \tag{43}$$

Extending standard arguments for admissible thermodynamic processes applied to Eq. 42,[38] the following constitutive equations are deduced for stresses [as the first

two terms in Eq. 42 cancel]:

$$\begin{aligned} \hat{\tau}_0 &= \frac{\partial \Psi}{\partial \epsilon_0}, \quad \hat{\tau}_1 = \frac{\partial \Psi}{\partial \epsilon_1}, \quad \hat{\tau}_2 = \frac{\partial \Psi}{\partial \epsilon_2}, \quad \hat{\tau}_3 = \frac{\partial \Psi}{\partial \epsilon_3}, \\ \hat{\tau}_4 &= \frac{\partial \Psi}{\partial \epsilon_4}, \quad \hat{\tau}_5 = \frac{\partial \Psi}{\partial \epsilon_5}, \quad \hat{\tau}_6 = \frac{\partial \Psi}{\partial \epsilon_6}; \end{aligned} \tag{44}$$

and entropy:

$$\eta = -\frac{\partial \Psi}{\partial T}. \tag{45}$$

The first of Eq. 44 corresponds to the more familiar thermodynamic relation

$$p = -J^{-1}\hat{\tau}_0 = -\frac{\partial \Psi}{\partial J}. \tag{46}$$

Constraints Eq. 25 and Eq. 33, which stipulate that not all terms in $\dot{\boldsymbol{\epsilon}}$ can be varied independently, have not been imposed in the derivation of Eq. 44. As such, for Eq. 44 to apply under such constraints, free energy Ψ must be specified consistently with

$$\frac{\partial \Psi}{\partial \epsilon_1} + \frac{\partial \Psi}{\partial \epsilon_2} + \frac{\partial \Psi}{\partial \epsilon_3} = 0. \tag{47}$$

Partial differentiation with respect to ϵ_i is performed with ϵ_j fixed for all $i \neq j$, regardless of Eq. 25.

The seven-element column vector of stress variables conjugate to strain attributes is

$$\hat{\boldsymbol{\tau}} = [\hat{\tau}_0, \hat{\tau}_1, \hat{\tau}_2, \hat{\tau}_3, \hat{\tau}_4, \hat{\tau}_5, \hat{\tau}_6]^{\mathrm{T}}. \tag{48}$$

Concisely, this is related to strain derivatives of free energy according to

$$\hat{\boldsymbol{\tau}} = \partial_{\boldsymbol{\epsilon}} \Psi = \frac{\partial \Psi}{\partial \boldsymbol{\epsilon}}. \tag{49}$$

With the seven stress components of Eq. 44 at hand, the physical stress tensor can be reconstructed from the inverse of Eq. 32:

$$\begin{aligned} s_{11} &= \hat{\tau}_0 + \frac{1}{3}(\hat{\tau}_1 - \hat{\tau}_3), \quad s_{22} = \hat{\tau}_0 + \frac{1}{3}(\hat{\tau}_2 - \hat{\tau}_1), \quad s_{33} = \hat{\tau}_0 + \frac{1}{3}(\hat{\tau}_3 - \hat{\tau}_2), \\ s_{12} &= s_{21} = \frac{b}{a}(\hat{\tau}_4 + \alpha\hat{\tau}_6), \quad s_{23} = s_{32} = \frac{c}{b}\hat{\tau}_5, \quad s_{13} = s_{31} = \frac{c}{a}\hat{\tau}_6. \end{aligned} \tag{50}$$

Other stress tensors can be obtained from $\boldsymbol{s}$ using Eq. 26.

From Eq. 41 and letting $T = T(\boldsymbol{\epsilon}, \eta, \boldsymbol{\chi}^\alpha, D)$,

$$\frac{\partial U}{\partial \boldsymbol{\epsilon}} = \frac{\partial \Psi}{\partial \boldsymbol{\epsilon}} + \frac{\partial \Psi}{\partial T}\frac{\partial T}{\partial \boldsymbol{\epsilon}} + \eta\frac{\partial T}{\partial \boldsymbol{\epsilon}}, \qquad \frac{\partial U}{\partial \eta} = \frac{\partial \Psi}{\partial T}\frac{\partial T}{\partial \eta} + \eta\frac{\partial T}{\partial \eta} + T. \tag{51}$$

Then, from Eq. 44 and Eq. 45, thermoelastic relations in terms of derivatives of internal energy are the independent stress variables

$$\begin{aligned} \hat{\tau}_0 &= \frac{\partial U}{\partial \epsilon_0}, \quad \hat{\tau}_1 = \frac{\partial U}{\partial \epsilon_1}, \quad \hat{\tau}_2 = \frac{\partial U}{\partial \epsilon_2}, \quad \hat{\tau}_3 = \frac{\partial U}{\partial \epsilon_3}, \\ \hat{\tau}_4 &= \frac{\partial U}{\partial \epsilon_4}, \quad \hat{\tau}_5 = \frac{\partial U}{\partial \epsilon_5}, \quad \hat{\tau}_6 = \frac{\partial U}{\partial \epsilon_6}; \end{aligned} \tag{52}$$

which in condensed notation corresponds to $\hat{\boldsymbol{\tau}} = \partial_{\boldsymbol{\epsilon}} U$, and the absolute temperature:

$$T = \frac{\partial U}{\partial \eta}. \tag{53}$$

Constraints analogous to Eq. 47 are imposed on the internal energy function U:

$$\frac{\partial U}{\partial \epsilon_1} + \frac{\partial U}{\partial \epsilon_2} + \frac{\partial U}{\partial \epsilon_3} = 0. \tag{54}$$

Many soft solids are so much stiffer in spherical tension or compression than in shear that they can be idealized as incompressible. In that case, $\epsilon_0 = 0$ identically, and ϵ_0 is removed as a state variable from the thermodynamic potentials. Pressure p does no mechanical work and is obtained from the incompressibility constraint and boundary conditions for a given problem. The first equality in each of Eq. 44 and Eq. 52 does not apply for incompressible materials, but the stress conjugates to the volume-preserving strain attributes ($\hat{\tau}_i$, $i > 0$) are obtained by the same constitutive equations listed in the remainder of these sets of equations. Particular models invoking the incompressibility assumption are not addressed further herein; finite compressibility, though perhaps very small, is presumed.

The residual dissipation inequality is what remains of Eq. 42:

$$-\sum_{\alpha=1}^{m} \frac{\partial \Psi}{\partial \boldsymbol{\chi}^\alpha} \cdot \dot{\boldsymbol{\chi}}^\alpha - \frac{\partial \Psi}{\partial D}\dot{D} - \frac{\boldsymbol{q} \cdot \nabla_0 T}{T} \geq 0. \tag{55}$$

3.3 Thermoelasticity and Dissipation

Let $c(\boldsymbol{\epsilon}, T, \boldsymbol{\chi}^\alpha, D)$ denote specific heat per unit reference volume at constant deformation, where from Eq. 45 and Eq. 53,

$$c = \frac{\partial U}{\partial T} = T\frac{\partial \eta}{\partial T} = -T\frac{\partial^2 \Psi}{\partial T^2}. \tag{56}$$

The rate of internal energy can be expanded as

$$\begin{aligned}
\dot{U} &= \dot{\Psi} + \eta\dot{T} + T\dot{\eta} \\
&= (\partial\Psi/\partial\boldsymbol{\epsilon}) : \dot{\boldsymbol{\epsilon}} + \sum_{\alpha=1}^{m}(\partial\Psi/\partial\boldsymbol{\chi}^\alpha)\cdot\dot{\boldsymbol{\chi}}^\alpha + (\partial\Psi/\partial D)\dot{D} + (\partial\Psi/\partial\eta)\dot{\eta} \\
&= \sum_{i=0}^{6}\hat{\tau}_i\dot{\epsilon}_i + T[(\partial\eta/\partial\boldsymbol{\epsilon}) : \dot{\boldsymbol{\epsilon}} + (\partial\eta/\partial T)\dot{T} + \sum_{\alpha=1}^{m}(\partial\eta/\partial\boldsymbol{\chi}^\alpha)\cdot\dot{\boldsymbol{\chi}}^\alpha + (\partial\eta/\partial D)\dot{D}] \\
&\qquad + \sum_{\alpha=1}^{m}(\partial\Psi/\partial\boldsymbol{\chi}^\alpha)\cdot\dot{\boldsymbol{\chi}}^\alpha + (\partial\Psi/\partial D)\dot{D}.
\end{aligned} \tag{57}$$

Substituting Eq. 34, Eq. 56, and Eq. 57 into Eq. 37 leads to the following temperature evolution equation:

$$\begin{aligned}
c\dot{T} = &-\sum_{\alpha=1}^{m}(\partial\Psi/\partial\boldsymbol{\chi}^\alpha)\cdot\dot{\boldsymbol{\chi}}^\alpha - (\partial\Psi/\partial D)\dot{D} - \nabla_0\cdot\boldsymbol{q} + r \\
&+ T\left[(\partial^2\Psi/\partial\boldsymbol{\epsilon}\partial T) : \dot{\boldsymbol{\epsilon}} + \sum_{\alpha=1}^{m}(\partial^2\Psi/\partial T\partial\boldsymbol{\chi}^\alpha)\cdot\dot{\boldsymbol{\chi}}^\alpha + (\partial^2\Psi/\partial T\partial D)\dot{D}\right].
\end{aligned} \tag{58}$$

Thermal stress coefficients $\boldsymbol{\kappa}$ and Grüneisen coefficients $\boldsymbol{g}$ are defined as

$$\boldsymbol{\kappa} = -\frac{\partial^2\Psi}{\partial\boldsymbol{\epsilon}\partial T} = c\boldsymbol{g}. \tag{59}$$

Isothermal and isentropic, respectively, second-order thermodynamic elastic coefficients (not necessarily constants) are

$$\mathbf{C}^T = \frac{\partial^2\Psi}{\partial\boldsymbol{\epsilon}\partial\boldsymbol{\epsilon}}, \qquad \mathbf{C}^\eta = \frac{\partial^2 U}{\partial\boldsymbol{\epsilon}\partial\boldsymbol{\epsilon}}. \tag{60}$$

Denote thermal expansion coefficients by $\boldsymbol{A} = \partial\boldsymbol{\epsilon}/\partial T$, with partial differentiation taken at constant stress and constant internal state. Denote specific heat at constant stress by c^s. Then relationships among thermoelastic coefficients can be derived by use of Maxwell-type equalities, following procedures derived elsewhere,[15] for example:

$$\boldsymbol{\kappa} = \boldsymbol{A} : \mathbf{C}^T, \qquad c^S - c = T\boldsymbol{A} : \boldsymbol{\kappa}, \qquad \mathbf{C}^\eta = \mathbf{C}^T + \frac{T}{c}\boldsymbol{\kappa} \otimes \boldsymbol{\kappa}. \tag{61}$$

Define conjugate thermodynamic forces to internal state variables as the negative derivatives

$$\boldsymbol{\zeta}^\alpha = -\frac{\partial \Psi}{\partial \boldsymbol{\chi}^\alpha}, \qquad F = -\frac{\partial \Psi}{\partial D}. \tag{62}$$

Substitution of Eq. 59 and Eq. 62 into Eq. 58 gives the energy balance in a more compact form:

$$c\dot{T} = -T\boldsymbol{\kappa} : \dot{\boldsymbol{\epsilon}} + \sum_{\alpha=1}^{m} [\boldsymbol{\zeta}^\alpha - T(\partial \boldsymbol{\zeta}^\alpha/\partial T)] \cdot \dot{\boldsymbol{\chi}}^\alpha + [F - T(\partial F/\partial T)]\dot{D} - \nabla_0 \cdot \boldsymbol{q} + r. \tag{63}$$

Any thermodynamically admissible standard model for heat conduction (e.g., Fourier conduction such that $-\boldsymbol{q} \cdot \nabla_0 T \geq 0$) is consistent with the present framework, so $\boldsymbol{q}$ will not be addressed further. The corresponding internal dissipation inequality and entropy production rate are then

$$\mathfrak{D} = \sum_{\alpha=1}^{m} \boldsymbol{\zeta}^\alpha \cdot \dot{\boldsymbol{\chi}}^\alpha + F\dot{D} \geq 0, \qquad T\dot{\eta} = \mathfrak{D} - \nabla_0 \cdot \boldsymbol{q} + r. \tag{64}$$

A complete constitutive model requires further specification of either of the two energy potential functions Ψ or U in Eq. 41. Also required are kinetic equations for the rate of damage variable, $\dot{D}$, and rates of viscoelastic internal state variables, $\{\dot{\boldsymbol{\chi}}^\alpha\}$, consistent with positive internal dissipation $\mathfrak{D}$ in Eq. 64. Thermoelasticity, viscoelasticity, and damage mechanics are considered in more detail via representative examples in subsequent sections.

4. Hyperelasticity

A fully hyperelastic model, in the absence of internal dissipation ($\mathfrak{D} = 0$), is enabled by the theory of Section 3 with internal state variables suppressed. Thermal and entropic effects are maintained. Free and internal energy densities of Eq. 41 reduce to the following functional forms for homogeneous continua:

$$\Psi = \Psi_0^\infty(\boldsymbol{\epsilon}, T), \qquad U = U_0^\infty(\boldsymbol{\epsilon}, \eta). \tag{65}$$

Superscript $(\cdot)^\infty$ is used to denote the equilibrium (i.e., infinite time) energy in the sense of viscoelasticity, and subscript $(\cdot)_0$ is used to denote the energy of the undamaged state. In the absence of dissipation (i.e., viscous effects and damage), the equilibrium and instantaneous responses are identical.

4.1 Symmetry Considerations

Formal arguments require that

$$\Psi_0^\infty[\boldsymbol{\epsilon}(\boldsymbol{F}), T] = \Psi_0^\infty[\boldsymbol{\epsilon}(\boldsymbol{FH}), T], \qquad U_0^\infty[\boldsymbol{\epsilon}(\boldsymbol{F}), \eta] = U_0^\infty[\boldsymbol{\epsilon}(\boldsymbol{FH}), \eta], \tag{66}$$

where $\boldsymbol{H}$ is any transformation of the material's reference configuration that leaves the free and internal energies invariant. The scalar invariants of the symmetric tensor $\boldsymbol{C}$ that enter energy potentials for standard material symmetry groups are well known in nonlinear elasticity based on Lagrangian strain measures.[39] In principle, invariants written as functions of six components of C_{IJ} could be expressed in terms of six nonzero components of R_{IJ}, which in turn could be expressed in terms of the deformation attributes $(a, b, c, \alpha, \beta, \gamma)$ and finally in terms of the strain attributes $\{\epsilon_i\}$. The end result, however, is exceedingly cumbersome, providing little insight into how particular potential energy functions with associated thermoelastic constants should be constructed.

A less formal and more intuitive approach is advocated by Srinivasa,[23] whereby geometric rather than group-theoretic arguments are invoked to deduce restrictions on strain energy potentials depending on R_{IJ} for solids of monoclinic, orthotropic, and transversely isotropic symmetries. This methodology is invoked here for materials with cubic and isotropic symmetries, in an approximate sense.

First consider a solid with cubic symmetry whose three cube axes align with the global Cartesian basis vectors $\{\boldsymbol{e}_I\}$. Diagonals connecting opposite corners of the cube comprise four axes of three-fold symmetry, and each cube axis is one of at least two-fold symmetry. The following geometric restrictions are imposed on strain energy potentials W depending on $(a, b, c, \alpha, \beta, \gamma)$ or $\{\epsilon_i\}$:

1. $W(a, b, c, \alpha, \beta, \gamma)$ should remain unchanged for any interchange or permutation of the elements in set (a, b, c): $W(a, b, c, \alpha, \beta, \gamma) = W(b, a, c, \alpha, \beta, \gamma)$ since any of the cube axes can be aligned arbitrarily with any of the global basis vectors;

2. $W(a, b, c, \alpha, \beta, \gamma)$ should remain unchanged for any interchange or permutation of elements in the set (α, β, γ): $W(a, b, c, \alpha, \beta, \gamma) = W(a, b, c, \beta, \alpha, \gamma)$ for the same reason;

3. $W(a, b, c, \alpha, \beta, \gamma)$ should remain unchanged for isolated changes of sign of elements in the set (α, β, γ), $W(a, b, c, \alpha, 0, 0) = W(a, b, c, -\alpha, 0, 0)$ since a reversal of the direction of simple shearing on any plane normal to a cube axes should not change the energy;

4. $W(\{\epsilon_i\})$ should remain unchanged for any change of sign of any of the squeeze modes $\epsilon_1, \epsilon_2, \epsilon_3$ since these represent stretch differences normal to the three cube axes;

5. $\Psi(\{\epsilon_i\}, T)$ or $U(\{\epsilon_i\}, \eta)$ should demonstrate isotropic thermoelastic coupling to first order, meaning thermal expansion should be spherical, a known result for cubic solids.[15]

The above restrictions are intuitively realistic but may or may not be necessary or sufficient for an energy potential to yield cubic symmetry in the formal sense of group theory. Potentials obeying restrictions 1 through 5 may not necessarily satisfy Eq. 66 for all $\boldsymbol{H}$ in the symmetry group for cubic symmetry.

Candidate energy potentials that obey this list of restrictions can be constructed readily from the following three scalar functions $\{\xi_j\}$, $j = 0, 1, 2$ of the seven

strain attributes $\{\epsilon_i\}$, $i = 0, \ldots, 6$:

$$\begin{aligned} \xi_0 &= \epsilon_0 = \ln J, \\ \xi_1 &= (\epsilon_1)^2 + (\epsilon_2)^2 + (\epsilon_3)^2, \\ \xi_2 &= (\epsilon_4)^2 + (\epsilon_5)^2 + (\epsilon_6)^2 = \alpha^2 + \beta^2 + \gamma^2. \end{aligned} \tag{67}$$

These functions are sufficient but are neither unique nor necessary to ensure cubic symmetry in the sense defined above: energy may depend on other combinations of strain attributes and still obey restrictions 1 through 5. A useful property of $W(\xi_0, \xi_1, \xi_2)$ is that the strain energy analog of Eq. 47 is identically satisfied via Eq. 25:

$$\begin{aligned} \frac{\partial W(\xi_0,\xi_1,\xi_2)}{\partial \epsilon_1} + \frac{\partial W(\xi_0,\xi_1,\xi_2)}{\partial \epsilon_2} + \frac{\partial W(\xi_0,\xi_1,\xi_2)}{\partial \epsilon_3} & \\ = \frac{\partial W(\xi_0,\xi_1,\xi_2)}{\partial \xi_1}\left[\frac{\partial \xi_1}{\partial \epsilon_1} + \frac{\partial \xi_1}{\partial \epsilon_2} + \frac{\partial \xi_1}{\partial \epsilon_3}\right] & \\ = \frac{\partial W(\xi_0,\xi_1,\xi_2)}{\partial \xi_1}\left[2(\epsilon_1 + \epsilon_2 + \epsilon_3)\right] & \\ = 0. & \end{aligned} \tag{68}$$

Identical relations would hold for $\Psi_0^\infty(\{\xi_j\}, T)$ or $U_0^\infty(\{\xi_j\}, \eta)$. Notable examples of free energy functions $\Psi_0^\infty(\{\xi_j\}, T)$ are considered in what follows next.

4.2 Quasi-Linear Cubic Solid

The current geometrically nonlinear model is said to approach linearity in the sense that scalar stress measures $\hat{\tau}_i$ and scalar strain attributes ϵ_i are linearly related through a set of (three) elastic constants, and the thermal stress coefficient is a constant. This is a three-mode solid in the terminology of Freed.[19] Let T_0 denote a reference temperature at which free energy vanishes, and let $\Delta T = T - T_0$. All material coefficients are constants measured at the reference state conditions $\boldsymbol{\epsilon} = \mathbf{0}$ and $T = T_0$. The free energy function is

$$\Psi_0^\infty(\{\xi_j\}, T) = \frac{1}{2} B_0^T (\xi_0)^2 + 3\mu_0 \xi_1 + \frac{1}{2} G_0 \xi_2 - \kappa_0 \xi_0 \Delta T - c_0 T \ln(T/T_0). \tag{69}$$

The isothermal bulk modulus at the reference state is B_0^T. The shear modulus at the reference state associated with squeeze modes is μ_0, and the shear modulus at

the reference state associated with simple shearing modes is G_0. The lone nonzero thermal stress coefficient in $\boldsymbol{\kappa}$ of Eq. 59 is

$$\kappa_0 = A_0 B_0^T = c_0 g_0, \tag{70}$$

where A_0 is the volumetric thermal expansion coefficient and g_0 is the Grüneisen parameter. A constant specific heat at fixed volume, $c = c_0$, is used. It follows from the last of Eq. 61 that all elastic coefficients except the bulk modulus are identical in isothermal or isentropic form. The isentropic bulk modulus obeys $B_0^\eta = B_0^T(1 + A_0 g_0 T_0)$.[15]

Conjugate stresses $\{\hat{\tau}_i\}$ are obtained via use of Eq. 44:

$$\begin{aligned} \hat{\tau}_0 &= B_0^T(\epsilon_0 - A_0 \Delta T), \\ \hat{\tau}_i &= 6\mu_0 \epsilon_i, \qquad\qquad (i = 1, 2, 3), \\ \hat{\tau}_i &= G_0 \epsilon_i, \qquad\qquad (i = 4, 5, 6). \end{aligned} \tag{71}$$

Pressure and rotated Kirchhoff stress components then follow, the latter from Eq. 50:

$$\begin{aligned} p &= -\frac{B_0^T}{J} \ln J + \frac{A_0}{J} \Delta T, \qquad (J = abc); \\ s_{11} &= -Jp + \frac{2}{3}\mu_0[\ln(a/b) + \ln(a/c)], \\ s_{22} &= -Jp + \frac{2}{3}\mu_0[\ln(b/a) + \ln(b/c)], \\ s_{33} &= -Jp + \frac{2}{3}\mu_0[\ln(c/b) + \ln(c/a)]; \\ s_{12} &= s_{21} = G_0 \frac{b}{a}\alpha(1 + \gamma), \quad s_{23} = s_{32} = G_0 \frac{c}{b}\beta, \quad s_{13} = s_{31} = G_0 \frac{c}{a}\gamma. \end{aligned} \tag{72}$$

In the limit of small deformations with $\boldsymbol{Q} \to \mathbf{1}$ in the QR decomposition, $\boldsymbol{\sigma} = \boldsymbol{k}/J \approx \boldsymbol{k} \to \boldsymbol{s}$, ϵ_0 approaches the trace of the small strain tensor, each of $\epsilon_1, \epsilon_2, \epsilon_3$ approaches a difference between two diagonal components of the small strain tensor, and each of $\epsilon_4, \epsilon_5, \epsilon_6$ approaches twice the value of an off-diagonal component of the small strain tensor. In this limit, if C_{11}, C_{12}, and C_{44} are the (isothermal) cubic elastic constants of usual Lagrangian elasticity,[15] then consistency with the present model is achieved by the correspondences

$$B_0^T = \frac{1}{3}(\mathsf{C}_{11} + 2\mathsf{C}_{12}), \qquad \mu_0 = \frac{1}{2}(\mathsf{C}_{11} - \mathsf{C}_{12}), \qquad G_0 = \mathsf{C}_{44}. \tag{73}$$

The present theory diverges from linear anisotropic thermoelasticity for large deformations since logarithmic strain attributes comprise the volumetric and squeeze entries of $\{\epsilon_i\}$, J may differ significantly from unity, and nonlinear factors enter the shear components of $s_{\alpha\beta}$ as is evident from Eq. 72.

An inherent advantage of this model is its reliance on only the usual thermoelastic constants B_0^T, μ_0, and G_0 that can be deduced immediately from the material's mechanical response under the decoupled respective loading protocols of volume change, pure shear, and simple shear according to Eq. 71. The coefficient of thermal expansion A_0 and specific heat at constant volume c_0 can also be obtained using standard methods since these constants obey their classical definitions.[15]

4.3 Cubic Solid with Equation-of-State and Pressure-Shear Coupling

The pressure-volume relation in Eq. 71 and Eq. 72 may be insufficient to account for nonlinear behavior at large deformations. For example, most solids decrease dramatically in compressibility as their specific volume shrinks towards zero. Denote the isothermal tangent bulk modulus by B^T and its pressure derivative under isothermal hydrostatic loading by B'^T. Let zero subscripts $(\cdot)|_0$ correspond to the reference state wherein $T = T_0$ and $\boldsymbol{\epsilon} = \mathbf{0}$. Then

$$B_0'^T = \left[\frac{\mathrm{d}}{\mathrm{d}p}B^T\right]\Big|_0 = \left[\frac{\mathrm{d}}{\mathrm{d}p}\left(-J\frac{\partial p}{\partial J}\right)\right]\Big|_{T=T_0,\boldsymbol{\epsilon}=\mathbf{0}} = \left[\frac{\mathrm{d}}{\mathrm{d}p}\left(\frac{\partial}{\partial \ln J}\frac{\partial \Psi}{\partial J}\right)\right]\Big|_{T=T_0,\boldsymbol{\epsilon}=\mathbf{0}}. \tag{74}$$

Furthermore, many solids demonstrate a change in tangent shear modulus under hydrostatic compression or tension.[40] Denote tangent shear moduli under squeeze and simple shear by μ and G, respectively. Their isothermal pressure derivatives are defined as

$$\mu_0' = \left[\frac{\mathrm{d}}{\mathrm{d}p}\mu\right]\Big|_0 = \left[\frac{\mathrm{d}}{\mathrm{d}p}\left(\frac{1}{6}\frac{\partial^2 \Psi}{\partial \epsilon_i^2}\right)\right]\Big|_{T=T_0,\boldsymbol{\epsilon}=\mathbf{0}}, \qquad (i = 1, 2, 3); \tag{75}$$

$$G_0' = \left[\frac{\mathrm{d}}{\mathrm{d}p}G\right]\Big|_0 = \left[\frac{\mathrm{d}}{\mathrm{d}p}\left(\frac{\partial^2 \Psi}{\partial \epsilon_i^2}\right)\right]\Big|_{T=T_0,\boldsymbol{\epsilon}=\mathbf{0}}, \qquad (i = 4, 5, 6). \tag{76}$$

Note that μ and G defined in this manner are tangent moduli with respect to corresponding strain attributes and do not necessarily correspond to wave propagation coefficients referred to Lagrangian or Eulerian coordinates. The quasi-linear model of Eq. 69 corresponds to a fixed value of $B_0'^T = 2$ verified by differentiation, and,

since pressure and shears are completely decoupled in Eq. 71, $\mu_0' = G_0' = 0$.

The nonlinear model forwarded in the present subsection includes a logarithmic equation-of-state[41,42] for the isothermal pressure-volume response and pressures-shear coupling to account for nonzero values of μ_0' and G_0':

$$\begin{aligned}\Psi_0^\infty(\{\xi_j\}, T) =& \frac{1}{2}B_0^T(\xi_0)^2\left[1 - \frac{1}{3}(B_0'^T - 2)\xi_0\right] - \kappa_0\xi_0\Delta T - c_0 T\ln(T/T_0) \\ &+ 3\mu_0\xi_1\left[1 - \frac{B_0^T}{\mu_0}\mu_0'\xi_0\right] + \frac{1}{2}G_0\xi_2\left[1 - \frac{B_0^T}{G_0}G_0'\xi_0\right].\end{aligned} \tag{77}$$

Constant thermal stress and specific heat coefficients are retained, and quantities in square braces reduce to unity for the quasi-linear model of Eq. 69.

Conjugate stresses $\{\hat{\tau}_i\}$ are again determined with Eq. 44:

$$\begin{aligned}\hat{\tau}_0 &= -Jp = B_0^T\epsilon_0\left[1 - \frac{1}{2}(B_0'^T - 2)\epsilon_0\right] - 3B_0^T\mu_0'\xi_1 - \frac{1}{2}B_0^T G_0'\xi_2 - B_0^T A_0\Delta T, \\ \hat{\tau}_i &= 6\mu_0\left[1 - \frac{B_0^T}{\mu_0}\mu_0'\xi_0\right]\epsilon_i, \qquad (i = 1, 2, 3), \\ \hat{\tau}_i &= G_0\left[1 - \frac{B_0^T}{G_0}G_0'\xi_0\right]\epsilon_i, \qquad (i = 4, 5, 6).\end{aligned} \tag{78}$$

Under spherical deformation, $\epsilon_i = 0$ for $i > 0$, so $\xi_1 = \xi_2 = 0$ and $\hat{\tau}_i = 0$ for $i > 0$. Thus, only pressure from the logarithmic equation-of-state and thermal stress arise for purely volumetric loading, and vice-versa: hydrostatic compression/tension corresponds to spherical deformation. However, under imposed shear deformations, volumetric compression ($\xi_0 = \epsilon_0 = \ln J < 0$) will amplify shear stresses $\hat{\tau}_i$ ($i > 0$) for positive values of μ_0' and G_0'. Since ξ_1 and ξ_2 are always non-negative, shear strains will induce a positive Cauchy pressure p under isochoric motions for positive μ_0' and G_0'.

The tangent isothermal bulk modulus corresponding to Eq. 77 is

$$B^T = -\left(J\frac{\partial p}{\partial J}\right)\bigg|_{T=T_0} = \frac{B_0}{J}\left[1 - \ln J\{1 + (B_0'^T - 2)\} + \frac{1}{2}(\ln J)^2(B_0'^T - 2)\right]. \tag{79}$$

An internal energy consistent with Eq. 77 is, with $\Delta\eta = \eta - \eta_0$ the entropy change

from the reference state,

$$U_0^\infty(\{\xi_j\},\eta) = \frac{1}{2}B_0^\eta(\xi_0)^2\left[1-\frac{1}{3}(B_0'^\eta-2)\xi_0\right]+T_0\Delta\eta[1-g_0\xi_0+(\Delta\eta)/(2c_0)] \\ +3\mu_0\xi_1\left[1-\frac{B_0^\eta}{\mu_0}\mu_0'\xi_0\right]+\frac{1}{2}G_0\xi_2\left[1-\frac{B_0^\eta}{G_0}G_0'\xi_0\right]. \tag{80}$$

Stresses can be obtained from internal energy using Eq. 52. Temperature is then, from Eq. 53,

$$T=\partial U_0^\infty/\partial T = T_0[1-g_0\ln J+\Delta\eta/c_0]. \tag{81}$$

This model requires only the nonlinear elastic parameters $B_0'^T$, μ_0', and G_0' above the base parameters of the model of Section 4.2. These are physically measured by monitoring changes in bulk, squeeze, and simple shear moduli as the pressure in the material is varied.

4.4 Pseudo-Isotropic Solids

Isotropy corresponds to permitting $\boldsymbol{H}$ in Eq. 66 to be any rotation, meaning $\boldsymbol{H}$ is any member of the 3-D orthogonal group with positive determinant [SO(3)]. The model advanced next, though not proven isotropic in such a group sense, is labeled pseudo-isotropic in that its linearization is consistent with linear isotropic elasticity theory.

Careful examination of the theory of Section 4.2 (e.g., Eq. 73) demonstrates that isotropic linear elasticity is recovered in the limit of small deformations when $G_0=\mu_0$. Accordingly a set of only two scalar functions $\{\Xi_j\}$, $j=0,1$, of the strain attributes is proposed:

$$\begin{aligned}\Xi_0&=\xi_0=\epsilon_0=\ln J,\\ \Xi_1&=6\xi_1+\xi_2=6[(\epsilon_1)^2+(\epsilon_2)^2+(\epsilon_3)^2]+\alpha^2+\beta^2+\gamma^2.\end{aligned} \tag{82}$$

Strain energy dependence on this set of variables is not claimed to be sufficient for isotropy in the formal sense of Eq. 66. The list of only two scalar variables in Eq. 82 is clearly incomplete because isotropic solids depend on three scalar invariants of $\boldsymbol{C}$. Since the material contains no intrinsic preferred directions (unlike the cubic solid), the global coordinate basis $\{\boldsymbol{e}_I\}$ is now chosen arbitrarily.

The quasi-linear, pseudo-isotropic free energy function is

$$\Psi_0^\infty(\{\Xi_j\},T) = \frac{1}{2}B_0^T(\Xi_0)^2 + \frac{1}{2}G_0\Xi_1 - \kappa_0\Xi_0\Delta T - c_0 T\ln(T/T_0). \tag{83}$$

The pressure-volume response is unchanged from the cubic model of Section 4.2, and the deviatoric response is identical to that of Eq. 72 with the substitution $\mu_0 = G_0$. Only the standard, physically measurable, isotropic linear thermoelastic constants enter this model.

Extending this idea to the nonlinear regime, a pseudo-isotropic free energy function can be constructed from the model of Section 4.3 by setting $\mu_0 = G_0$ and $\mu_0' = G_0'$:

$$\begin{aligned}\Psi_0^\infty(\{\Xi_j\},T) =& \frac{1}{2}B_0^T(\Xi_0)^2\left[1-\frac{1}{3}(B_0'^T-2)\Xi_0\right] + \frac{1}{2}G_0\Xi_1\left[1-\frac{B_0^T}{G_0}G_0'\Xi_0\right] \\ &- \kappa_0\Xi_0\Delta T - c_0 T\ln\left(\frac{T}{T_0}\right),\end{aligned} \tag{84}$$

$$\begin{aligned}U_0^\infty(\{\Xi_j\},\eta) =& \frac{1}{2}B_0^\eta(\Xi_0)^2\left[1-\frac{1}{3}(B_0'^\eta-2)\Xi_0\right] + \frac{1}{2}G_0\Xi_1\left[1-\frac{B_0^\eta}{G_0}G_0'\Xi_0\right] \\ &+ T_0\Delta\eta\left[1-g_0\Xi_0+\frac{\Delta\eta}{2c_0}\right].\end{aligned} \tag{85}$$

Stresses, entropy, and temperature follow readily from differentiation that is omitted here. Only the standard linear thermoelastic constants plus the measurable nonlinear constants $B_0'^T$ and G_0' enter this model.

A final example proposes a nonlinear pseudo-isotropic model with exponential stress-strain response. Such descriptions are widely used for biological tissues.[2,43,44] The following free and internal energy functions are proposed that combine distinct exponential pressure and shear responses with potential pressure-shear stiffness coupling:

$$\begin{aligned}\Psi_0^\infty(\{\Xi_j\},T) =& \frac{1}{2}\frac{B_0^T}{c_1}\{\exp[c_1(\Xi_0)^2]-1\} + \frac{1}{2}\frac{G_0}{c_2}\{\exp[c_2\Xi_1]-1\}\left[1-\frac{B_0^T}{G_0}G_0'\Xi_0\right] \\ &- \kappa_0\Xi_0\Delta T - c_0 T\ln\left(\frac{T}{T_0}\right),\end{aligned} \tag{86}$$

$$U_0^\infty(\{\Xi_j\},\eta) = \frac{1}{2}\frac{B_0^\eta}{c_1}\{\exp[c_1(\Xi_0)^2]-1\} + \frac{1}{2}\frac{G_0}{c_2}\{\exp[c_2\Xi_1]-1\}\left[1-\frac{B_0^\eta}{G_0}G_0'\Xi_0\right] + T_0\Delta\eta\left[1-g_0\Xi_0+\frac{\Delta\eta}{2c_0}\right]. \tag{87}$$

All parameters that have been introduced already in prior models (e.g., referential bulk and shear moduli) have identical physical and mathematical meanings and are readily measurable. This model has a fixed initial pressure derivative of the bulk moduli $B_0'^T = B_0'^\eta = 2$. Parameters c_1 and c_2 control the exponential scaling; these should be non-negative for strain energy to be positive in compression. These parameters can be calibrated to the very large strain response of the material under hydrostatic and shear loading, respectively. The quasi-linear theory of Eq. 83 is recovered in the limit $c_1, c_2 \to 0$ and $G_0' = 0$.

Conjugate thermodynamic stresses are

$$\begin{aligned}
\hat{\tau}_0 &= -Jp = B_0^T\epsilon_0\exp[c_1(\epsilon_0)^2] - \frac{1}{2}B_0^T G_0'\Xi_1 - B_0^T A_0\Delta T, \\
\hat{\tau}_i &= 6G_0\epsilon_i\left[1-\frac{B_0^T}{G_0}G_0'\epsilon_0\right]\exp[c_2(\Xi_1)], \qquad (i=1,2,3), \\
\hat{\tau}_i &= G_0\epsilon_i\left[1-\frac{B_0^T}{G_0}G_0'\epsilon_0\right]\exp[c_2(\Xi_1)], \qquad (i=4,5,6).
\end{aligned} \tag{88}$$

The absolute temperature T can be obtained from differentiation of Eq. 87 with respect to η, producing a result identical to Eq. 81.

The tangent isothermal bulk modulus corresponding to Eq. 86 is

$$B^T = -\left(J\frac{\partial p}{\partial J}\right)\Big|_{T=T_0} = \frac{B_0^T}{J}\left[1+\ln J(2c_1\ln J-1)\right]\exp\{c_1(\ln J)^2\}. \tag{89}$$

Compared in Fig. 2 are normalized Cauchy pressure p and tangent isothermal bulk modulus B^T for the logarithmic equation-of-state inherent in Eq. 84 and the exponential equation-of-state inherent in Eq. 86. Deformation is spherical (i.e., $\boldsymbol{F} = J^{1/3}\mathbf{1}$) and isothermal at $T = T_0$. Different choices of nonlinear elasticity parameters $B_0'^T$ and c_1 are evaluated, where $B_0'^T = 2$ corresponds to the quasi-linear theory of Eq. 83. All results in Fig. 2a demonstrate increasing pressure with a reduction in volume, and with the exception of the logarithmic model with $B_0'^T = 0$, a bulk

modulus that increases steadily under compression in Fig. 2b.

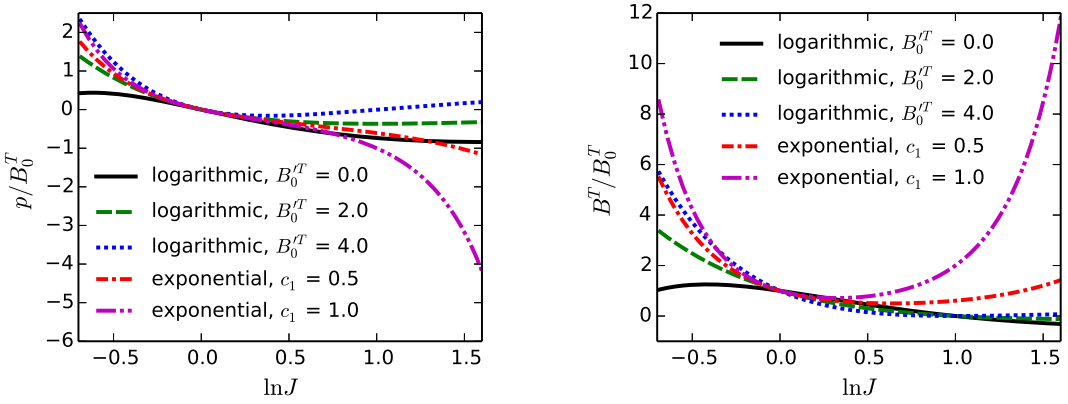

(a) pressure (b) bulk modulus

Fig. 2 Predictions for isothermal spherical elastic deformation, normalized by reference bulk modulus B_0^T: a) Cauchy pressure p computed from Eq. 78 (logarithmic model) or Eq. 88 (exponential model) and b) tangent isothermal bulk modulus B^T computed from Eq. 79 (logarithmic model) or Eq. 89 (exponential model)

Results in Fig. 2 show how the present theoretical framework successfully encompasses behaviors representative of stiff and soft solids depending on the choice of free energy function Ψ_0^∞. The logarithmic model is physically realistic for many strong single and polycrystalline solids deformed to large compression, as encountered in structural engineering materials (ceramics) and geomechanics (rocks and minerals).[41,42,45,46] It has also been used as a standard model of compressible neo-Hookean elasticity, appropriate for nearly incompressible rubber and some other polymers.[8,47] The logarithmic theory predicts a negative bulk modulus for $B_0'^T \leq 2$ and $J \geq 2.8$, implying instability under large dilatation is possible depending on nonlinear elastic parameters.

The exponential model is physically realistic for soft solids including biological tissues[1,2,30,48–50] that exhibit a very compliant response at small deformation and stiffen considerably at large extensional strain. Such behavior is characteristic of biological fibers containing elastin and collagen.[28] Under large expansion, the exponential model predicts an increasing bulk modulus that can significantly exceed the initial modulus B_0^T. Such stiffening, which occurs both in tension and compression at large deformations, is amplified by increasing the value of parameter c_1.

5. Viscoelasticity

The finite strain thermo-viscoelastic framework of Holzapfel and Simo,[9] which in turn implements some features from earlier work of Simo,[8] is adapted for use in the present formulation. A fundamental distinction is that, in the present approach, scalar viscous stress components conjugate to strain-like internal variables mirror elastic strain attributes of the QR kinematics. In contrast, used in other theories[9,10] are various viscous second Piola-Kirchhoff stress tensors conjugate to tensor internal state variables that mirror the Lagrangian deformation tensor $\boldsymbol{C}$ or Lagrangian strain tensor $\boldsymbol{E} = \frac{1}{2}(\boldsymbol{C} - \boldsymbol{1})$. The general theory posited herein admits isotropic or anisotropic viscoelastic responses depending on the particular forms prescribed for the equilibrium and configurational energy potentials.

5.1 General Thermodynamics

Attention is restricted here to a free energy-based formulation, for which the first of Eq. 41 in the absence of damage [$(\cdot)_0$ subscripts] is written

$$\Psi = \Psi_0(\boldsymbol{\epsilon}, T, \boldsymbol{\chi}^\alpha) = \Psi_0^\infty(\boldsymbol{\epsilon}, T) + \Upsilon_0(\boldsymbol{\epsilon}, T, \boldsymbol{\chi}^\alpha). \tag{90}$$

Dimensionless viscoelastic state variables are $\{\chi_i^\alpha\}$, $i = 0, \dots, 6$ and $\boldsymbol{\chi}^\alpha$, $\alpha = 1, \dots, m$, where the latter are defined in the second of Eq. 40. The first term on the right, Ψ_0^∞, accounts for the equilibrium (i.e., infinite-time) hyperelastic response, where examples have been given in Section 4. The second term on the right, Υ_0, accounts for the configurational free energy from which viscous effects on stress and entropy emerge. Each α corresponds to a different relaxation process affiliated with time scale t_α.

Substitution of Eq. 90 into Eq. 44, Eq. 45, and Eq. 64 provides the conjugate stress measures, entropy density, and dissipation inequality:

$$\begin{aligned}
&\hat{\tau}_0 = \frac{\partial \Psi_0^\infty}{\partial \epsilon_0} + \frac{\partial \Upsilon_0}{\partial \epsilon_0}, \qquad \hat{\tau}_1 = \frac{\partial \Psi_0^\infty}{\partial \epsilon_1} + \frac{\partial \Upsilon_0}{\partial \epsilon_1}, \qquad \hat{\tau}_2 = \frac{\partial \Psi_0^\infty}{\partial \epsilon_2} + \frac{\partial \Upsilon_0}{\partial \epsilon_2}, \\
&\hat{\tau}_3 = \frac{\partial \Psi_0^\infty}{\partial \epsilon_3} + \frac{\partial \Upsilon_0}{\partial \epsilon_3}, \qquad \hat{\tau}_4 = \frac{\partial \Psi_0^\infty}{\partial \epsilon_4} + \frac{\partial \Upsilon_0}{\partial \epsilon_4}, \qquad \hat{\tau}_5 = \frac{\partial \Psi_0^\infty}{\partial \epsilon_5} + \frac{\partial \Upsilon_0}{\partial \epsilon_5}, \\
&\hat{\tau}_6 = \frac{\partial \Psi_0^\infty}{\partial \epsilon_6} + \frac{\partial \Upsilon_0}{\partial \epsilon_6};
\end{aligned} \tag{91}$$

$$\eta = -\frac{\partial \Psi_0^\infty}{\partial T} - \frac{\partial \Upsilon_0}{\partial T} = \eta^\infty - \frac{\partial \Upsilon_0}{\partial T}; \tag{92}$$

$$\mathfrak{D} = \sum_{\alpha=1}^{m} \boldsymbol{\zeta}^\alpha \cdot \dot{\boldsymbol{\chi}}^\alpha \geq 0, \qquad \boldsymbol{\zeta}^\alpha = -\frac{\partial \Upsilon_0}{\partial \boldsymbol{\chi}^\alpha} = -\partial_{\boldsymbol{\chi}^\alpha} \Upsilon_0. \tag{93}$$

The conjugate internal force vector $\boldsymbol{\zeta}^\alpha$ is defined as a usual negative partial derivative (i.e., thermodynamic force) according to Eq. 62. Components are, from Eq. 90,

$$\boldsymbol{\zeta}^\alpha = [\zeta_0^\alpha, \zeta_1^\alpha, \zeta_2^\alpha, \zeta_4^\alpha, \zeta_5^\alpha, \zeta_6^\alpha]^{\mathrm{T}} = -\partial_{\boldsymbol{\chi}^\alpha} \Psi_0 = -\partial_{\boldsymbol{\chi}^\alpha} \Upsilon_0; \tag{94}$$

$$\begin{aligned} \zeta_0^\alpha &= -\frac{\partial \Upsilon_0}{\partial \chi_0^\alpha}, \quad \zeta_1^\alpha = -\frac{\partial \Upsilon_0}{\partial \chi_1^\alpha}, \quad \zeta_2^\alpha = -\frac{\partial \Upsilon_0}{\partial \chi_2^\alpha}, \quad \zeta_3^\alpha = -\frac{\partial \Upsilon_0}{\partial \chi_3^\alpha}, \\ \zeta_4^\alpha &= -\frac{\partial \Upsilon_0}{\partial \chi_4^\alpha}, \quad \zeta_5^\alpha = -\frac{\partial \Upsilon_0}{\partial \chi_5^\alpha} \quad \zeta_6^\alpha = -\frac{\partial \Upsilon_0}{\partial \chi_6^\alpha}. \end{aligned} \tag{95}$$

These viscous stress components are defined analogously to elastic stress components in Eq. 91 such that dissipation from the sum of products of seven scalar attributes equals that from the dot product of the seven-element vectors of thermodynamic conjugates:

$$\sum_{i=0}^{6} \zeta_i^\alpha \dot{\chi}_i^\alpha = \boldsymbol{\zeta}^\alpha \cdot \dot{\boldsymbol{\chi}}^\alpha \quad \Rightarrow \quad \mathfrak{D} = \sum_{\alpha=1}^{m} \sum_{i=0}^{6} \hat{\zeta}_i^\alpha \dot{\chi}_i^\alpha. \tag{96}$$

5.2 General Kinetics

A kinetic law for evolution of $\boldsymbol{\chi}^\alpha$ and a configurational free energy Υ_0, both consistent with the dissipation requirement Eq. 93, are needed. Positive dissipation can be ensured by prescribing, where $\mathbf{V}^\alpha = \mathbf{V}^\alpha(\boldsymbol{\epsilon}, T, \boldsymbol{\chi}^\alpha)$ is a positive definite 6×6 matrix of inverse viscosities,

$$\dot{\boldsymbol{\chi}}^\alpha = \mathbf{V}^\alpha \boldsymbol{\zeta}^\alpha, \tag{97}$$

which in turn requires specification of the viscous stresses $\boldsymbol{\zeta}^\alpha$.

A realistic and flexible kinetic model for viscous stresses, motivated by the standard viscoelasticity model of (i) a spring element for equilibrium response in parallel with (ii) m Maxwell (i.e., spring-dashpot) elements, is expressed in tensor form in other works.[9,10] In the present kinematic and thermodynamic framework, the analogous differential equations and initial conditions (i.e., instantaneous internal

stresses measured when a load is applied at $t = 0$) are, respectively,

$$\dot{\boldsymbol{\zeta}}^{\alpha} + \frac{1}{t_{\alpha}}\boldsymbol{\zeta}^{\alpha} = \frac{\mathrm{d}}{\mathrm{d}t}\left[\partial_{\boldsymbol{\epsilon}}\Psi_0^{\alpha}\right] - \boldsymbol{\omega}^{\alpha}, \qquad \boldsymbol{\zeta}^{\alpha}|_{t=0} = \boldsymbol{\zeta}_0^{\alpha} = \partial_{\boldsymbol{\epsilon}}\Psi_0^{\alpha}\big|_{\boldsymbol{\epsilon},T \text{ at } t=0}. \tag{98}$$

Denoted by $\Psi_0^{\alpha} = \Psi_0^{\alpha}(\boldsymbol{\epsilon}, T)$ is a free energy function that corresponds to relaxation process α with time scale $t_{\alpha} > 0$. Though not mandatory, these configurational energy potentials should logically be constructed such that they inherit the same material symmetry as the equilibrium free energy Ψ_0^{∞}.

The coupling function $\boldsymbol{\omega}^{\alpha}$ accounts for temperature-dependent viscous properties and will be defined in more detail later. The solution of Eq. 98 can be written in the form of a convolution integral for each α:

$$\boldsymbol{\zeta}^{\alpha}(t) = \exp\left(\frac{-t}{t_{\alpha}}\right)\boldsymbol{\zeta}_0^{\alpha} + \int_{0^+}^{t} \exp\left[\frac{-(t-s)}{t_{\alpha}}\right]\left(\frac{\mathrm{d}}{\mathrm{d}s}\left[\partial_{\boldsymbol{\epsilon}}\Psi_0^{\alpha}(s)\right] - \boldsymbol{\omega}^{\alpha}(s)\right)\mathrm{d}s. \tag{99}$$

The present model, like those formulated elsewhere,[9,10] is geometrically and materially nonlinear and admits up to any number m of discrete relaxation times t_{α} that may be needed to capture the relaxation spectrum. However, the exponential kernel in Eq. 99 that results from the differential equation assigned in Eq. 98 is reminiscent of linear viscoelasticity. It remains to be seen if this approach is capable of addressing the highly nonlinear cyclic viscoelastic response of some biological tissues,[3,29,43] or if modifications are necessary. Notably, a large number of Kelvin elements—each Kelvin element being an aforementioned Maxwell spring-dashpot unit and spring unit in parallel—have been recommended for describing the frequency response of soft tissues.[2]

Extending the propositions of Holzapfel and Simo[9] to the present context, the following three assumptions are imposed in addition to Eq. 98, beginning with

$$\partial_{\boldsymbol{\chi}^{\alpha}}\partial_{\boldsymbol{\chi}^{\beta}}\Upsilon_0 = \mu_{\alpha}\delta_{\alpha\beta}\mathbf{I}, \qquad \mu_{\alpha} = \mu_{\alpha}(T), \tag{100}$$

with $\mu_{\alpha} \geq 0$ a temperature-dependent parameter for each α with dimensions of elastic stiffness and $\mathbf{I}$ the 7×7 identity matrix. The second assumption is that the thermo-viscoelastic coupling function obeys

$$\boldsymbol{\omega}^{\alpha} = \dot{\mu}_{\alpha}\boldsymbol{\chi}^{\alpha} = \mu'_{\alpha}\dot{T}\boldsymbol{\chi}^{\alpha}, \qquad \mu'_{\alpha} = \mathrm{d}\mu_{\alpha}/\mathrm{d}T. \tag{101}$$

The third assumption is that internal dissipation is of the form

$$\mathfrak{D} = \sum_{\alpha=1}^{m} \frac{1}{\nu_\alpha} \boldsymbol{\zeta}^\alpha \cdot \boldsymbol{\zeta}^\alpha = \sum_{\alpha=1}^{m} \frac{1}{\mu_\alpha t_\alpha} |\boldsymbol{\zeta}^\alpha|^2 \geq 0, \qquad \nu_\alpha = \mu_\alpha t_\alpha, \tag{102}$$

with $\nu_\alpha \geq 0$ a viscosity coefficient.

The configurational free energy that emerges from these assumptions is

$$\Upsilon_0(\boldsymbol{\epsilon}, T, \boldsymbol{\chi}^\alpha) = \sum_{\alpha=1}^{m} \left[\frac{1}{2} \mu_\alpha(T) |\boldsymbol{\chi}^\alpha|^2 - \partial_{\boldsymbol{\epsilon}} \Psi_0^\alpha(\boldsymbol{\epsilon}, T) \cdot \boldsymbol{\chi}^\alpha + \Psi_0^\alpha(\boldsymbol{\epsilon}, T) \right]. \tag{103}$$

The proof follows the same steps as those in prior work,[9] albeit with different definitions for elastic and viscous stress-strain variables. Comparing Eq. 96 and Eq. 97 with Eq. 102,

$$\boldsymbol{\zeta}^\alpha = \nu_\alpha \dot{\boldsymbol{\chi}}^\alpha, \qquad \mathbf{V}^\alpha = (1/\nu_\alpha)\mathbf{I}. \tag{104}$$

Integrating Eq. 100 successively gives

$$\partial_{\boldsymbol{\chi}^\alpha} \Upsilon_0 = \mu_\alpha \boldsymbol{\chi}^\alpha + \boldsymbol{\Xi}^\alpha, \qquad \boldsymbol{\Xi}^\alpha = \boldsymbol{\Xi}^\alpha(\boldsymbol{\epsilon}, T); \tag{105}$$

$$\Upsilon_0(\boldsymbol{\epsilon}, T, \boldsymbol{\chi}^\alpha) = \sum_{\alpha=1}^{m} \left[\frac{1}{2} \mu_\alpha(T) |\boldsymbol{\chi}^\alpha|^2 + \boldsymbol{\Xi}^\alpha(\boldsymbol{\epsilon}, T) \cdot \boldsymbol{\chi}^\alpha \right] + \tilde{\Upsilon}(\boldsymbol{\epsilon}, T). \tag{106}$$

Differentiating Eq. 105 with respect to strain and temperature, respectively, provides

$$\partial_{\boldsymbol{\epsilon}} \partial_{\boldsymbol{\chi}^\alpha} \Upsilon_0 = \partial_{\boldsymbol{\epsilon}} \boldsymbol{\Xi}^\alpha, \qquad \partial_T \partial_{\boldsymbol{\chi}^\alpha} \Upsilon_0 = \mu_\alpha' \boldsymbol{\chi}^\alpha + \partial_T \boldsymbol{\Xi}^\alpha. \tag{107}$$

The material time derivative of the second of Eq. 93 is

$$\dot{\boldsymbol{\zeta}}^\alpha = -\frac{\mathrm{d}}{\mathrm{d}t} \left(\partial_{\boldsymbol{\chi}^\alpha} \Upsilon_0 \right) = -\sum_{\beta=1}^{m} \left([\partial_{\boldsymbol{\chi}^\alpha} \partial_{\boldsymbol{\chi}^\beta} \Upsilon_0] \cdot \dot{\boldsymbol{\chi}}^\beta \right) - [\partial_{\boldsymbol{\epsilon}} \partial_{\boldsymbol{\chi}^\alpha} \Upsilon_0] \cdot \dot{\boldsymbol{\epsilon}} - [\partial_T \partial_{\boldsymbol{\chi}^\alpha} \Upsilon_0] \cdot \dot{T}. \tag{108}$$

Substitution of Eq. 100, Eq. 101, Eq. 104, and Eq. 107 into Eq. 108 results in

$$\dot{\boldsymbol{\zeta}}^\alpha + \frac{\mu_\alpha}{\nu_\alpha} \boldsymbol{\zeta}^\alpha = -\partial_{\boldsymbol{\epsilon}} \boldsymbol{\Xi}^\alpha \cdot \dot{\boldsymbol{\epsilon}} - \dot{T} \partial_T \boldsymbol{\Xi}^\alpha - \boldsymbol{\omega}^\alpha. \tag{109}$$

The left side of Eq. 109 is identical to the left side of Eq. 98. Equating the right

sides of Eq. 98 and Eq. 109 then integrating with respect to time gives

$$\Xi^\alpha(\boldsymbol{\epsilon}, T) = -\partial_{\boldsymbol{\epsilon}} \Psi_0^\alpha(\boldsymbol{\epsilon}, T). \tag{110}$$

Finally, defining the integration scalar $\tilde{\Upsilon} = \sum_{\alpha=1}^{m} \Psi_0^\alpha$ and substituting Eq. 110 into Eq. 106 produces the internal configurational energy of Eq. 103.

The resulting important constitutive equations are summarized as follows. Total free energy of Eq. 90 is

$$\Psi_0(\boldsymbol{\epsilon}, T, \boldsymbol{\chi}^\alpha) = \Psi_0^\infty(\boldsymbol{\epsilon}, T) + \sum_{\alpha=1}^{m} \left[\frac{1}{2} \mu_\alpha(T) |\boldsymbol{\chi}^\alpha|^2 - \partial_{\boldsymbol{\epsilon}} \Psi_0^\alpha(\boldsymbol{\epsilon}, T) \cdot \boldsymbol{\chi}^\alpha + \Psi_0^\alpha(\boldsymbol{\epsilon}, T) \right]. \tag{111}$$

The thermodynamic stress vector $\hat{\boldsymbol{\tau}}$ is a sum of equilibrium elastic and m viscous parts:

$$\hat{\boldsymbol{\tau}} = \frac{\partial \Psi_0}{\partial \boldsymbol{\epsilon}} = \frac{\partial \Psi_0^\infty}{\partial \boldsymbol{\epsilon}} + \sum_{\alpha=1}^{m} \left[\frac{\partial \Psi_0^\alpha}{\partial \boldsymbol{\epsilon}} - \frac{\partial^2 \Psi_0^\alpha}{\partial \boldsymbol{\epsilon} \partial \boldsymbol{\epsilon}} \cdot \boldsymbol{\chi}^\alpha \right]. \tag{112}$$

Entropy $\eta = -\partial_T \Psi_0$ can be obtained from differentiation of Eq. 111 as an analogous sum of equilibrium elastic and m viscous contributions. The evolution equation for viscous internal stresses is Eq. 98 with general solution Eq. 99.

Internal strains and their rates obey, from Eq. 105 and Eq. 104,

$$\boldsymbol{\chi}^\alpha = \frac{1}{\mu_\alpha} \left[\frac{\partial \Psi_0^\alpha}{\partial \boldsymbol{\epsilon}} - \boldsymbol{\zeta}^\alpha \right], \qquad \dot{\boldsymbol{\chi}}^\alpha = \frac{1}{\nu_\alpha} \boldsymbol{\zeta}^\alpha, \qquad (\nu_\alpha = \mu_\alpha t_\alpha > 0). \tag{113}$$

Comparing Eq. 112 and Eq. 113, total thermodynamic stress is the direct sum of equilibrium stress and m conjugate internal stresses $\boldsymbol{\zeta}^\alpha$ when the following inessential constraints are imposed:

$$\frac{\partial^2 \Psi_0^\alpha}{\partial \boldsymbol{\epsilon} \partial \boldsymbol{\epsilon}} \cdot \boldsymbol{\chi}^\alpha = \mu_\alpha \boldsymbol{\chi}^\alpha \quad \Rightarrow \quad \hat{\boldsymbol{\tau}} = \frac{\partial \Psi_0^\infty}{\partial \boldsymbol{\epsilon}} + \sum_{\alpha=1}^{m} \boldsymbol{\zeta}^\alpha. \tag{114}$$

Temperature can be computed via use of Eq. 63 with $\dot{D} = 0$, where the summation over m internal configurational variables accounts for viscous heating, for example.

The initial internal stress is calculated as follows, from which the internal strain

vanishes at $t = 0$ according to the first of Eq. 113:

$$\boldsymbol{\zeta}_0^\alpha = \left.\frac{\partial \Psi_0^\alpha}{\partial \boldsymbol{\epsilon}}\right|_{t=0}, \qquad \boldsymbol{\chi}_0^\alpha = \boldsymbol{\chi}^\alpha|_{t=0} = \mathbf{0}. \tag{115}$$

The instantaneous total stress at $t = 0$ is then, from Eq. 112, regardless of whether Eq. 114 applies:

$$\hat{\boldsymbol{\tau}}_0 = \hat{\boldsymbol{\tau}}|_{t=0} = \frac{\partial \Psi_0^\infty}{\partial \boldsymbol{\epsilon}} + \sum_{\alpha=1}^{m} \boldsymbol{\zeta}_0^\alpha. \tag{116}$$

The condition imposed for thermodynamic equilibrium is that internal stresses vanish at infinite time, which leads to the following limiting thermoelastic relations, from Eq. 113:

$$\boldsymbol{\zeta}_\infty^\alpha = \boldsymbol{\zeta}^\alpha|_{t\to\infty} = \mathbf{0} \quad \Rightarrow \quad \boldsymbol{\chi}_\infty^\alpha = \boldsymbol{\chi}^\alpha|_{t\to\infty} = \frac{1}{\mu_\alpha}\frac{\partial \Psi_0^\alpha}{\partial \boldsymbol{\epsilon}}, \quad \dot{\boldsymbol{\chi}}_\infty^\alpha = \mathbf{0}. \tag{117}$$

Furthermore, when special condition Eq. 114 applies, then the equilibrium stress is simply $\hat{\boldsymbol{\tau}}_\infty = \partial \Psi_0^\infty / \partial \boldsymbol{\epsilon}$.

The model is complete upon specification of the free energy potentials Ψ_0^∞ and Ψ_0^α for $\alpha = 1, \ldots, m$ along with the viscoelastic stiffness function(s) $\mu_\alpha(T)$ and the relaxation time constant(s) t_α. Three representative examples are presented in what follows subsequently.

5.3 Quadratic Configurational Energy

The first example of the framework of Section 5.1 and Section 5.2 invokes the quasi-linear, pseudo-isotropic free energy of Section 4.4 for the equilibrium thermoelastic response in combination with a simple quadratic form summation for the configurational free energy that obeys Eq. 114:

$$\Psi_0^\alpha = \frac{1}{2}\mu_\alpha |\boldsymbol{\epsilon}|^2 \qquad \Rightarrow \qquad \Upsilon_0 = \sum_{\alpha=1}^{m} \frac{1}{2}\mu_\alpha |\boldsymbol{\epsilon} - \boldsymbol{\chi}^\alpha|^2. \tag{118}$$

The total free energy in Eq. 90 is the sum of Eq. 83 in square brackets below and

the latter sum of quadratic forms from Eq. 118:

$$\begin{aligned}\Psi_0 &= \Psi_0^\infty + \Upsilon_0 \\ &= \left[\frac{1}{2}B_0^T(\Xi_0)^2 + \frac{1}{2}G_0\Xi_1 - \kappa_0\Xi_0\Delta T - c_0 T\ln(T/T_0)\right] + \frac{1}{2}\sum_{\alpha=1}^{m}\mu_\alpha|\boldsymbol{\epsilon}-\boldsymbol{\chi}^\alpha|^2.\end{aligned} \tag{119}$$

An equilibrium thermodynamic stress vector is defined as follows (not necessarily at $t \to \infty$, which will be demonstrated later):

$$\hat{\boldsymbol{\tau}}_\infty = \partial_{\boldsymbol{\epsilon}}\Psi_0^\infty = \{\hat{\tau}_i\}_\infty = \begin{Bmatrix}\hat{\tau}_0\\ \hat{\tau}_1\\ \hat{\tau}_2\\ \hat{\tau}_3\\ \hat{\tau}_4\\ \hat{\tau}_5\\ \hat{\tau}_6\end{Bmatrix}_\infty = \begin{Bmatrix}B_0^T(\epsilon_0 - A_0\Delta T)\\ 6G_0\epsilon_1\\ 6G_0\epsilon_2\\ 6G_0\epsilon_3\\ G_0\epsilon_4\\ G_0\epsilon_5\\ G_0\epsilon_6\end{Bmatrix}. \tag{120}$$

The viscous stress vector is

$$\boldsymbol{\zeta}^\alpha = -\partial_{\boldsymbol{\chi}^\alpha}\Upsilon_0 = \partial_{\boldsymbol{\epsilon}}\Psi_0^\alpha - \mu_\alpha\boldsymbol{\chi}^\alpha = \mu_\alpha(\boldsymbol{\epsilon}-\boldsymbol{\chi}^\alpha) = \nu_\alpha\dot{\boldsymbol{\chi}}^\alpha = \mu_\alpha t_\alpha\dot{\boldsymbol{\chi}}^\alpha. \tag{121}$$

Total stresses at any time are the sum of Eq. 120 and Eq. 121:

$$\hat{\boldsymbol{\tau}} = \partial_{\boldsymbol{\epsilon}}\Psi_0 = \begin{Bmatrix}B_0^T(\epsilon_0 - A_0\Delta T) + \sum_{\alpha=1}^m \mu_\alpha(\epsilon_0 - \chi_0^\alpha)\\ 6G_0\epsilon_1 + \sum_{\alpha=1}^m \mu_\alpha(\epsilon_1 - \chi_1^\alpha)\\ 6G_0\epsilon_2 + \sum_{\alpha=1}^m \mu_\alpha(\epsilon_2 - \chi_2^\alpha)\\ 6G_0\epsilon_3 + \sum_{\alpha=1}^m \mu_\alpha(\epsilon_3 - \chi_3^\alpha)\\ G_0\epsilon_4 + \sum_{\alpha=1}^m \mu_\alpha(\epsilon_4 - \chi_4^\alpha)\\ G_0\epsilon_5 + \sum_{\alpha=1}^m \mu_\alpha(\epsilon_5 - \chi_5^\alpha)\\ G_0\epsilon_6 + \sum_{\alpha=1}^m \mu_\alpha(\epsilon_6 - \chi_6^\alpha)\end{Bmatrix}. \tag{122}$$

The evolution equation for internal stresses with initial conditions is

$$\dot{\boldsymbol{\zeta}}^\alpha + \frac{1}{t_\alpha}\boldsymbol{\zeta}^\alpha = \mu_\alpha\dot{\boldsymbol{\epsilon}} + \mu'_\alpha(\boldsymbol{\epsilon}-\boldsymbol{\chi}^\alpha)\dot{T}, \qquad \boldsymbol{\zeta}_0^\alpha = \boldsymbol{\zeta}^\alpha(\boldsymbol{\epsilon}_0, T_0) = \mu_\alpha(T_0)\boldsymbol{\epsilon}_0. \tag{123}$$

The general solution is obtained by Eq. 99 with straightforward substitutions. Initial

total stresses are given in Eq. 122 with $\chi_i^\alpha = 0$. Internal strains and their rates are obtained from Eq. 113:

$$\boldsymbol{\chi}^\alpha = \boldsymbol{\epsilon} - \boldsymbol{\zeta}^\alpha/\mu_\alpha, \qquad \dot{\boldsymbol{\chi}}^\alpha = \boldsymbol{\zeta}^\alpha/\nu_\alpha, \qquad (\nu_\alpha = \mu_\alpha t_\alpha > 0). \tag{124}$$

The equilibrium values of internal variables are, from Eq. 117 and the first of Eq. 118,

$$\boldsymbol{\chi}_\infty^\alpha = \boldsymbol{\chi}^\alpha|_{t\to\infty} = \frac{1}{\mu_\alpha}\frac{\partial \Psi_0^\alpha}{\partial \boldsymbol{\epsilon}} = \boldsymbol{\epsilon}. \tag{125}$$

This verifies in Eq. 122 that $\hat{\boldsymbol{\tau}} \to \hat{\boldsymbol{\tau}}_\infty$ as $t \to \infty$. Furthermore, the condition Eq. 39 is now imposed for the internal strains entering the free energy function Υ_0. With this constraint in place along with Eq. 25, verification is straightforward that $\hat{\tau}_1 + \hat{\tau}_2 + \hat{\tau}_3 = 0$, thus satisfying the restrictions in Eq. 33 and Eq. 47.

If $\alpha = m = 1$, then parameters t_α and μ_α can be obtained from an isothermal stress relaxation test, presuming the hyperelastic potential Ψ_0^∞ is known. Consider a 1-D shear relaxation test where $\boldsymbol{\epsilon}$ has the lone nonzero component $\epsilon_4 = \gamma = \gamma_0 =$ constant and T is held fixed at T_0. In this constant strain and constant temperature case, the right side of the differential equation in Eq. 123 vanishes identically, as does the convolution integral in Eq. 99. The lone nonzero shear stress component relaxes according to

$$\hat{\tau}_4(t, T_0) = \gamma_0[G_0 + \mu_1(T_0)\exp(-t/t_1)]. \tag{126}$$

If the initial total stress is measured, then $\mu_1(T_0) = \hat{\tau}_4(0, T_0)/\gamma_0 - G_0$. The relaxation time t_1 can be obtained by fitting the decay behavior for $t > 0$. The ease at which the two physically relevant viscoelastic parameters is calibrated in this case is clear. However, this simple model may be overly restrictive since the same viscoelastic parameters (stiffness, relaxation times, and thus viscosity) are assigned to volumetric and shear behaviors.

5.4 Proportional Configurational Energy

A second, perhaps more realistic, approach follows ideas in a different prior work on nonlinear viscoelasticity.[10] In lieu of the first of Eq. 118, the configurational free

energy for process α is assigned proportional to the equilibrium free energy:

$$\Psi_0^\alpha(\boldsymbol{\epsilon}, T) = \beta_\alpha \Psi_0^\infty(\boldsymbol{\epsilon}, T), \qquad \beta_\alpha \in (0, \infty), \qquad (\alpha = 1, \ldots, m), \tag{127}$$

where β_α are constants for a given material. The total free energy of Eq. 111 becomes

$$\Psi_0 = \Psi_0^\infty + \Upsilon_0 = \Psi_0^\infty + \sum_{\alpha=1}^{m} \left[\frac{1}{2} \mu_\alpha |\boldsymbol{\chi}^\alpha|^2 - \beta_\alpha (\boldsymbol{\tau}_\infty \cdot \boldsymbol{\chi}^\alpha - \Psi_0^\infty) \right]. \tag{128}$$

Note that the inessential relation Eq. 114 does not generally apply for this model.

The viscous stress vector is

$$\boldsymbol{\zeta}^\alpha = -\partial_{\boldsymbol{\chi}^\alpha} \Upsilon_0 = \beta_\alpha \boldsymbol{\tau}_\infty - \mu_\alpha \boldsymbol{\chi}^\alpha = \nu_\alpha \dot{\boldsymbol{\chi}}^\alpha = \mu_\alpha t_\alpha \dot{\boldsymbol{\chi}}^\alpha. \tag{129}$$

The total thermodynamic stress vector of Eq. 112 is

$$\begin{aligned} \hat{\boldsymbol{\tau}} = \frac{\partial \Psi_0}{\partial \boldsymbol{\epsilon}} &= \frac{\partial \Psi_0^\infty}{\partial \boldsymbol{\epsilon}} + \sum_{\alpha=1}^{m} \beta_\alpha \left[\frac{\partial \Psi_0^\infty}{\partial \boldsymbol{\epsilon}} - \frac{\partial^2 \Psi_0^\infty}{\partial \boldsymbol{\epsilon} \partial \boldsymbol{\epsilon}} \cdot \boldsymbol{\chi}^\alpha \right] \\ &= \boldsymbol{\tau}_\infty + \sum_{\alpha=1}^{m} \beta_\alpha \left[\boldsymbol{\tau}_\infty - \mathbf{C}_\infty^T \cdot \boldsymbol{\chi}^\alpha \right], \end{aligned} \tag{130}$$

where $\mathbf{C}_\infty^T = \partial \boldsymbol{\tau}_\infty / \partial \boldsymbol{\epsilon}$ is the 7×7 equilibrium isothermal tangent elastic stiffness matrix with respect to $\boldsymbol{\epsilon}$.

The same quasi-linear form of Ψ_0^∞ is invoked as in the previous example, so Eq. 120 still holds for the equilibrium stress vector. For the thermoelastic potential of Eq. 83,

$$\mathbf{C}_\infty^T = \begin{bmatrix} B_0^T & 0 & 0 & 0 & 0 & 0 & 0 \\ 0 & 6G_0 & 0 & 0 & 0 & 0 & 0 \\ 0 & 0 & 6G_0 & 0 & 0 & 0 & 0 \\ 0 & 0 & 0 & 6G_0 & 0 & 0 & 0 \\ 0 & 0 & 0 & 0 & G_0 & 0 & 0 \\ 0 & 0 & 0 & 0 & 0 & G_0 & 0 \\ 0 & 0 & 0 & 0 & 0 & 0 & G_0 \end{bmatrix}. \tag{131}$$

Substituting Eq. 120 and Eq. 131 into Eq. 130 produces

$$\hat{\boldsymbol{\tau}} = \partial_{\boldsymbol{\epsilon}}\Psi_0 = \left\{ \begin{array}{c} B_0^T[(\epsilon_0 - A_0\Delta T) + \sum_{\alpha=1}^m \beta_\alpha(\epsilon_0 - A_0\Delta T - \chi_0^\alpha)] \\ 6G_0[\epsilon_1 + \sum_{\alpha=1}^m \beta_\alpha(\epsilon_1 - \chi_1^\alpha)] \\ 6G_0[\epsilon_2 + \sum_{\alpha=1}^m \beta_\alpha(\epsilon_2 - \chi_2^\alpha)] \\ 6G_0[\epsilon_3 + \sum_{\alpha=1}^m \beta_\alpha(\epsilon_3 - \chi_3^\alpha)] \\ G_0[\epsilon_4 + \sum_{\alpha=1}^m \beta_\alpha(\epsilon_4 - \chi_4^\alpha)] \\ G_0[\epsilon_5 + \sum_{\alpha=1}^m \beta_\alpha(\epsilon_5 - \chi_5^\alpha)] \\ G_0[\epsilon_6 + \sum_{\alpha=1}^m \beta_\alpha(\epsilon_6 - \chi_6^\alpha)] \end{array} \right\}. \tag{132}$$

Again, Eq. 39 is imposed for internal strains entering Υ_0. Upon use of this constraint in conjunction with Eq. 25, verification is straightforward that Eq. 33 and Eq. 47 are satisfied.

The evolution equation for internal stresses with initial conditions is

$$\dot{\boldsymbol{\zeta}}^\alpha + \frac{1}{t_\alpha}\boldsymbol{\zeta}^\alpha = \beta_\alpha\dot{\boldsymbol{\tau}}_\infty - \mu'_\alpha\boldsymbol{\chi}^\alpha\dot{T}, \qquad \boldsymbol{\zeta}_0^\alpha = \boldsymbol{\zeta}^\alpha(\boldsymbol{\epsilon}_0, T_0) = \beta_\alpha\partial_{\boldsymbol{\epsilon}}\Psi_0^\infty(\boldsymbol{\epsilon}_0, T_0). \tag{133}$$

The general solution is obtained by integration of Eq. 99 with the appropriate substitutions. Initial total stresses are given by Eq. 132 with $\chi_i^\alpha = 0$. Internal strains and their rates are obtained from Eq. 113:

$$\boldsymbol{\chi}^\alpha = \frac{1}{\mu_\alpha}\left[\beta_\alpha\boldsymbol{\tau}_\infty - \boldsymbol{\zeta}^\alpha\right], \qquad \dot{\boldsymbol{\chi}}^\alpha = \boldsymbol{\zeta}^\alpha/\nu_\alpha, \qquad (\nu_\alpha = \mu_\alpha t_\alpha > 0). \tag{134}$$

At equilibrium as $t \to \infty$ from Eq. 117 and Eq. 127, $\boldsymbol{\chi}_\infty^\alpha = \beta_\alpha\boldsymbol{\tau}_\infty/\mu_\alpha$.

For this model, three independent material parameters are needed for each viscosity mode α: the energy factor β_α, the relaxation time t_α, and the stiffness factor μ_α, where the latter two are related to viscosity via the rightmost expression in Eq. 134. Consider a simple shear stress relaxation test of the same form as that discussed for the previous model of Section 5.3. For the present model, Eq. 126 is replaced with the following, where $\mu_1 = \mu_1(T_0)$:

$$\hat{\tau}_4(t) = G_0\gamma_0\left[1 + \beta_1\{1 - \frac{\beta_1 G_0}{\mu_1}[1 - \exp(-t/t_1)]\}\right]. \tag{135}$$

An obvious logical choice is $\beta_1 = \mu_1/G_0$, which yields behavior identical to

Eq. 126:

$$\hat{\tau}_4(t, T_0) = G_0\gamma_0 \left[1 + \beta_1 \exp(-t/t_1)\right]. \tag{136}$$

The analogous equation to Eq. 135 for isothermal spherical stress (i.e., pressure) relaxation at constant volume [$J = J_0 = \exp(\epsilon_0) =$ constant] is

$$p(t) = -\frac{\hat{\tau}_0(t)}{J_0} = -\frac{B_0^T \epsilon_0}{J_0}\left[1 + \beta_1\{1 - \frac{\beta_1 B_0^T}{\mu_1}[1 - \exp(-t/t_1)]\}\right]. \tag{137}$$

Notice that although viscous stress contributions are scaled by different factors for $t > 0$, the initial total stress is $(1 + \beta_1)$ times the equilibrium stress for different loading protocols in Eq. 135 and Eq. 137, regardless of the choice of μ_1. The model presented next rectifies this situation, albeit at the expense of one additional material parameter per viscous mode α.

5.5 Proportional Configurational Energy with Volumetric-Shear Split

The equilibrium free energy density is next assumed additively separable into volumetric and shear contributions, where all thermal effects are embedded in the former and pressure coupling is included in the latter. All example thermoelastic potentials presented in Section 4 can be represented in this format.

Specifically, considering pseudo-isotropic formulations of Section 4.4,

$$\begin{aligned}\Psi_0^{\infty}(\Xi_j, T) &= \Psi_0^{V\infty}(\Xi_0, T) + \Psi_0^{\Delta\infty}(\Xi_0, \Xi_1) \\ &= \Psi_0^{v\infty}(\Xi_0, T) + \psi^{\infty}(T) + \Psi_0^{\delta\infty}(\Xi_1)\iota(\Xi_0),\end{aligned} \tag{138}$$

recalling from Eq. 82 that $\Xi_0 = \epsilon_0 = \ln J$ and Ξ_1 is a scalar function of the squeeze and simple shearing modes $\{\epsilon_i\}, i \geq 1$. The coupling function $\iota(\epsilon_0)$ accounts for pressure dependence of the tangent shear modulus. The total thermal-volumetric energy $\Psi_0^{V\infty}$ is further decomposed into a sum of thermoelastic strain energy $\Psi_0^{v\infty}$ and purely thermal energy $\psi^{\infty}(T)$, where the latter accounts for specific heat. For all models with constant specific heat presented in Section 4, $\psi^{\infty} = -c_0 T \ln(T/T_0)$.

The superscript and subscript notation used for energy potentials is summarized below for ease of reference:

- $(\cdot)^V$: volumetric part *with* thermal energy ψ;

- $(\cdot)^v$: volumetric part *without* thermal energy ψ;
- $(\cdot)^\Delta$: deviatoric part *with* pressure coupling ι;
- $(\cdot)^\delta$: deviatoric part *without* pressure coupling ι;
- $(\cdot)^\infty$: equilibrium thermoelastic part;
- $(\cdot)_0$: damage-free part;
- $(\cdot)^\alpha$: part corresponding to viscoelastic mode α.

The present model invokes the following generalization of Eq. 127:

$$\begin{aligned}\Psi_0^\alpha(\boldsymbol{\epsilon}, T) = \beta_\alpha^V \Psi_0^{V\infty}(\epsilon_0, T) + \beta_\alpha^\Delta \Psi_0^{\Delta\infty}(\epsilon_i)|_{i\geq 0}; \\ \left[\beta_\alpha^V, \beta_\alpha^\Delta \in (0,\infty), \quad (\alpha = 1, \ldots, m)\right],\end{aligned} \tag{139}$$

where β_α^V and β_α^Δ are constants for a given material. When $\beta_\alpha^V = \beta_\alpha^\Delta \forall \alpha \in [1, m]$, then the model of Section 5.4 is recovered.

Define the following modified stress vector that is obtained from differentiation of Eq. 139 with respect to $\boldsymbol{\epsilon}$ for each α:

$$\tilde{\boldsymbol{\tau}}_\infty^\alpha = \partial_{\boldsymbol{\epsilon}} \Psi_0^\alpha = \{\tilde{\tau}_i\}_\infty^\alpha = \left\{ \begin{array}{c} \beta_\alpha^V(\partial \Psi_0^{V\infty}/\partial \epsilon_0) + \beta_\alpha^\Delta \Psi_0^{\delta\infty}(\mathrm{d}\iota/\mathrm{d}\epsilon_0) \\ \beta_\alpha^\Delta(\partial \Psi_1^{\Delta\infty}/\partial \epsilon_1) \\ \beta_\alpha^\Delta(\partial \Psi_1^{\Delta\infty}/\partial \epsilon_2) \\ \beta_\alpha^\Delta(\partial \Psi_1^{\Delta\infty}/\partial \epsilon_3) \\ \beta_\alpha^\Delta(\partial \Psi_1^{\Delta\infty}/\partial \epsilon_4) \\ \beta_\alpha^\Delta(\partial \Psi_1^{\Delta\infty}/\partial \epsilon_5) \\ \beta_\alpha^\Delta(\partial \Psi_1^{\Delta\infty}/\partial \epsilon_6) \end{array} \right\}. \tag{140}$$

The total free energy and viscous stress vectors of Eq. 128 and Eq. 129 are then generalized to

$$\Psi_0 = \Psi_0^\infty + \Upsilon_0 = \Psi_0^\infty + \sum_{\alpha=1}^m \left[\frac{1}{2}\mu_\alpha |\boldsymbol{\chi}^\alpha|^2 - \tilde{\boldsymbol{\tau}}_\infty^\alpha \cdot \boldsymbol{\chi}^\alpha + \beta_\alpha^V \Psi_0^{V\infty} + \beta_\alpha^\Delta \Psi_0^{D\infty} \right]. \tag{141}$$

$$\boldsymbol{\zeta}^\alpha = -\partial_{\boldsymbol{\chi}^\alpha} \Upsilon_0 = \tilde{\boldsymbol{\tau}}_\infty^\alpha - \mu_\alpha \boldsymbol{\chi}^\alpha = \nu_\alpha \dot{\boldsymbol{\chi}}^\alpha = \mu_\alpha t_\alpha \dot{\boldsymbol{\chi}}^\alpha. \tag{142}$$

The quasi-linear hyperelastic potential of Eq. 83 is now selected, as was the case in the prior two viscoelastic examples. With regard to Eq. 138, $\iota = 1$ and

$$\begin{aligned}\Psi_0^{V\infty} &= \frac{1}{2}B_0^T(\epsilon_0)^2 - B_0^T A_0 \epsilon_0 \Delta T - c_0 T \ln(T/T_0),\\ \Psi_0^{\Delta\infty} &= \frac{1}{2}G_0\{6[(\epsilon_1)^2 + (\epsilon_2)^2 + (\epsilon_3)^2] + (\epsilon_4)^2 + (\epsilon_5)^2 + (\epsilon_6)^2\}.\end{aligned} \tag{143}$$

With this potential, Eq. 140 becomes

$$\tilde{\boldsymbol{\tau}}_\infty^\alpha = \left\{\begin{array}{c} \beta_\alpha^V B_0^T(\epsilon_0 - A_0\Delta T) \\ 6\beta_\alpha^\Delta G_0 \epsilon_1 \\ 6\beta_\alpha^\Delta G_0 \epsilon_2 \\ 6\beta_\alpha^\Delta G_0 \epsilon_3 \\ \beta_\alpha^\Delta G_0 \epsilon_4 \\ \beta_\alpha^\Delta G_0 \epsilon_5 \\ \beta_\alpha^\Delta G_0 \epsilon_6 \end{array}\right\}. \tag{144}$$

The total thermodynamic stress vector of Eq. 112 is

$$\hat{\boldsymbol{\tau}} = \frac{\partial \Psi_0}{\partial \boldsymbol{\epsilon}} = \frac{\partial \Psi_0^\infty}{\partial \boldsymbol{\epsilon}} + \sum_{\alpha=1}^{m}\left[\frac{\partial \Psi_0^\alpha}{\partial \boldsymbol{\epsilon}} - \frac{\partial^2 \Psi_0^\alpha}{\partial \boldsymbol{\epsilon}\partial \boldsymbol{\epsilon}} \cdot \boldsymbol{\chi}^\alpha\right] = \tilde{\boldsymbol{\tau}}_\infty + \sum_{\alpha=1}^{m}\left[\tilde{\boldsymbol{\tau}}_\infty^\alpha - \mathbf{C}_\infty^{T\alpha} \cdot \boldsymbol{\chi}^\alpha\right], \tag{145}$$

where $\mathbf{C}_\infty^{T\alpha} = \partial \tilde{\boldsymbol{\tau}}_\infty^\alpha / \partial \boldsymbol{\epsilon}$ is the 7×7 equilibrium isothermal tangent elastic stiffness matrix of Ψ_0^α with respect to $\boldsymbol{\epsilon}$. For the thermoelastic potential of Eq. 143 with Eq. 139,

$$\mathbf{C}_\infty^{T\alpha} = \begin{bmatrix} \beta_\alpha^V B_0^T & 0 & 0 & 0 & 0 & 0 & 0 \\ 0 & 6\beta_\alpha^\Delta G_0 & 0 & 0 & 0 & 0 & 0 \\ 0 & 0 & 6\beta_\alpha^\Delta G_0 & 0 & 0 & 0 & 0 \\ 0 & 0 & 0 & 6\beta_\alpha^\Delta G_0 & 0 & 0 & 0 \\ 0 & 0 & 0 & 0 & \beta_\alpha^\Delta G_0 & 0 & 0 \\ 0 & 0 & 0 & 0 & 0 & \beta_\alpha^\Delta G_0 & 0 \\ 0 & 0 & 0 & 0 & 0 & 0 & \beta_\alpha^\Delta G_0 \end{bmatrix}. \tag{146}$$

Substituting Eq. 144 and Eq. 146 into Eq. 145 produces

$$\hat{\boldsymbol{\tau}} = \partial_{\boldsymbol{\epsilon}} \Psi_0 = \left\{ \begin{array}{c} B_0^T[(\epsilon_0 - A_0\Delta T) + \sum_{\alpha=1}^m \beta_\alpha^V(\epsilon_0 - A_0\Delta T - \chi_0^\alpha)] \\ 6G_0[\epsilon_1 + \sum_{\alpha=1}^m \beta_\alpha^\Delta(\epsilon_1 - \chi_1^\alpha)] \\ 6G_0[\epsilon_2 + \sum_{\alpha=1}^m \beta_\alpha^\Delta(\epsilon_2 - \chi_2^\alpha)] \\ 6G_0[\epsilon_3 + \sum_{\alpha=1}^m \beta_\alpha^\Delta(\epsilon_3 - \chi_3^\alpha)] \\ G_0[\epsilon_4 + \sum_{\alpha=1}^m \beta_\alpha^\Delta(\epsilon_4 - \chi_4^\alpha)] \\ G_0[\epsilon_5 + \sum_{\alpha=1}^m \beta_\alpha^\Delta(\epsilon_5 - \chi_5^\alpha)] \\ G_0[\epsilon_6 + \sum_{\alpha=1}^m \beta_\alpha^\Delta(\epsilon_6 - \chi_6^\alpha)] \end{array} \right\}. \tag{147}$$

Constraint Eq. 39 is imposed for this Υ_0. As such, with Eq. 25, verification is straightforward that Eq. 33 and Eq. 47 hold as desired.

The evolution equation for internal stresses and initial conditions are, respectively,

$$\dot{\boldsymbol{\zeta}}^\alpha + \frac{1}{t_\alpha}\boldsymbol{\zeta}^\alpha = \frac{\mathrm{d}}{\mathrm{d}t}\tilde{\boldsymbol{\tau}}_\infty^\alpha - \mu'_\alpha \boldsymbol{\chi}^\alpha \dot{T}, \qquad \boldsymbol{\zeta}_0^\alpha = \boldsymbol{\zeta}^\alpha(\boldsymbol{\epsilon}_0, T_0) = \tilde{\boldsymbol{\tau}}_\infty^\alpha(\boldsymbol{\epsilon}_0, T_0). \tag{148}$$

The general solution is again obtained by Eq. 99 with the straightforward substitutions. Initial total stresses are given by Eq. 122 with $\chi_i^\alpha = 0$. Internal strains and their rates are obtained from Eq. 113:

$$\boldsymbol{\chi}^\alpha = \frac{1}{\mu_\alpha}\left[\tilde{\boldsymbol{\tau}}_\infty^\alpha - \boldsymbol{\zeta}^\alpha\right], \qquad \dot{\boldsymbol{\chi}}^\alpha = \boldsymbol{\zeta}^\alpha/\nu_\alpha, \qquad (\nu_\alpha = \mu_\alpha t_\alpha > 0). \tag{149}$$

As $t \to \infty$ from Eq. 117 and Eq. 139, $\boldsymbol{\chi}_\infty^\alpha = \tilde{\boldsymbol{\tau}}_\infty^\alpha/\mu_\alpha$.

Four independent material parameters are needed for each viscosity mode α: the energy factors β_α^V and β_α^Δ, the relaxation time t_α, and the stiffness factor μ_α, where the latter two are related to viscosity via the rightmost expression in Eq. 149. Consider again an isothermal, simple shear, stress relaxation test whereby $\epsilon_4 = \gamma_0 =$ constant, $T = T_0 =$ constant, and $\mu_1 = \mu_1(T_0)$. For the present model, Eq. 126 of Section 5.3 is replaced with

$$\hat{\tau}_4(t) = G_0\gamma_0\left[1 + \beta_1^\Delta\{1 - \frac{\beta_1^\Delta G_0}{\mu_1}[1 - \exp(-t/t_1)]\}\right]. \tag{150}$$

Analogously, for isothermal spherical stress (i.e., pressure) relaxation at constant

volume [$J = J_0 = \exp(\epsilon_0) =$ constant],

$$p(t) = -\frac{\hat{\tau}_0(t)}{J_0} = -\frac{B_0^T \epsilon_0}{J_0}\left[1 + \beta_1^V\{1 - \frac{\beta_1^V B_0^T}{\mu_1}[1 - \exp(-t/t_1)]\}\right]. \tag{151}$$

Unlike the previous two examples, here the initial total stress is $(1+\beta_1^\Delta)$ or $(1+\beta_1^V)$ times the equilibrium stress for shear and pressure loading protocols in Eq. 150 and Eq. 151, which is more amenable to data fitting, albeit at the expense of an additional parameter for each viscous mode α. Thus, the energy factors β_1^Δ and β_1^V are physically related to initial stress and can be calibrated from the ratios of initial to equilibrium stresses for respective simple shear and hydrostatic pressure loadings. The time-dependent relaxation behavior can then be used to obtain μ_1 and t_1.

Though perhaps overly restrictive, upon choosing $\beta_1^\Delta = \mu_1/G_0$, the response in Eq. 126 can be obtained, where $\hat{\tau}_4 \to G_0\gamma_0$ as $t \to \infty$:

$$\tau(t) = \hat{\tau}_4(t) = G_0\gamma_0\left[1 + \beta_1^\Delta \exp(-t/t_1)\right]. \tag{152}$$

Choosing $\beta_1^V = \mu_1/B_0^T$ gives similarly, with the equilibrium response $pJ_0 \to -B_0^T\epsilon_0$ as $t \to \infty$,

$$p(t) = -\frac{\hat{\tau}_0(t)}{J_0} = -\frac{B_0^T \epsilon_0}{J_0}\left[1 + \beta_1^V \exp\left(\frac{-t}{t_1}\right)\right]. \tag{153}$$

Shown in Fig. 3a is the shear stress relaxation response predicted by Eq. 152 for different prescriptions of β_1^Δ and t_1, where $\tau = \hat{\tau}_4$. Denoted by t_0 is an arbitrary time constant for normalization. Faster decay corresponds to lower t_1. The instantaneous (dynamic) simple shear modulus is $G_0 \cdot (1 + \beta_1^\Delta)$. Evolution of the corresponding shear component of internal configurational strain, reported in Fig. 3b, for this shearing mode is given by the first of Eq. 149:

$$\chi = \chi_4^1 = \frac{\beta_1^\Delta G_0\gamma_0}{\mu_1}\left[1 - \exp\left(\frac{-t}{t_1}\right)\right] = \gamma_0\left[1 - \exp\left(\frac{-t}{t_1}\right)\right]. \tag{154}$$

Notably, the internal strain increases independently of parameters β_1^Δ, μ_1, and G_0. As $t \to \infty$, $\chi = \chi_4^1 \to \epsilon_4 = \gamma_0$ in Eq. 147, and the total shear stress degenerates to the equilibrium shear stress: $\hat{\tau}_4 \to G_0\epsilon_4 = G_0\gamma_0$. Results in Fig. 3 demonstrate the

capability of the present formulation to address a physically meaningful viscoelastic response. Specifically, the exponential decay to an equilibrium value under stress relaxation experiments is characteristic of standard (e.g., linear and quasi-linear) viscoelastic media,[30,51] including rubber and other polymers,[9,10] as well as many soft biological tissues.[2,52,53] Analogous relaxation behaviors can be well-represented by the model for pressure, pure shear, and their combinations such as uniaxial loading.

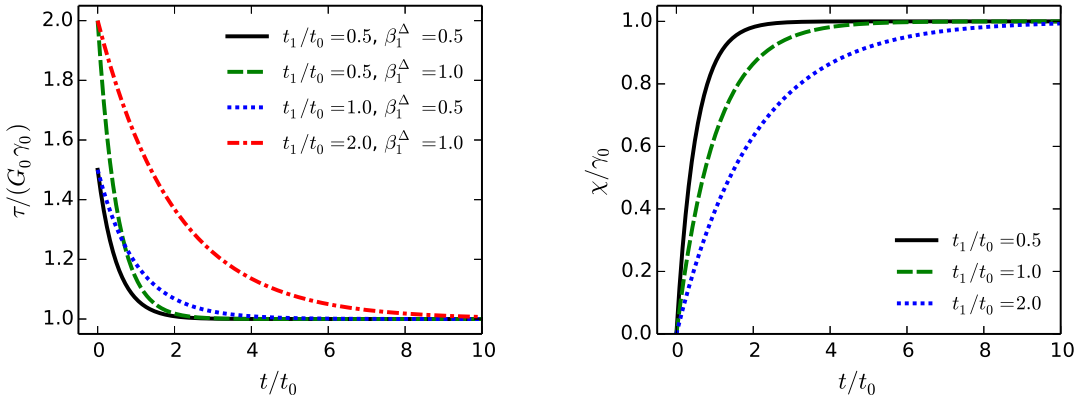

(a) shear stress (b) internal strain

Fig. 3 Predictions for isothermal viscoelastic stress relaxation of a solid with equilibrium shear modulus G_0 under constant simple shear deformation γ_0: a) shear stress τ computed from Eq. 152 and b) internal state variable (internal shear strain) χ computed from Eq. 154

6. Damage

Mechanics and thermodynamics of damage, described mathematically via internal state variable D first introduced in Section 3, are now addressed. The theory initiated by Simo[8] for coupled finite viscoelasticity and damage is adapted in the present work to consider nonlinear elastic and viscoelastic models based on the QR decomposition and stress-strain attributes. More descriptive degradation functions and kinetic equations than those proposed elsewhere[8] are also advanced herein, capable of addressing a variety of behaviors observed in stiff materials (e.g., polycrystals, plastics) and softer solids such as rubbery polymers and biomaterials.

6.1 General Theory

A free-energy based theory is considered, corresponding to the first of Eq. 41. This is consistent with the viscoelastic framework set forth in Section 5 and is most

suitable for isothermal problems. Internal energy-based models are often more convenient for adiabatic events (e.g., most wave propagation problems) and will be addressed in future work.

Recall that Ψ_0 corresponds to free energy when the material is undamaged (i.e., when $D = 0$). In some cases damage can reasonably be assumed to affect total free energy multiplicatively through a single degradation function f:

$$\Psi(\boldsymbol{\epsilon}, T, \boldsymbol{\chi}^\alpha, D) = f(D) \cdot \Psi_0(\boldsymbol{\epsilon}, T, \boldsymbol{\chi}^\alpha); \qquad f \in [0,1], \quad f(0) = 1. \tag{155}$$

For example, the familiar model of classical continuum damage mechanics[54] advocated elsewhere[8] takes $f = 1 - D$ for isothermal problems. The quadratic degradation function $f = (1-D)^2$ is standard in variational and phase field representations of fracture[55–57] and other generalized continuum theories,[58–60] though in the current framework, surface energies associated with material gradients of D are omitted. More elaborate continuum damage theories consistent with the laws of thermodynamics are described in the literature,[15,37,61] for example. Correspondence between D and microstructure depends on the particular material under consideration. Particular linkages of damage variable D to physical entities such as cracks and voids will be provided subsequently in demonstrative examples in Section 6.2 and Section 6.3, respectively.

Limiting the present scope to materials of cubic or isotropic elastic symmetry, free energy of Eq. 41 in the undamaged state is further decomposed into volumetric, thermal, and shearing contributions generalizing the scheme outlined in Section 5.5:

$$\begin{aligned}\Psi_0 = \Psi(\xi_0, \xi_1, \xi_2, T, \boldsymbol{\chi}^\alpha, 0) &= \Psi_0^V(\xi_0, T, \chi_0^\alpha) + \Psi_0^\Delta(\xi_0, \xi_1, \xi_2, \{\chi_j^\alpha\}|_{j\geq 0}) \\ &= \Psi_0^v(\xi_0, T, \chi_0^\alpha) + \psi(T) + \Psi_0^\Delta(\xi_0, \xi_1, \xi_2, \{\chi_j^\alpha\}|_{j\geq 0}).\end{aligned} \tag{156}$$

Recall from Eq. 67 that $\xi_0 = \epsilon_0 = \ln J$, and that ξ_1 and ξ_2 account for isochoric pure and simple shearing deformations, respectively. Energy function ψ accounts for specific heat but not thermoelastic coupling, which is embedded in Ψ_0^v. Effective deviatoric energy Ψ_0^Δ includes possible dependence on (ϵ_0, χ_0) as results from pressure-shear coupling (e.g., $\iota \neq 1$ in Eq. 138). Any of the example hyperelastic potentials presented in Section 4 can be partitioned according to the forms in Eq. 156, as can the example viscoelastic potentials in Section 5.

The basic model of Eq. 155 is extended and applied as follows, where now degradation functions $f^v(D,q)$ and $f^\Delta(D)$ are possibly distinct scalar multipliers:

$$\begin{aligned}\Psi(\xi_i, T, \chi_i^\alpha, D) = f^v(D,q) \cdot \Psi_0^v(\xi_0, T, \chi_0^\alpha) \\ + f^\Delta(D) \cdot \Psi_0^\Delta(\xi_0, \xi_1, \xi_2, \{\chi_j^\alpha\}|_{j\geq 0}) + \psi(T).\end{aligned} \tag{157}$$

The sign of volumetric strain is $q = \text{sgn}(\epsilon_0)$ and is used as an indicator in f^v to account for potentially different deterioration of the tangent bulk modulus in tension versus compression.[56,57] Notably, in compression when cracks and voids are fully closed, the tangent bulk modulus may not appreciably differ from that of its reference value in the absence of damage. This is in contrast to dilatation (i.e., volumetric expansion), whereby open cracks and voids should increase compliance.

The following constraints are imposed:

$$\begin{aligned}&f^v, f^\Delta \in [0,1], \qquad f^v(0,q) = f^\Delta(0) = 1; \\ &f'^v = \partial f^v / \partial D \leq 0, \quad f'^\Delta = \mathrm{d}f^\Delta / \mathrm{d}D \leq 0.\end{aligned} \tag{158}$$

Accordingly, volumetric and deviatoric strain energy densities are degraded via possibly different functions f^V and f^Δ, respectively, and the thermal energy ψ (e.g., specific heat capacity) is not affected by damage. The latter assumption implies that a material with cracks or tears requires the same amount of heat energy to raise its temperature as an undamaged material. Bounds on f^v and f^Δ ensure that damage does not cause the free energy to change sign or the tangent elastic stiffness to increase above its nominal initial value. The rightmost two inequalities lead to monotonically decreasing degradation multipliers as D increases.

With the prescription in Eq. 157, dissipation due to damage in Eq. 64 is

$$-\frac{\partial \Psi}{\partial D}\dot{D} = F\dot{D} = F^v\dot{D} + F^\Delta\dot{D} = -f'^v\Psi_0^v\dot{D} - f'^\Delta\Psi_0^\Delta\dot{D} \geq 0, \tag{159}$$

and is here forced to be non-negative according to the rightmost inequality. Motivated by the derived forms of driving forces F^v and F^Δ, the following dimensionless energies and their maximums achieved over the time history of deformation are

introduced:

$$\begin{aligned}\varphi^v(t) =& \left\langle \frac{2\Psi_0^v(t)}{B_0^T} \right\rangle^R, \quad \varphi_m^v(t) = \max_{s\in(-\infty,t]}[\varphi^v(s), \varphi_0^v];\\ \varphi^\Delta(t) =& \left\langle \frac{2\Psi_0^\Delta(t)}{G_0} \right\rangle^R, \quad \varphi_m^\Delta(t) = \max_{s\in(-\infty,t]}[\varphi^\Delta(s), \varphi_0^\Delta].\end{aligned} \tag{160}$$

Angled brackets parse positive values: $\langle X\rangle = \frac{1}{2}(X + |X|)$. Dimensionless material parameter $R > 0$ modulates the strength of the driving force. Dimensionless threshold energies for the onset of damage growth are the non-negative constants φ_0^v and φ_0^Δ.

A kinetic law for damage is proposed as follows, where $\mathrm{H}(\cdot)$ is the Heaviside function:

$$\begin{aligned}\dot{D}(\varphi^v, \dot{\varphi}_m^v, \varphi^\Delta, \dot{\varphi}_m^\Delta, D, q) &= \frac{\mathrm{d}D}{\mathrm{d}t}(\varphi^v, \dot{\varphi}_m^v, \varphi^\Delta, \dot{\varphi}_m^\Delta, D, q)\\ &= \left[\alpha_v(\varphi^v, \varphi^\Delta, q)\dot{\varphi}_m^v + \alpha_\Delta(\varphi^v, \varphi^\Delta, q)\dot{\varphi}_m^\Delta\right] \cdot \mathrm{H}(1 - D)\\ &\geq 0.\end{aligned} \tag{161}$$

Dimensionless material dependent functions are denoted by α_v and α_D; these obey $\alpha_v \geq 0$ and $\alpha_\Delta \geq 0$. The Heaviside function caps maximum damage at $D = 1$.

Rates of φ_m^v and φ_m^Δ are non-negative by definition:

$$\frac{\mathrm{d}}{\mathrm{d}t}\varphi_m^v = \dot{\varphi}_m^v = \begin{cases} \dot{\varphi}^v & \text{if} \quad \dot{\varphi}^v > 0 \quad \text{and} \quad \varphi^v = \varphi_m^v,\\ 0 & \text{otherwise;}\end{cases} \tag{162}$$

$$\frac{\mathrm{d}}{\mathrm{d}t}\varphi_m^\Delta = \dot{\varphi}_m^\Delta = \begin{cases} \dot{\varphi}^\Delta & \text{if} \quad \dot{\varphi}^\Delta > 0 \quad \text{and} \quad \varphi^\Delta = \varphi_m^\Delta,\\ 0 & \text{otherwise.}\end{cases} \tag{163}$$

These rates are positive only when respective initial thresholds $\phi_0^v \geq 0$ and $\phi_0^\Delta \geq 0$ are exceeded, meaning when strain energy densities Ψ_0^v or Ψ_0^Δ are non-negative as imposed from Eq. 160.

According to Eq. 161, damage increases in the material only when conjugate strain energy densities are increasing above prior maximums or their initial thresholds. It follows from Eq. 158 and Eq. 161 that dissipation in Eq. 159 is unconditionally

non-negative.

The kinetic model of Eq. 161–Eq. 163 could equivalently be expressed in terms of loading criteria from a damage surface in state space, extending the viewpoint of Simo.[8] If the volumetric-deviatoric split and q are omitted, the conjugate force φ is defined instead as $\sqrt{2\Psi_0}$ with historic maximum φ_m, and $R = \frac{1}{2}$ are imposed, then the present kinetic model reduces to that proposed elsewhere.[8] In other words, a dissipation potential could be constructed in strain space to arrive at a similar (or even identical, under less mathematically restrictive conditions) kinetic equation for damage evolution. Both the present, direct evolution equation and the potential function of Simo[8] ensure thermodynamic admissibility (i.e., non-negative dissipation), and ultimately, both require similar material parameters either calibrated to macroscopic test data or derived/extracted from micromechanics or other multi-scale methods. See also approaches for modeling damage kinetics of biomaterials invoking a damage surface[4] and a conditional, history-dependent evolution equation[5] similar to Eq. 161.

Examples in the following two subsections demonstrate how the foregoing damage theory is superimposed on representative hyperelastic and viscoelastic models introduced in Section 4 and Section 5, respectively. The first shows how damage D can be related physically to micro-cracks distributed in a hyperelastic material. The second shows how D can be related physically to porosity from voids in a viscoelastic material.

6.2 Nonlinear Hyperelastic Solid with Isotropic Damage from Micro-Cracks

In the present example, the free energy functional of Eq. 83 for the undamaged solid is invoked. This energy is partitioned according to Eq. 156 as follows, noting that $\boldsymbol{\chi}^\alpha$ are not needed in the absence of viscosity:

$$\Psi_0(\{\Xi_j\}, T) = \Psi_0^\infty(\{\Xi_j\}, T) = \Psi_0^{v\infty}(\Xi_0, T) + \psi^\infty(T) + \Psi_0^{\Delta\infty}(\Xi_1); \tag{164}$$

$$\Psi_0^{v\infty} = \frac{1}{2} B_0^T (\Xi_0)^2 - B_0^T A_0 \Xi_0 \Delta T, \tag{165}$$

$$\Psi_0^{\Delta\infty} = \frac{1}{2} G_0 \Xi_1, \tag{166}$$

$$\psi^{\infty} = -c_0 T \ln(T/T_0). \tag{167}$$

Damage consists of an isotropic distribution of penny-shaped micro-cracks. The mean radius of micro-cracks contained in a volume element at $\boldsymbol{X}$ and time t is denoted by $a_c(\boldsymbol{X}, t)$. The number of micro-cracks per unit reference volume is denoted by $n_c(\boldsymbol{X}, t)$. The damage variable is defined as

$$D(\boldsymbol{X}, t) = 8[a_c(\boldsymbol{X}, t)]^3 \cdot n_c(\boldsymbol{X}, t). \tag{168}$$

At percolation, $D \to 1$ corresponds to one micro-crack of radius a_c per cubic volume element of material of edge length $2a_c$. Define the Poisson's ratio of the undamaged material at its initial state by the usual isotropic linear elastic relation:

$$\nu_0 = (3B_0^T - 2G_0)/(6B_0^T + 2G_0). \tag{169}$$

The bulk modulus and shear modulus are then presumed to degrade according to the linear elastic theory of Bristow,[32] in the absence of analytical formulae relating cracks to moduli in nonlinear elastic materials of the present type with strain energy corresponding to Eq. 164. Two coefficients depending on Poisson's ratio are defined as

$$\kappa^v = \frac{2}{9}\frac{1-\nu_0^2}{1-2\nu_0}, \qquad \kappa^{\Delta} = \frac{4}{45}(1-\nu_0)(5-\nu_0). \tag{170}$$

The following degradation functions are then used for $0 \leq D < 1$, based on work of Bristow[32]:

$$f^v(D,q) = \begin{cases} 1 - \kappa^v D & \text{if } q \geq 0 \text{ and } D < 1/\kappa^v, \\ 0 & \text{if } q \geq 0 \text{ and } D \geq 1/\kappa^v, \\ 1 & \text{if } q < 0; \end{cases} \tag{171}$$

$$f^{\Delta}(D) = \begin{cases} 1 - \kappa^{\Delta} D & \text{if } D < 1/\kappa^{\Delta}, \\ 0 & \text{if } D \geq 1/\kappa^{\Delta}. \end{cases}$$

The value of q indicates compression ($q < 0$) versus tension ($q > 0$) or neutral loading ($q = 0$) such that under volumetric compression with $\epsilon_0 < 0 \Rightarrow q = -1 \Rightarrow f^v = 1$, the volumetric strain energy density $\Psi_0^{v\infty}$ is not degraded. Under compressive pressure, closed cracks are presumed to leave the bulk modulus unaffected.[56,57] This way, the material's response becomes akin to a compressible fluid when the

tangent shear modulus is fully degraded due to damage, preventing interpenetration of matter that might occur were the bulk modulus reduced to zero in compression. If $\kappa^v \geq 1$ or $\kappa^\Delta \geq 1$, the corresponding minimum of f^v or f^Δ is set to zero when $D \geq 1/\kappa^v$ or $D \geq 1/\kappa^\Delta$, respectively.

At percolation, when $D = 1$, a physically reasonable limiting assumption is that the tangent bulk modulus degrades to zero in tension or neutral loading, and the tangent shear modulus vanishes (i.e., frictionless crack surfaces):

$$f^v(1,q) = \begin{cases} 0 & \text{if } q \geq 0, \\ 1 & \text{if } q < 0; \end{cases} \qquad f^\Delta(1) = 0. \tag{172}$$

Constraints $f^v \in [0,1]$ and $f^\Delta \in [0,1]$ as required from Eq. 158 always hold from Eq. 171 and Eq. 172.

Shown in Fig. 4 are effective bulk and shear moduli obtained from Eq. 171 for $D \in [0,1)$. The bulk modulus decreases more rapidly with increasing crack content as Poisson's ratio increases. The shear modulus demonstrates the converse behavior, decreasing more rapidly as Poisson's ratio decreases. When $D = 1$, moduli drop abruptly to 0 according to Eq. 172; this behavior is not shown in Fig. 4.

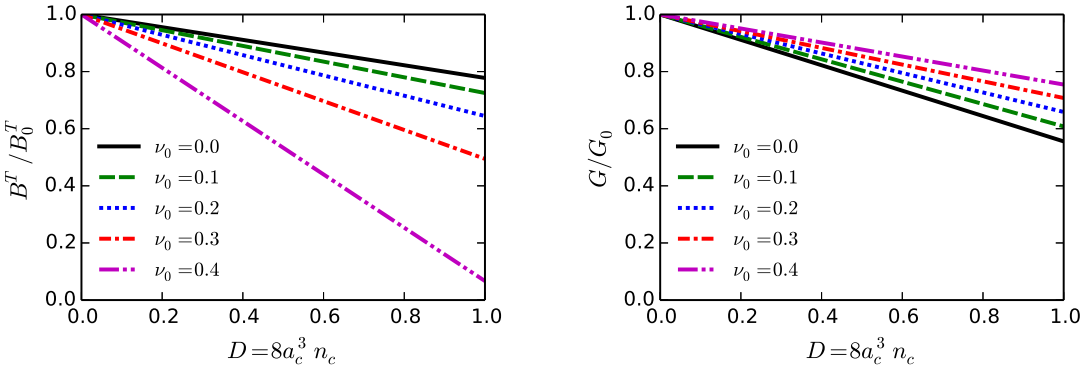

(a) bulk modulus (b) shear modulus

Fig. 4 Effects of damage D from isotropic distribution of penny-shaped micro-cracks of radius a_c and number per unit reference volume n_c: a) tangent bulk isothermal modulus B^T for $q \geq 0$ (neutral or tensile loading) and b) shear modulus G, both measured at null applied strain. Relations among moduli and crack variables extracted from literature.[32]

Derivatives of Eq. 171 with respect to damage $D \in [0, 1)$ obey, with thermodynamic bounds $-1 < \nu_0 < \frac{1}{2}$ on Poisson's ratio,

$$f'^{v}(D, q) = \begin{cases} -\kappa^v < 0 & \text{if } q \geq 0,\ D < 1/\kappa^v, \\ 0 & \text{otherwise;} \end{cases}$$
$$f'^{\Delta}(D) = \begin{cases} -\kappa^\Delta < 0 & \text{if } D < 1/\kappa^\Delta, \\ 0 & \text{otherwise.} \end{cases} \tag{173}$$

If conditions in Eq. 172 are invoked, then $f'^{v} = f'^{\Delta} = 0$ when the material element fails by total fracture at $D = 1$. Therefore, Eq. 171 and Eq. 172 collectively obey all required constraints in Eq. 158 for $D \in [0, 1]$.

Conjugate stresses to the strain attributes, $\{\hat{\tau}_i\}$, are computed using Eq. 44:

$$\begin{aligned} \hat{\tau}_0(\epsilon_0, D, T) &= f^v(D, \epsilon_0) \cdot B_0^T \left[\epsilon_0 - A_0 \Delta T\right], \\ \hat{\tau}_i(\epsilon_i, D) &= 6 f^\Delta(D) G_0 \epsilon_i, \qquad (i = 1, 2, 3); \\ \hat{\tau}_i(\epsilon_i, D) &= f^\Delta(D) G_0 \epsilon_i, \qquad (i = 4, 5, 6). \end{aligned} \tag{174}$$

The temperature rate equation Eq. 63 becomes

$$c_0 \dot{T} = -f^v B_0^T A_0 T \dot{\epsilon}_0 + [F - T(\partial F/\partial T)]\dot{D} - \nabla_0 \cdot \boldsymbol{q} + r. \tag{175}$$

The total thermodynamic force conjugate to D and its temperature derivative are

$$F = F^v + F^\Delta = -f'^{v} \Psi_0^{v\infty} - f'^{\Delta} \Psi_0^{\Delta\infty} \tag{176}$$

and

$$\frac{\partial F}{\partial T} = -f'^{v} \partial_T \Psi_0^{v\infty} = f'^{v} B_0^T A_0 \epsilon_0. \tag{177}$$

The model is complete upon specification of evolution law Eq. 161 with initial conditions D_0 on the distribution of damage:

$$\dot{D} = \left[\alpha_v \cdot \dot{\varphi}_m^v + \alpha_\Delta \cdot \dot{\varphi}_m^\Delta\right] \cdot \mathrm{H}(1 - D), \qquad D(\boldsymbol{X}, 0) = D_0(\boldsymbol{X}). \tag{178}$$

If no cracks exist initially, then $D_0 = 0$; however, many brittle solids (e.g., rocks and ceramics) have a non-negligible content of micro-cracks in their natural, as-

fabricated, or as-received states.

Time differentiation of Eq. 168 provides a relationship between the damage growth rate and the rates of extension and nucleation of micro-cracks:

$$\dot{D}(\boldsymbol{X},t) = 8[a_c(\boldsymbol{X},t)]^2 \cdot [3\dot{a}_c(\boldsymbol{X},t) \cdot n_c(\boldsymbol{X},t) + a_c(\boldsymbol{X},t) \cdot \dot{n}_c(\boldsymbol{X},t)]\,. \tag{179}$$

Driving forces for damage in Eq. 160 whose rates enter Eq. 178 are

$$\begin{aligned}
\varphi^v &= \left\langle \frac{2\Psi_0^v}{B_0^T} \right\rangle^R = \langle \epsilon_0(\epsilon_0 - 2A_0\Delta T)\rangle^R, \\
\varphi^\Delta &= \left\langle \frac{2\Psi_0^\Delta}{G_0} \right\rangle^R = (\Xi_1)^R = \{6[(\epsilon_1)^2 + (\epsilon_2)^2 + (\epsilon_3)^2] + (\epsilon_4)^2 + (\epsilon_5)^2 + (\epsilon_6)^2\}^R.
\end{aligned} \tag{180}$$

When $R = \frac{1}{2}$ and α_v and α_Δ are constants, then the damage growth rate is proportional to a measure of strain rate, or an effective stress rate via Eq. 174, for isothermal deformation. The effective stress in this context would be that in the material were its moduli not degraded by damage. Furthermore, under monotonic loading at constant rate, D would increase proportionally to strain or effective stress exceeding threshold values for these model choices. In practice, constant R and functions α_v and α_D can be calibrated to some combination of macroscopic stress-strain and tangent modulus data and microscopic information on evolving densities and/or mean radii of micro-cracks under different loading protocols. Such steps are beyond the present generic treatment, since micro-crack kinetics are complex and highly material dependent. Representative examples of damage growth laws for different brittle solids (ceramics, minerals, concrete) are available elsewhere.[62–65]

6.3 Nonlinear Viscoelastic Pseudo-Isotropic Solid with Voids

In the final example, the thermo-viscoelastic model of Section 5 is extended to account for damage, with full nonlinearity maintained via inclusion of parameters $B_0'^T$ and G_0'. Free energy function of Eq. 138 for the undamaged solid in the equilibrium limit is invoked. Variable D is explicitly related to void volume fraction later in this section.

The total free energy of the undamaged solid, including configuration energy, is

Eq. 141 .This energy is partitioned according to Eq. 156 as follows:

$$\Psi_0 = \Psi_0^{\infty} + \Upsilon_0 = \Psi_0^{V} + \Psi_0^{\Delta}; \tag{181}$$

$$\begin{aligned}\Upsilon_0 &= \sum_{\alpha=1}^{m}\left[\frac{1}{2}\mu_\alpha|\boldsymbol{\chi}^\alpha|^2 - \tilde{\boldsymbol{\tau}}_\infty^\alpha\cdot\boldsymbol{\chi}^\alpha + \Psi_0^\alpha\right]\\ &= \sum_{\alpha=1}^{m}\left[\frac{1}{2}\mu_\alpha|\boldsymbol{\chi}^\alpha|^2 - \tilde{\boldsymbol{\tau}}_\infty^\alpha\cdot\boldsymbol{\chi}^\alpha + \beta_\alpha^V\Psi_0^{V\infty} + \beta_\alpha^\Delta\Psi_0^{\Delta\infty}\right];\end{aligned} \tag{182}$$

$$\begin{aligned}\Psi_0^\alpha(\boldsymbol{\epsilon},T) &= \beta_\alpha^V\Psi_0^{V\infty}(\epsilon_0,T) + \beta_\alpha^{D\alpha}\Psi_0^{\Delta\infty}(\epsilon_i)|_{i\geq 0}\\ &\qquad\left[\beta_\alpha^V,\beta_\alpha^\Delta\in(0,\infty),\qquad(\alpha=1,\ldots,m)\right];\end{aligned} \tag{183}$$

$$\begin{aligned}\Psi_0^\infty(\Xi_j,T) &= \Psi_0^{V\infty}(\Xi_0,T) + \Psi_0^{\Delta\infty}(\Xi_0,\Xi_1)\\ &= \Psi_0^{v\infty}(\Xi_0,T) + \psi^\infty(T) + \Psi_0^{\delta\infty}(\Xi_1)\iota(\Xi_0),\end{aligned} \tag{184}$$

$$\begin{aligned}\Psi_0^{v\infty} &= \frac{1}{2}B_0^T(\Xi_0)^2\left[1-\frac{1}{3}(B_0'^T-2)\Xi_0\right] - B_0^TA_0\Xi_0\Delta T,\\ \Psi_0^{\Delta\infty} &= \frac{1}{2}G_0\Xi_1\left[1-\frac{B_0^T}{G_0}G_0'\Xi_0\right];\end{aligned} \tag{185}$$

$$\Psi_0^v = \Psi_0^{v\infty} + \sum_{\alpha=1}^{m}\left[\frac{1}{2}\mu_\alpha(\chi_0^\alpha)^2 - \beta_\alpha^V\left(\frac{\partial\Psi_0^{V\infty}}{\partial\epsilon_0}\chi_0^\alpha - \Psi_0^{v\infty}\right)\right], \tag{186}$$

$$\Psi_0^\Delta = \Psi_0^{D\infty} + \sum_{\alpha=1}^{m}\left[\frac{1}{2}\mu_\alpha(\sum_{i\neq 0}\chi_i^\alpha)^2 - \beta_\alpha^\Delta\left(\sum_{i\neq 0}\frac{\partial\Psi_i^{\Delta\infty}}{\partial\epsilon_i}\chi_i^\alpha + \Psi_0^{\delta\infty}\frac{\mathrm{d}\iota}{\mathrm{d}\epsilon_0}\chi_0^\alpha - \Psi_0^{\Delta\infty}\right)\right], \tag{187}$$

$$\psi = \psi^\infty\cdot(1-\sum_{\alpha=1}^{m}\beta_\alpha^V) = -c_0T\ln(T/T_0)\cdot(1-\sum_{\alpha=1}^{m}\beta_\alpha^V). \tag{188}$$

Define the following modified stress vector that is obtained from differentiation of

Eq. 183 with respect to $\boldsymbol{\epsilon}$ for each α:

$$\begin{aligned}\tilde{\boldsymbol{\tau}}^{\alpha}_{\infty} = \partial_{\boldsymbol{\epsilon}}\Psi^{\alpha}_{0} = \{\tilde{\tau}_i\}^{\alpha}_{\infty} &= \begin{Bmatrix} \beta^{V}_{\alpha}(\partial\Psi^{V\infty}_{0}/\partial\epsilon_0) + \beta^{\Delta}_{\alpha}\Psi^{\delta\infty}_{0}(\mathrm{d}\iota/\mathrm{d}\epsilon_0) \\ \beta^{\Delta}_{\alpha}(\partial\Psi^{\Delta\infty}_{1}/\partial\epsilon_1) \\ \beta^{\Delta}_{\alpha}(\partial\Psi^{\Delta\infty}_{1}/\partial\epsilon_2) \\ \beta^{\Delta}_{\alpha}(\partial\Psi^{\Delta\infty}_{1}/\partial\epsilon_3) \\ \beta^{\Delta}_{\alpha}(\partial\Psi^{\Delta\infty}_{1}/\partial\epsilon_4) \\ \beta^{\Delta}_{\alpha}(\partial\Psi^{\Delta\infty}_{1}/\partial\epsilon_5) \\ \beta^{\Delta}_{\alpha}(\partial\Psi^{\Delta\infty}_{1}/\partial\epsilon_6) \end{Bmatrix} \\ &= \begin{Bmatrix} \beta^{V}_{\alpha}B^{T}_{0}[\epsilon_0 - \frac{1}{2}(B'^{T}_{0} - 2)(\epsilon_0)^2 - A_0\Delta T] - \beta^{\Delta}_{\alpha}B^{T}_{0}[\frac{1}{2}G'_0\Xi_1] \\ 6\beta^{\Delta}_{\alpha}G_0\epsilon_1[1 - (B^{T}_{0}/G_0)G'_0\epsilon_0] \\ 6\beta^{\Delta}_{\alpha}G_0\epsilon_2[1 - (B^{T}_{0}/G_0)G'_0\epsilon_0] \\ 6\beta^{\Delta}_{\alpha}G_0\epsilon_3[1 - (B^{T}_{0}/G_0)G'_0\epsilon_0] \\ \beta^{\Delta}_{\alpha}G_0\epsilon_4[1 - (B^{T}_{0}/G_0)G'_0\epsilon_0] \\ \beta^{\Delta}_{\alpha}G_0\epsilon_5[1 - (B^{T}_{0}/G_0)G'_0\epsilon_0] \\ \beta^{\Delta}_{\alpha}G_0\epsilon_6[1 - (B^{T}_{0}/G_0)G'_0\epsilon_0] \end{Bmatrix}. \end{aligned} \tag{189}$$

The total viscous stress vector (now undegraded) is redefined from Eq. 62 as

$$\boldsymbol{\zeta}^{\alpha} = -\partial_{\boldsymbol{\chi}^{\alpha}}\Psi_0 = -\partial_{\boldsymbol{\chi}^{\alpha}}\Upsilon_0 = \tilde{\boldsymbol{\tau}}^{\alpha}_{\infty} - \mu_{\alpha}\boldsymbol{\chi}^{\alpha} = \nu_{\alpha}\dot{\boldsymbol{\chi}}^{\alpha} = \mu_{\alpha}t_{\alpha}\dot{\boldsymbol{\chi}}^{\alpha}. \tag{190}$$

The kinetic equation for internal stresses with initial conditions is

$$\dot{\boldsymbol{\zeta}}^{\alpha} + \frac{1}{t_{\alpha}}\boldsymbol{\zeta}^{\alpha} = \frac{\mathrm{d}}{\mathrm{d}t}\tilde{\boldsymbol{\tau}}^{\alpha}_{\infty} - \mu'_{\alpha}\boldsymbol{\chi}^{\alpha}\dot{T}, \qquad \boldsymbol{\zeta}^{\alpha}_{0} = \boldsymbol{\zeta}^{\alpha}(\boldsymbol{\epsilon}_0, T_0) = \tilde{\boldsymbol{\tau}}^{\alpha}_{\infty}(\boldsymbol{\epsilon}_0, T_0). \tag{191}$$

The general solution obeys Eq. 99 with convolution integrand containing the rate of Eq. 189. Internal strains and their rates are obtained from Eq. 190:

$$\boldsymbol{\chi}^{\alpha} = \frac{1}{\mu_{\alpha}}\left[\tilde{\boldsymbol{\tau}}^{\alpha}_{\infty} - \boldsymbol{\zeta}^{\alpha}\right], \qquad \dot{\boldsymbol{\chi}}^{\alpha} = \boldsymbol{\zeta}^{\alpha}/\nu_{\alpha}, \qquad (\nu_{\alpha} = \mu_{\alpha}t_{\alpha} > 0). \tag{192}$$

Terminal equilibrium values of internal strains are found by use of Eq. 183 in Eq. 117: $\boldsymbol{\chi}^{\alpha}_{\infty} = \tilde{\boldsymbol{\tau}}^{\alpha}_{\infty}/\mu_{\alpha}$. The preceding formulae in Eq. 181–Eq. 192 are unaffected by damage variable D.

Following Eq. 157, the total free energy function including damage is

$$\begin{aligned}\Psi(\Xi_i, T, \chi_i^\alpha, D) = f^v(D,q)\cdot\Psi_0^v(\Xi_0, T, \chi_0^\alpha) \\ + f^\Delta(D)\cdot\Psi_0^\Delta(\Xi_0, \Xi_1, \{\chi_j^\alpha\}|_{j\geq 0}) + \psi(T).\end{aligned} \tag{193}$$

Possible degradation functions f^v and f^Δ will be prescribed later, after derivation of total stresses. The latter, in thermodynamic form, are

$$\boldsymbol{\tau} = \frac{\partial\Psi}{\partial\boldsymbol{\epsilon}} = f^v\frac{\partial\Psi_0^v}{\partial\boldsymbol{\epsilon}} + f^\Delta\frac{\partial\Psi_0^\Delta}{\partial\boldsymbol{\epsilon}}. \tag{194}$$

Substituting Eq. 181–Eq. 187 into Eq. 194 gives

$$\hat{\boldsymbol{\tau}} = \left\{\begin{array}{c} f^v B_0^T[\{\epsilon_0 - \frac{1}{2}\bar{B}(\epsilon_0)^2 - A_0\Delta T\} + \sum_{\alpha=1}^m \beta_\alpha^V\{\epsilon_0 - \frac{1}{2}\bar{B}(\epsilon_0)^2 - \dots \\ \dots - A_0\Delta T - (1-\bar{B}\epsilon_0)\chi_0^\alpha\}] - \bar{\tau}_0 \\ 6f^\Delta G_0[1-(B_0^T/G_0)G_0'\epsilon_0][\epsilon_1 + \sum_{\alpha=1}^m \beta_\alpha^\Delta(\epsilon_1 - \chi_1^\alpha)] - \bar{\tau}_1 \\ 6f^\Delta G_0[1-(B_0^T/G_0)G_0'\epsilon_0][\epsilon_2 + \sum_{\alpha=1}^m \beta_\alpha^\Delta(\epsilon_2 - \chi_2^\alpha)] - \bar{\tau}_2 \\ 6f^\Delta G_0[1-(B_0^T/G_0)G_0'\epsilon_0][\epsilon_3 + \sum_{\alpha=1}^m \beta_\alpha^\Delta(\epsilon_3 - \chi_3^\alpha)] - \bar{\tau}_3 \\ f^\Delta G_0[1-(B_0^T/G_0)G_0'\epsilon_0][\epsilon_4 + \sum_{\alpha=1}^m \beta_\alpha^\Delta(\epsilon_4 - \chi_4^\alpha)] - \bar{\tau}_4 \\ f^\Delta G_0[1-(B_0^T/G_0)G_0'\epsilon_0][\epsilon_5 + \sum_{\alpha=1}^m \beta_\alpha^\Delta(\epsilon_5 - \chi_5^\alpha)] - \bar{\tau}_5 \\ f^\Delta G_0[1-(B_0^T/G_0)G_0'\epsilon_0][\epsilon_6 + \sum_{\alpha=1}^m \beta_\alpha^\Delta(\epsilon_6 - \chi_6^\alpha)] - \bar{\tau}_6 \end{array}\right\}, \tag{195}$$

where $\bar{B} = B_0'^T - 2$ and pressure-shear coupling is

$$\begin{aligned}
\bar{\tau}_0 &= f^\Delta B_0^T G_0'\Bigg[\frac{\Xi_1}{2} \\
&\qquad + \sum_{\alpha=1}^m \beta_\alpha^\Delta\{\frac{\Xi_1}{2}\chi_0^\alpha - 6(\epsilon_1\chi_1^\alpha + \epsilon_2\chi_2^\alpha + \epsilon_3\chi_3^\alpha) - (\epsilon_4\chi_4^\alpha + \epsilon_5\chi_5^\alpha + \epsilon_6\chi_6^\alpha)\}\Bigg], \\
\bar{\tau}_1 &= -6f^\Delta B_0^T G_0'\sum_{\alpha=1}^m \beta_\alpha^\Delta\epsilon_1\chi_0^\alpha, \qquad \bar{\tau}_2 = -6f^\Delta B_0^T G_0'\sum_{\alpha=1}^m \beta_\alpha^\Delta\epsilon_2\chi_0^\alpha, \\
\bar{\tau}_3 &= -6f^\Delta B_0^T G_0'\sum_{\alpha=1}^m \beta_\alpha^\Delta\epsilon_3\chi_0^\alpha, \qquad \bar{\tau}_4 = -f^\Delta B_0^T G_0'\sum_{\alpha=1}^m \beta_\alpha^\Delta\epsilon_4\chi_0^\alpha, \\
\bar{\tau}_5 &= -f^\Delta B_0^T G_0'\sum_{\alpha=1}^m \beta_\alpha^\Delta\epsilon_5\chi_0^\alpha, \qquad \bar{\tau}_6 = -f^\Delta B_0^T G_0'\sum_{\alpha=1}^m \beta_\alpha^\Delta\epsilon_6\chi_0^\alpha.
\end{aligned} \tag{196}$$

The condition Eq. 39 is invoked for internal strains entering the configurational energy function Υ_0. With this constraint in place and Eq. 25, verification is straightfor-

ward that $\hat{\tau}_1+\hat{\tau}_2+\hat{\tau}_3 = 0$; thus restrictions in Eq. 33 and Eq. 47 are obeyed. Initial total stresses are given by Eq. 195 with $\chi_i^\alpha = 0$ and $f^v = f^\Delta = 1$, presuming that the material is undamaged initially; otherwise initial conditions $D(t=0) = D_0 > 0$ should be used in f^v and f^Δ.

Entropy density is

$$\begin{aligned}\eta = -\frac{\partial \Psi}{\partial T} = c_0[1+\ln(T/T_0)]\left(1+\sum_{\alpha=1}^{m}\beta_\alpha^V\right) + f^v B_0^T A_0 \epsilon_0 \\ + \sum_{\alpha=1}^{m}[f^v \beta_\alpha^V B_0^T A_0(\epsilon_0 - \chi_0^\alpha) - \frac{1}{2}\{f^v \mu'_\alpha (\chi_0^\alpha)^2 + f^\Delta \mu'_\alpha \sum_{i\neq 0}(\chi_i^\alpha)^2\}].\end{aligned} \tag{197}$$

Temperature evolution can be calculated via Eq. 63:

$$\begin{aligned}c_0\dot{T} = -f^v B^T A_0 T\left(1+\sum_{\alpha=1}^{m}\beta_\alpha^V\right)\dot{\epsilon}_0 \\ + \sum_{\alpha=1}^{m}\nu_\alpha[f^v(\dot{\chi}_0^\alpha)^2 + f^\Delta\sum_{i\neq 0}(\dot{\chi}_i^\alpha)^2] \\ + T\sum_{\alpha=1}^{m}[f^v\{\beta_\alpha^V B_0^T A_0 + \mu'_\alpha \chi_0^\alpha\}\dot{\chi}_0^\alpha + f^\Delta \mu'_\alpha \sum_{i\neq 0}\chi_i^\alpha \cdot \dot{\chi}_i^\alpha] \\ + [F - T(\partial F/\partial T)]\dot{D} - \nabla_0 \cdot \boldsymbol{q} + r,\end{aligned} \tag{198}$$

with, from Eq. 159,

$$\begin{aligned}F &= -f'^v \Psi_0^v - f'^\Delta \Psi_0^\Delta, \\ \frac{\partial F}{\partial T} &= f'^v\{B_0^T A_0 \epsilon_0 + \sum_{\alpha=1}^{m}[\beta_\alpha^V B_0^T A_0(\epsilon_0 - \chi_0^\alpha) - \frac{1}{2}\mu'_\alpha(\chi_0^\alpha)^2]\} \\ &\quad - \frac{1}{2}f'^\Delta \sum_{\alpha=1}^{m}\mu'_\alpha \sum_{i\neq 0}(\chi_i^\alpha)^2,\end{aligned} \tag{199}$$

where Ψ_0^v and Ψ_0^Δ are given in Eq. 186 and Eq. 187, respectively.

The internal dissipation inequality in the first of Eq. 64 becomes

$$\mathfrak{D} = -\sum_{\alpha=1}^{M}\left(f^v \frac{\partial \Psi_0^v}{\partial \boldsymbol{\chi}^\alpha} + f^\Delta \frac{\partial \Psi_0^\Delta}{\partial \boldsymbol{\chi}^\alpha}\right)\cdot \dot{\boldsymbol{\chi}}^\alpha + F\dot{D} \geq 0. \tag{200}$$

The viscoelasticity theory of Section 5 ensures that Eq. 93 and Eq. 102 are unconditionally satisfied, that is,

$$-\sum_{\alpha=1}^{M}\left(\frac{\partial\Psi_0^v}{\partial\boldsymbol{\chi}^\alpha}+\frac{\partial\Psi_0^\Delta}{\partial\boldsymbol{\chi}^\alpha}\right)\cdot\dot{\boldsymbol{\chi}}^\alpha\geq 0 \tag{201}$$

follows directly from the total and configurational energy functions Eq. 181 and Eq. 182 in conjunction with kinetic law Eq. 191. Obviously when $f^v = f^\Delta \geq 0$, then the viscoelastic contribution to Eq. 200 is always non-negative. Physics permitting, this would be a preferred choice to ensure thermodynamic consistency; otherwise, functions f^v and f^Δ should be constrained such that Eq. 200 holds over the loading regime to which the model is applied. The term $F\dot{D}$ in Eq. 200 is always non-negative when the damage degradation constitutive equations and kinetic framework of Section 6.1 are imposed.

A simple phenomenological degradation model, and perhaps the most prevalent for rubbery solids and other polymers[8,54] as well as biological tissues,[5] that fulfills all properties in Eq. 158 is

$$f^v = f^\Delta = f = 1 - D, \qquad f' = \mathrm{d}f/\mathrm{d}D = -1. \tag{202}$$

A specific form of Eq. 161 is needed; an example kinetic law like Eq. 178 is equally applicable to the present setting. Parameters entering the damage framework should ideally be calibrated after viscoelastic properties are determined. The former are preferably obtained by consideration of the time-dependent response when loading at intensities below the threshold(s) for damage initiation. Subsequently, the material parameters controlling degradation and damage kinetics can be calibrated by considering the response to more severe loadings above these threshold(s). A similar approach to calibration was undertaken elsewhere,[5] where hyperelastic and damage properties were calibrated for biological tissues for respective loadings in physiological and supra-physiological domains.

An alternative degradation model rooted in micromechanics explicitly defines D as the void volume fraction $\hat{\phi}$:

$$D(\boldsymbol{X},t) = \hat{\phi}(\boldsymbol{X},t) = 1 - \frac{\hat{\rho}(\boldsymbol{X},t)}{\rho_0(\boldsymbol{X})}. \tag{203}$$

where $\rho_0 > 0$ is the mass density of the material in the unloaded reference state without any voids, and $\hat{\rho}$ is the mass density of the material, externally unloaded at the reference temperature, with voids. Since $0 \leq \hat{\rho} \leq \rho_0$, bounds $D \in [0,1]$ are fulfilled by this physical definition. Following the scheme used for modulus degradation in the presence of micro-cracks in Section 6.2, dilatational and deviatoric free energy densities now are affected by voids using coefficients obtained from the isotropic elastic analysis of Mackenzie,[31] with Poisson's ratio ν_0 defined in Eq. 169:

$$\kappa^v = \frac{3(1-\nu_0)}{(1+\nu_0)D + 2(1-2\nu_0)}, \qquad \kappa^\Delta = \frac{15(1-\nu_0)}{(7-5\nu_0)}. \tag{204}$$

Note that the first of Eq. 204 is not a constant since it depends on $D = \hat{\phi}$. The following degradation functions are then used for $0 \leq D < 1$, based on the above-quoted theory[31] for effective moduli:

$$f^v(D,q) = \begin{cases} 1 - \kappa^v D & \text{if } q \geq 0 \text{ and } D < 1/\kappa^v, \\ 0 & \text{if } q \geq 0 \text{ and } D \geq 1/\kappa^v, \\ 1 & \text{if } q < 0; \end{cases} \tag{205}$$

$$f^\Delta(D) = \begin{cases} 1 - \kappa^\Delta D & \text{if } D < 1/\kappa^\Delta, \\ 0 & \text{if } D \geq 1/\kappa^\Delta. \end{cases}$$

Recall that $q = \text{sgn}(\epsilon_0)$ indicates compression ($q < 0$, $J < 1$) versus tension ($q > 0$, $J > 1$) or neutral loading ($q = 0$, $J = 1$) such that under volumetric compression, the volumetric strain energy density $\Psi_0^{v\infty}$ is not degraded. Under compressive pressure, voids collapse in viscoelastic solids and are presumed to leave the bulk modulus unaltered.[56,57] Interpenetration of matter that might occur were the bulk modulus to reduce to zero in compression is thereby avoided. If $\kappa^v \geq 1$ or $\kappa^\Delta \geq 1$, the corresponding minimum of f^v or f^Δ is set to zero when $D \geq 1/\kappa^v$ or $D \geq 1/\kappa^\Delta$, respectively.

Relations from the literature[31] for κ^v and κ^Δ are accurate to $\text{O}(D^3)$ and $\text{O}(D^2)$, respectively, in linear isotropic elastic solids. They are extrapolations for nonlinear elastic solids like the one considered here, since analogous analytical formulae do not exist. If $D = 1$ occurs in a material element, then that element is completely voided, with no solid material. Although this extreme limiting condition can never be fully realized physically, the tangent bulk modulus degrades to zero by default

for $q \geq 0$ in Eq. 205, and vanishing of the tangent shear modulus results automatically as $D \to 1$ since $\kappa^{\Delta} > 1$ for $-1 < \nu_0 < \frac{1}{2}$: $f^v(1,q) = f^{\Delta}(1) = 0$. Constraints $f^v \in [0,1]$ and $f^{\Delta} \in [0,1]$, as required from Eq. 158, always hold from Eq. 205. Derivatives of Eq. 205 with respect to damage $D \in [0,1]$ can be verified, using thermodynamic bounds $B_0^T > 0$ and $G_0 > 0$, to satisfy $f'^v(D,q) \leq 0$ and $f'^{\Delta}(D) \leq 0$. Therefore, Eq. 205 obeys all required constraints in Eq. 158 for $D \in [0,1]$.

Shown in Fig. 5 are effective bulk and shear moduli obtained from Eq. 205 for $D \in [0,1]$. The bulk modulus decreases more rapidly with increasing void volume fraction as Poisson's ratio increases. The shear modulus demonstrates the converse behavior, decreasing more rapidly as Poisson's ratio decreases. The minimum value of G is capped at 0 at some damage level $0.46 \lesssim D \lesssim 0.6$ for the cases shown per Eq. 205, since $\kappa^{\Delta} > 1$. When $D = 1$, moduli all equate to 0 according to Eq. 205; this feature need not be manually imposed according to results in Fig. 5.

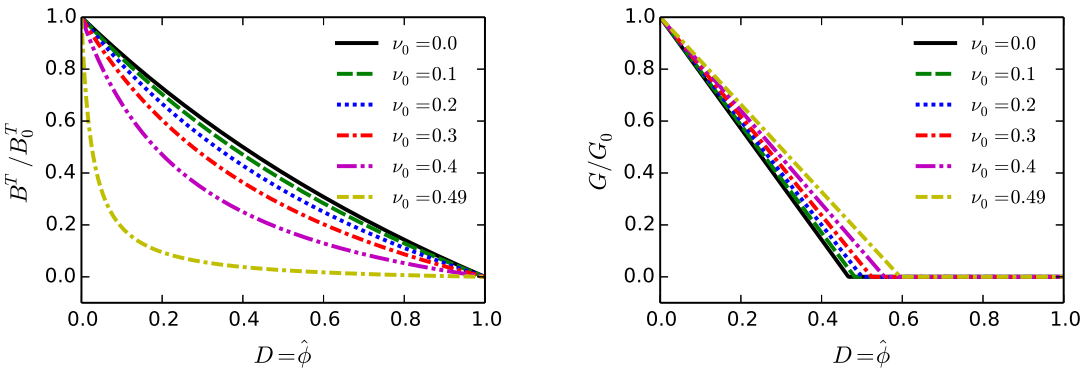

(a) bulk modulus (b) shear modulus

Fig. 5 Effects of damage D from isotropic distribution of spherical voids of volume fraction $\hat{\phi}$: a) tangent bulk isothermal modulus B^T for $q \geq 0$ (neutral or tensile loading) and b) shear modulus G, both measured at null applied strain. Relations among moduli and porosity extracted from literature[31] are most realistic for small $\hat{\phi}$.

Under tensile loading, many rubber solids and other ductile polymers fail by void nucleation, growth, and coalescence. Nucleation often occurs by debonding of a matrix phase from small particles of a dilute, stiffer second phase. Analytical, numerical, and experimental studies have related the onset of void formation to a threshold cavitation pressure p_C.[58,66,67] The present model framework is now adapted to address this phenomenon in a rubbery solid in the quasi-static isothermal limit.

The material is assumed nearly incompressible, with $\nu_0 = 0.49$ and a default value of $\bar{B} = 0$. Temperature is fixed at $T = T_0$. The deformation gradient for spherical expansion is $\boldsymbol{F} = J^{1/3}\mathbf{1}$, with $J \geq 1$, so $\epsilon_0 = \ln J \geq 0$ and $q \geq 0$. Furthermore, since squeeze and shear strain attributes vanish, $\Xi_1 = 0$. In the quasi-static limit, $\chi^0_\alpha \to \epsilon_0$ and $\Upsilon_0 \to 0$ with $\mu_\alpha = \beta_\alpha B_0^T$, such that viscoelasticity does not subsequently enter the analysis. Free energy, the degradation function, the single nonzero stress component in Eq. 195, and Cauchy pressure become, respectively,

$$\begin{aligned} \Psi &= \frac{1}{2}[1 - \kappa^v(D) \cdot D] B_0^T (\ln J)^2, \qquad & \kappa^v(D) &= \frac{3(1-\nu_0)}{(1+\nu_0)D + 2(1-2\nu_0)}; \\ \hat{\tau}_0 &= [1 - \kappa^v(D) \cdot D] B_0^T \ln J, & p &= -[1 - \kappa^v(D) \cdot D] B_0^T \frac{\ln J}{J}. \end{aligned} \tag{206}$$

The static driving force for damage is, since $J \geq 1$,

$$\varphi^v = (\ln J)^{2R}. \tag{207}$$

Porosity initiates when cavitation pressure $p = -p_C$ is attained, where the latter is defined as positive in tension. Let J_C be the volume ratio of a material element at this pressure, and ϕ^v_0 the corresponding threshold driving force:

$$\frac{p_C}{B_0^T} = \frac{\ln J_C}{J_C}, \qquad \varphi^v_0 = (\ln J_C)^{2R}. \tag{208}$$

Experimental or theoretical knowledge of p_C thus allows identification of damage initiation threshold φ^v_0 through implicit solution of Eq. 208.

The damage rate in Eq. 161 is equal to the rate of void volume fraction through Eq. 203:

$$\frac{\mathrm{d}}{\mathrm{d}t}\hat{\phi} = \dot{D} = \alpha_v \cdot \dot{\varphi}^v_m \cdot \mathrm{H}(1 - D), \qquad \varphi^v_m(t) = \max_{t \in (-\infty, s]} [\varphi^v(s), \varphi^v_0]. \tag{209}$$

The simplest physically plausible version of Eq. 209 invokes $\alpha_v =$constant. Making this choice, along with initial condition $D(t = 0) = 0$, Eq. 209 can be integrated analytically for monotonic tensile expansion:

$$D(J) = \min[\alpha_v \langle (\ln J)^{2R} - \varphi^v_0 \rangle, 1]. \tag{210}$$

For this simple model under hydrostatic expansion, two elastic constants and three

damage parameters suffice: the initial bulk modulus B_0^T, the initial Poisson's ratio ν_0, the cavitation pressure p_C, and the void kinetic parameters α_v and R. The latter two require calibration to macroscopic pressure-volume data and/or transient measurements of void volume fraction $D = \hat{\phi}$. Since these are highly material- and microstructure-dependent, they are varied parametrically in what follows rather than assigned absolute values. As remarked already, for a rubbery solid, $\nu_0 = 0.49$ is deemed reasonable. Energy and pressure can be normalized by B_0^T so that the latter does not affect normalized results of the model. Following analysis reviewed elsewhere,[66] $p_C = \frac{5}{2}G_0$ is appropriate for nearly incompressible isotropic hyperelastic solids. With $\nu_0 = 0.49$, this estimate yields $p_C = \frac{1}{20}B_0^T$, giving $J_C = 1.0542$.

Predictions of the model are shown in Fig. 6. Damage (i.e., void volume fraction) is reported in Fig. 6a versus volume expansion as computed from kinetic law Eq. 210. Cauchy pressure computed from Eq. 206, normalized by cavitation pressure p_C, is shown in Fig. 6b. At fixed R, increasing α_v increases void growth and reduces the normalized pressure more rapidly with increasing J. At fixed α_v, decreasing R has a similar effect on trends in evolution of porosity and pressure since $0 \leq \epsilon_0 < 1$ for results shown here. The case with $R = \frac{1}{2}$ and $\alpha_v = 2$ attains the total failure condition $D = 1$ at $J \approx 1.6J_C$. The other cases never achieve this maximum in D over the range of J reported in Fig. 6a, but all would attain $D = 1$ eventually at larger J. The very stiff response when damage is omitted is shown for reference in Fig. 6b.

When $R = \frac{1}{2}$, the magnitude of pressure peaks at p_C and drops abruptly thereafter with further expansion. When $R = 1$, the maximum tensile load supported exceeds the initial cavitation pressure ($-p > p_C$ for $J > J_C$) , and strain softening due to damage is more gradual with increasing J. Both types of behavior (i.e., abrupt failure and gradual softening) have been observed in different rubbers and glassy polymers,[68–70] though plastic deformation that may emerge in some such materials under local, non-hydrostatic stress states is omitted here. This simple damage mechanics framework enables representation of either trend when parameters are chosen appropriately. It is understood that more elaborate models are required to account complex behaviors of degradation of viscoelastic polymers and biomaterials observed under dynamic cyclic loading.[5,8]

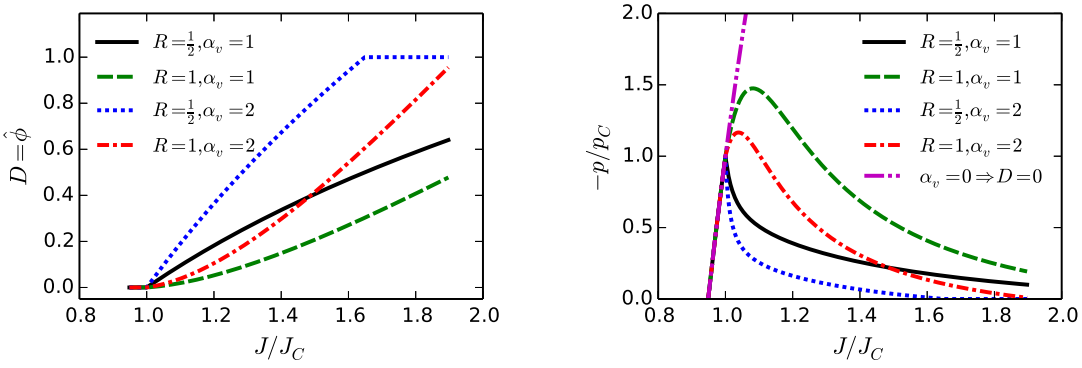

(a) void volume (b) pressure

Fig. 6 Model predictions for evolution of damage under static isothermal, spherical expansion J of a nearly incompressible solid with $\nu_0 = 0.49$: a) damage-equivalent void volume fraction $\hat{\phi}$ and b) Cauchy pressure p accounting for degraded bulk modulus from voids.[31] Expansion ratio at onset of cavitation is J_C corresponding to cavitation pressure $p_C = \frac{1}{20}B_0^T$.

7. Conclusions

A comprehensive theoretical framework for finite deformation mechanics and thermodynamics of continuous bodies has been constructed in the context of the Gram-Schmidt (QR) decomposition of the deformation gradient. The present work appears to be the first to apply QR kinematics of total deformation towards both viscoelastic and damage phenomena, though a different kinematic formulation with upper triangular residual deformation and a flow rule for its evolution were invoked elsewhere[16] in the context of thermo-viscoelasticity. More specifically, noteworthy developments reported herein include the following:

- A geometrically nonlinear thermodynamic and internal variable framework complementing the QR description of conjugate stress-strain attributes;
- Finite hyperelasticity with temperature and entropy effects, including examples for quasi-linear and fully nonlinear solids with certain cubic or isotropic symmetries in the context of QR kinematics;
- Nonlinear thermo-viscoelasticity with configurational energies and kinetics obeying physical and thermodynamically admissible behaviors;

- Continuum damage mechanics accounting for initial thresholds of damage growth, differing behaviors in spherical tension/compression and shear, and simultaneous viscoelasticity.

Advantages of the present strain attribute-based framework over classical $\boldsymbol{C}$-invariant-based theories discussed in the context of (hyper)elastic response[16,20,21,23–25] are retained in the current hyperelastic-thermo-viscoelastic-damage framework.

Various examples presented herein have considered physically relevant energy potentials and kinetic relations. Effective moduli for solids with micro-cracks and pores have been incorporated. Solutions for simple 1-D cases have been discussed in the context of isothermal hyperelastic pressure-volume response, isothermal shear stress relaxation, and void nucleation and growth under static expansion. Physically reasonable trends are apparent in results for each case.

The present theory can be used for any classes of materials demonstrating a hyperelastic response in conjunction with possible viscoelasticity or damage mechanisms, including biological tissues, polymers, and even (poly)crystalline solids in the absence of plastic flow. Inelastic deformation and remnant strains are not considered here and thus await extension of the theory.[20] Proper definition of a reference state is crucial and often challenging for soft tissues[43,71]; this will be given detailed consideration in subsequent applications. Notably, future work will apply the theory towards modeling and simulation of a compressible soft biological tissue.[50]

8. References

1. Fung YC. Biomechanics: motion, flow, stress, and growth. New York (NY): Springer; 1990.

2. Fung YC. Biomechanics: mechanical properties of living tissues. Second ed. New York (NY): Springer; 1993.

3. Humphrey J. Continuum biomechanics of soft biological tissues. Proceedings of the Royal Society of London A. 2003;459:3–46.

4. Rodríguez J, Cacho F, Bea J, Doblaré M. A stochastic-structurally based three dimensional finite-strain damage model for fibrous soft tissue. Journal of the Mechanics and Physics of Solids. 2006;54:864–886.

5. Balzani D, Brinkhues S, Holzapfel G. Constitutive framework for the modeling of damage in collagenous soft tissues with application to arterial walls. Computer Methods in Applied Mechanics and Engineering. 2012;213:139–151.

6. Regueiro R, Zhang B, Wozniak S. Large deformation dynamic three-dimensional coupled finite element analysis of soft biological tissues treated as biphasic porous media. Computer Modeling in Engineering and Sciences (CMES). 2014;98:1–39.

7. Fankell D, Regueiro R, Kramer E, Ferguson V, Rentschler M. A small deformation thermoporomechanics finite element model and its application to arterial tissue fusion. Journal of Biomechanical Engineering. 2018;140:031007.

8. Simo J. On a fully three-dimensional finite-strain viscoelastic damage model: formulation and computational aspects. Computer Methods in Applied Mechanics and Engineering. 1987;60:153–173.

9. Holzapfel G, Simo J. A new viscoelastic constitutive model for continuous media at finite thermomechanical changes. International Journal of Solids and Structures. 1996;33:3019–3034.

10. Holzapfel G. On large strain viscoelasticity: continuum formulation and finite element applications to elastomeric structures. International Journal for Numerical Methods in Engineering. 1996;39:3903–3926.

11. Liu H, Holzapfel G, Skallerud B, Prot V. Anisotropic finite strain viscoelasticity: constitutive modeling and finite element implementation. Journal of the Mechanics and Physics of Solids. 2019;124:172–188.

12. Reese S, Govindjee S. A theory of finite viscoelasticity and numerical aspects. International Journal of Solids and Structures. 1998;35:3455–3482.

13. Clayton J, McDowell D, Bammann D. A multiscale gradient theory for elastoviscoplasticity of single crystals. International Journal of Engineering Science. 2004;42:427–457.

14. Clayton J. A continuum description of nonlinear elasticity, slip and twinning, with application to sapphire. Proceedings of the Royal Society of London A. 2009;465:307–334.

15. Clayton J. Nonlinear mechanics of crystals. Dordrecht (Netherlands): Springer; 2011.

16. Ghosh P, Srinivasa A. Development of a finite strain two-network model for shape memory polymers using QR decomposition. International Journal of Engineering Science. 2014;81:177–191.

17. Flory P. Thermodynamic relations for high elastic materials. Transactions of the Faraday Society. 1961;57:829–838.

18. Freed A, Zamani S. On the use of convected coordinate systems in the mechanics of continuous media derived from a QR factorization of F. International Journal of Engineering Science. 2018;127:145–161.

19. Freed A, Zamani S. Elastic Kelvin-Poisson-Poynting solids described through scalar conjugate stress/strain pairs derived from a QR factorization of F. Journal of the Mechanics and Physics of Solids. 2019;129:278–293.

20. Freed A, Graverend JB, Rajagopal K. A decomposition of Laplace stretch with applications in inelasticity. Acta Mechanica. 2019;230:3423–3429.

21. Criscione J. A constitutive framework for tubular structures that enables a semi-inverse solution to extension and inflation. Journal of Elasticity. 2004;77:57–81.

22. McLellan A. Finite strain coordinates and the stability of solid phases. Journal of Physics C: Solid State Physics. 1976;9:4083-4094.

23. Srinivasa A. On the use of the upper triangular (or QR) decomposition for developing constitutive equations for Green-elastic materials. International Journal of Engineering Science. 2012;60:1–12.

24. Freed A, Erel V, Moreno M. Conjugate stress/strain base pairs for planar analysis of biological tissues. Journal of Mechanics of Materials and Structures. 2017;12:219–247.

25. Freed A. A note on stress/strain conjugate pairs: explicit and implicit theories of thermoelasticity for anisotropic materials. International Journal of Engineering Science. 2017;120:155–171.

26. Rajagopal K, Srinivasa A. On the response of non-dissipative solids. Proceedings of the Royal Society A. 2006;463:357–367.

27. Freed A, Einstein D. An implicit elastic theory for lung parenchyma. International Journal of Engineering Science. 2013;62:31–47.

28. Freed A, Rajagopal K. A promising approach for modeling biological fibers. Acta Mechanica. 2016;227:1609–1619.

29. Freed A, Rajagopal K. A viscoelastic model for describing the response of biological fibers. Acta Mechanica. 2016;227:3367–3380.

30. Freed A. Soft solids. Cham (Switzerland): Birkhauser; 2016.

31. Mackenzie J. The elastic constants of a solid containing spherical holes. Proceedings of the Physical Society B. 1950;63:2–11.

32. Bristow J. Microcracks, and the static and dynamic elastic constants of annealed and heavily cold-worked metals. British Journal of Applied Physics. 1960;11:81–85.

33. Budiansky B, O'Connell R. Elastic moduli of a cracked solid. International Journal of Solids and Structures. 1976;12:81–97.

34. Rice J. Continuum mechanics and thermodynamics of plasticity in relation to microscale deformation mechanisms. In: Constitutive Equations in Plasticity; Argon A, editor. Cambridge (MA): Massachusetts Institute of Technology Press; 1975; p. 23–79.

35. Clayton J. Differential geometry and kinematics of continua. Singapore (Singapore): World Scientific; 2014.

36. Clayton J. On anholonomic deformation, geometry, and differentiation. Mathematics and Mechanics of Solids. 2012;17:702–735.

37. Voyiadjis G, Kattan P. Advances in damage mechanics: metals and metal matrix composites. Amsterdam (Netherlands): Elsevier; 1999.

38. Coleman B, Noll W. The thermodynamics of elastic materials with heat conduction and viscosity. Archive for Rational Mechanics and Analysis. 1963;13:167–178.

39. Truesdell C, Noll W. The non-linear field theories of mechanics. Berlin (Germany): Springer; 1965.

40. Guinan M, Steinberg D. Pressure and temperature derivatives of the isotropic polycrystalline shear modulus for 65 elements. Journal of the Physics and Chemistry of Solids. 1974;35:1501–1512.

41. Poirier JP, Tarantola A. A logarithmic equation of state. Physics of the Earth and Planetary Interiors. 1998;109:1–8.

42. Clayton J. Analysis of shock compression of strong single crystals with logarithmic thermoelastic-plastic theory. International Journal of Engineering Science. 2014;79:1–20.

43. Fung YC. Elasticity of soft tissues in simple elongation. American Journal of Physiology. 1967;213:1532–1544.

44. Vawter D, Fung YC, West J. Constitutive equation of lung tissue elasticity. Journal of Biomechanical Engineering. 1979;101:38–45.

45. Clayton J. Crystal thermoelasticity at extreme loading rates and pressures: analysis of higher-order energy potentials. Extreme Mechanics Letters. 2015;3:113–122.

46. Clayton J. Nonlinear elastic and inelastic models for shock compression of crystalline solids. Cham (Switzerland): Springer; 2019.

47. Simo J, Pister K. Remarks on rate constitutive equations for finite deformation problems: computational implications. Computer Methods in Applied Mechanics and Engineering. 1984;46:201–215.

48. Fung YC, Patitucci P, Tong P. Stress and strain in the lung. ASCE Journal of Engineering Mechanics. 1978;104:201–223.

49. Lee G, Frankus A. Elasticity properties of lung parenchyma derived from experimental distortion data. Biophysical Journal. 1975;15:481–493.

50. Clayton J, Banton R, Freed A. A nonlinear thermoelastic-viscoelastic continuum model of lung mechanics for shock wave analysis. In: Shock Compression of Condensed Matter; AIP Conference Proceedings; 2019, Forthcoming.

51. Wineman A. Nonlinear viscoelastic solids–a review. Mathematics and Mechanics of Solids. 2009;14:300–366.

52. Hughes R, May A, Widdicombe J. Stress relaxation in rabbits' lungs. Journal of Physiology. 1959;146:85–97.

53. Zeng Y, Yager D, Fung Y. Measurement of the mechanical properties of the human lung tissue. Journal of Biomechanical Engineering. 1987;109:169–174.

54. Krajcinovic D. Damage mechanics. Amsterdam (Netherlands): North-Holland; 1996.

55. Bourdin B, Francfort G, Marigo JJ. The variational approach to fracture. Journal of Elasticity. 2008;91:5–148.

56. Clayton J, Knap J. A geometrically nonlinear phase field theory of brittle fracture. International Journal of Fracture. 2014;189:139–148.

57. Clayton J, Knap J. Phase field modeling of coupled fracture and twinning in single crystals and polycrystals. Computer Methods in Applied Mechanics and Engineering. 2016;312:447–467.

58. Clayton J. Finsler geometry of nonlinear elastic solids with internal structure. Journal of Geometry and Physics. 2017;112:118–146.

59. Clayton J. Generalized finsler geometric continuum physics with applications in fracture and phase transformations. Zeitschrift fur Angewandte Mathematik und Physik (ZAMP). 2017;68:9.

60. Clayton J, Knap J. Continuum modeling of twinning, amorphization, and fracture: theory and numerical simulations. Continuum Mechanics and Thermodynamics. 2018;30:421–455.

61. Marshall J, Naghdi P, Srinivasa A. A macroscopic theory of microcrack growth in brittle materials. Philosophical Transactions of the Royal Society of London A. 1991;335:455–485.

62. Rajendran A. Modeling the impact behavior of AD85 ceramic under multiaxial loading. International Journal of Impact Engineering. 1994;15:749–768.

63. Espinosa H, Zavattieri P, Dwivedi S. A finite deformation continuum-discrete model for the description of fragmentation and damage in brittle materials. Journal of the Mechanics and Physics of Solids. 1998;46:1909–1942.

64. Clayton J. A model for deformation and fragmentation in crushable brittle solids. International Journal of Impact Engineering. 2008;35:269–289.

65. Clayton J. Deformation, fracture, and fragmentation in brittle geologic solids. International Journal of Fracture. 2010;173:151–172.

66. Fond C. Cavitation criterion for rubber materials: a review of void-growth models. Journal of Polymer Science B. 2001;39:2081–2096.

67. Hang-Sheng H, Abeyaratne R. Cavitation in elastic and elastic-plastic solids. Journal of the Mechanics and Physics of Solids. 1992;40:571–592.

68. Steenbrink A, Van Der Giessen E, Wu P. Void growth in glassy polymers. Journal of the Mechanics and Physics of Solids. 1997;45:405–437.

69. Volokh K. Cavitation instability in rubber. International Journal of Applied Mechanics. 2011;3:299–311.

70. Voyiadjis G, Shojaei A, Li G. A generalized coupled viscoplastic-viscodamage-viscohealing theory for glassy polymers. International Journal of Plasticity. 2012;28:21–45.

71. Rajagopal K, Srinivasa A. On a class of non-dissipative materials that are not hyperelastic. Proceedings of the Royal Society A. 2008;465:493–500.

1 (PDF) DEFENSE TECHNICAL INFORMATION CTR DTIC OCA

1 (PDF) CCDC ARL FCDD RLD CL TECH LIB

1 (PDF) GOVT PRINTG OFC A MALHOTRA

ABERDEEN PROVING GROUND

28 (PDF) CCDC ARL
FCDD RLC HC
J KNAP
FCDD RLW
A RAWLETT
S SCHOENFELD
J ZABINSKI
FCDD RLW MB
G GAZONAS
FCDD RLW PB
T BAUMER
C HOPPEL
M KLEINBERGER
K RAFAELS
S SATAPATHY
M SCHEIDLER
FCDD RLW PC
R BECKER
J BERRY
J CAZAMIAS
J CLAYTON
M FERMEN-COKER
A FREED
M GREENFIELD
R LEAVY
J LLOYD
C MEREDITH
R REGUEIRO
S SEGLETES
L SHANNAHAN
A TONGE
S TURNEAGE
C WILLIAMS
FCDD RLW PG
R BANTON